The role of ABC transporters for neurogenic functions of the adult and diseased brain

Dissertation

zur

Erlangung des akademischen Grades

doctor rerum naturalium (Dr. rer. nat.)

der Mathematisch-Naturwissenschaftlichen Fakultät

der Universität Rostock

Vorgelegt von Toni Schumacher

Geboren am 14.03.1982 in Rostock

Gutachter:

1. Gutachter: Prof. Dr. rer. nat. Hubert Bahl
   Institut für Biowissenschaften Universität Rostock

2. Gutachter: Prof. Dr. med. Dr. rer. nat. Jens Pahnke
   Universitätsklinik für Neurologie Magdeburg

3. Gutachter: Prof. Dr. rer. nat. Reinhard Walther
   Institut für Medizinische Biochemie und Molekularbiologie Universität
   Greifswald

Datum der Einreichung: 11. Mai 2012
Datum der Verteidigung: 26. November 2012

"I love fools' experiments. I am always making them."

- Charles Darwin -

Content

Table of Figures

List of Tables

List of Abbreviations

°C	degree Celsius
ABC	ATP binding cassette
aCSF	artificial cerebrospinal fluid
AD	Alzheimer's disease
APP	amyloid precursor protein
ATP	adenosine-triphosphate
Aβ	β-amyloid
$A\beta_{42}$	β-amyloid of 42 amino acids of length
BrdU	5-bromo-2'-deoxyuridine
C	concentration
CCI	controlled cortical injury
Cy2	carbocyanine 2
Cy3	carbocyanine 3
DAPI	4',6-diamidino-2-phenylindole
DCX	Doublecortin
DNA	deoxyribonucleic acid
EDTA	ethylenediaminetetraacetic acid
EGF	endothelial growth factor
eGFP	enhanced green fluorescent protein
EPM	elevated plus maze
FGF	fibroblast growth factor
for	forward
GAPDH	glyceraldehyde 3-phosphate dehydrogenase
GFAP	glial fibrilary acid protein
GZ	granular zone (of the dentate gyrus)
hAPP	human amyloid precursor protein
IPC	intermediate progenitor
Ko	knock out
LDB	light/dark-box
Mash1	archaete scute homologe 1
MibI	mindbomb1
mRNA	messenger ribonucleic acid
MW	molar weight
NBD	nucleic binding domain
NeuN	neuronal nuclear antigen
NICD1	notch intracellular domain 1
nIPC	neural intermediate progenitor
NS	neural stem cells
NSPC	neural stem and progenitor cells
oIPC	oligodendrocytic intermediate progenitor
p	level of significance
PBS	phosphate buffer saline
PCR	polymerase chain reactions
PFA	paraformaldehyde

PS1	preseneline 1
qRT-PCR	quantitative realtime PCR
Rev	reverse
RMS	rostral migratory stream
RNA	ribonucleic acid
SEM	standard error of the mean
SGZ	subgranular zone
Sox2	sex determining region Y-box 2
SP	side population
SVZ	subventricular zone
TMD	transmembrane domain
Tuj1	clone name for anti-β-III-tubulin antibody
V	volume
Wt	wild type

1   Summary

The family of ATP binding cassette (ABC) transporters comprises a number of export proteins which are responsible for the organismic homeostasis and are expressed at endothelial barriers of different tissues. Furthermore, recent findings of ABC transporters being transiently expressed in stem and progenitor cells of various tissues, also suggest them to play a functional role in sustaining cellular homeostasis for maintaining their stem cell character. Not least these proteins are of fundamental importance for the brain homeostasis by regulating transport of metabolites across the blood brain barrier and were therefore recently linked to neurodegenerative proteopathies of the brain like Alzheimer's disease (AD). Here, ABC transporters have been found directly responsible for the efflux of the toxic β-amyloid or Aβ which is the origin of neurodegenerative Aβ-plaques.

This study was carried out to assess the involvement of ABC transporters in neurogenic functions of the healthy and diseased adult brain. To do so, neurogenic progenitors in the hippocampal dentate gyrus were quantified in adult ABC deficient mouse strains which lacked either ABCB1 (ABCB1$^{0/0}$), ABCG2 (ABCG2$^{0/0}$) or ABCC1 (ABCC1$^{0/0}$), using immunofluorescence techniques. These analyzes revealed significantly impaired neuronal differentiation in the adult NSPC pool of ABCB1$^{0/0}$ mice. Additionally, analogues and comparative analyzes were performed in brains after utilization of a controlled cortical injury (CCI). The CCI was used to model neuroregeneration after brain injuries and for triggering neurogenesis. The neuroregeneration was assumed as to be impaired as a result of ABC depletion. Interestingly, deficit of ABCC1 did not seem to affect adult neurogenesis in the healthy brain, while these animals suffered from significantly impaired neuroregeneration after cortical injury as like as ABCB1 deficient mice did. Adult neurogenesis was also assessed in transgenic mouse strains expressing the human amyloid precursor protein (hAPP) and presenelin 1 (hPS1) when simultaneously lacking either one of the three questioned ABC transporters. These analyzes were carried out to assess neurogenic processes in brains suffering from β-amyloid proteopathy. While ABC transporters were already known to be involved in AD pathology, the question remained in which way ABC deficiency would contribute to neurogenic processes in the AD-affected brain. The experiments showed, as like previous studies stated for distinct other AD mouse models, that adult neurogenesis is triggered in the AD-affected brain. The relative increase in neurogenesis during β-amyloid deposition compared to the non-transgenic counterparts was most significantly increased in ABCG2$^{0/0}$ transgenic APP/PS1$^{+/0}$ mice.

Analyzes were also performed *in vitro* to answer the question whether ABC transporter activity is of cell-intrinsic importance for stem cell functions using primary NSPC cultures isolated from the ABC deficient mouse strains. The cultured NSPCs were used for proliferation and differentiation analyzes to find possible impairments as a result of ABC depletion. Also synthetic Aβ was used to observe NSPC functions with regard to AD pathology and ABC transporter functions *in vitro*. The results showed that only proliferation was significantly increased by lack of ABCG2, while capability for neuronal differentiation was not affected by ABC depletion. Aβ administration only showed a significant pro-neuronal effect during NSPC differentiation in cells of the control line without revealing significant deficits as a result of lacking ABC expression.

To assess possible alterations of ABC-depletion on brain ontogenesis, histological analyzes were performed and revealed minor alterations in the cortical cytoarchitecture in ABCB1 and ABCC1 deficient animals. As a result of alterations in adult neurogenesis and altered cortical cytoarchitecture found in ABC deficient animals, behavioral assessments were carried out to find possible impairments in behavioral phenotypes. Again $ABCB1^{0/0}$ and $ABCC1^{0/0}$ mice revealed significantly altered anxiety and activity levels.

The overall outcome of this study concluded in the finding that ABC transporters are indeed involved in neurogenic processes of the adult brain. But otherwise than suggested in former studies, deficit of single ABC transporters do not necessarily contribute to impaired NSPC functions on a cellular level. Rather deficiency of distinct ABC transporters seem to have far ranging effects on the brain homeostasis, especially on that of the stem cell niche, resulting in impaired neuroregenerative functions in the adult brain. Therefore impaired stem cell functions should be considered much more as a result of altered brain homeostasis. These resulting deficits seem to affect even brain ontogenesis leading to distinct behavioral phenotypes as well.

2 Introduction

2.1 Adult neurogenesis

For a long time the dogma of neurogenesis occurring only during prenatal brain ontogenesis and ending with birth was well accepted in the scientific community, assuming a slow loss of neuronal cells during neurodegenerative events until death. While first speculations about some "indifferent cells" or "medulloblasts", possibly giving birth to neurons in the adult brain, came up at the beginning of the 20th century, it took until the 1960s when Sidman, Altman and colleagues published first evidence supporting such theories.

By intrathecal injection of the radioactive nucleotide $[H^3]$-thymidine, newly generated cells were labeled as a result of $[H^3]$-thymidine incorporation into the DNA and allowing their identification by histological means [1]. By analyzing autoradiograms of brain slices of rats, Altman and colleagues found individual positive cells in the neocortex while a vast number of cells in the ependymal and subependymal layers of the lateral ventricles, as well as in the granular cell layer of the hippocampal dentate gyrus also showed robust $[H^3]$-thymidine labeling [2]. These early findings were controversially discussed and not well accepted in the scientific community. Some years later, studies of Kaplan and colleagues supported the earlier findings of Altman and the theory of adult neurogenesis. Here also $[H^3]$-thymidine labeling was used to mark proliferating cells, but the further analysis of ultra-structural properties of those cells revealed them as to be in fact neurons [3]. Still the question remained whether these single generated neurons really contribute to neuronal circuitry and thereby to neuroregenerative effects. Than in 1984 Paton and Nottebohm proved for the first time the functional integration of newly generated neurons in songbirds. By combining $[H^3]$-thymidine labeling prior to *in vivo* measurements of neuronal depolarization after acoustic stimuli and *in vivo* cell labeling of the measured cells, they could later document by utilizing immunohistochemical methods that a small amount of the measured cells were indeed positive for $[H^3]$-thymidine. Thereby the functional integration of newly generated neurons in the adult brain was proven, at least in birds [4].

Also more sophisticated cell culturing methods contributed to the growing knowledge of neural stem cells in the adult brain. In 1992 two workgroups could show independently the proliferative potential of isolated primary cells from the rodent striatum and their ability to differentiate into neural linage cells. Reynolds and colleagues could show that virtually all *in*

vitro proliferated cells were expressing Nestin, a cytoskeletal protein only expressed in neural stem and progenitor cells. They also showed the dependency of proliferation on the presence EGF and a non-adhesive matrix [5]. With a similar approach Richards and his group managed to differentiate these primary NSPCs into neurons *in vitro* and thereby evidenced the existence of stem cells in the adult brain [6].

Rapid gain of knowledge about adult neurogenesis was achieved after the introduction of 5-bromo-2'0-deoxyuridine (BrdU). Incorporation of this nucleotide analog into newly synthesized DNA and the ability of labeling BrdU incorporation by means of immunohistochemistry allowed easy lineage tracking of proliferating cells. This new tool led to observations of adult neurogenesis in virtually all analyzed mammalian brains and even in humans [7]. Much progress was made and it became clear that neurogenesis occurred only in distinct regions of the brain. It was observed that neurogenesis only occurred in two brain areas the hippocampus, were the dentate gyrus gives rise to new neurons, and the subventricular zones of virtually all ventricles. Here it was also observed that neurons from the subventricular region enter the rostral migratory stream and migrate to the olfactory bulb to become interneurons throughout adulthood [8].

As a result of a vast number of previous studies in the field of neuroregenerative potential of NSPCs, we already have a quite good understanding about the general mechanisms of NSPC differentiation and know the cellular markers expressed in each of the transient steps from early progenitors to mature neurons. It has been shown that apart from minor differences between hippocampal and subventricular NSPCs, neurogenic functions are based upon the proliferation and differentiation capacity of special astrocyte-like cells, the so-called radial glia or type-1 cells [9, 10]. It is believed that radial glial cells are remnants from neuroepithelial cells. They give rise directly to neurons (during embryonal development only) or intermediate progenitor cells (IPC) by asymmetrical diversion which are also referred to as type-2 cells [10]. Different early committed progenitors of neuronal (nIPC) or oligodendrocytic lineage (oIPC) are possible. During brain development the radial glia cells become less frequent and seem to be substituted by so called B-cells, which still reflect the morphological features of radial glia (e.g. morphology and marker expression (GFAP/Nestin)) and have the stem cell-like property of giving birth to all neural linage cells [9].
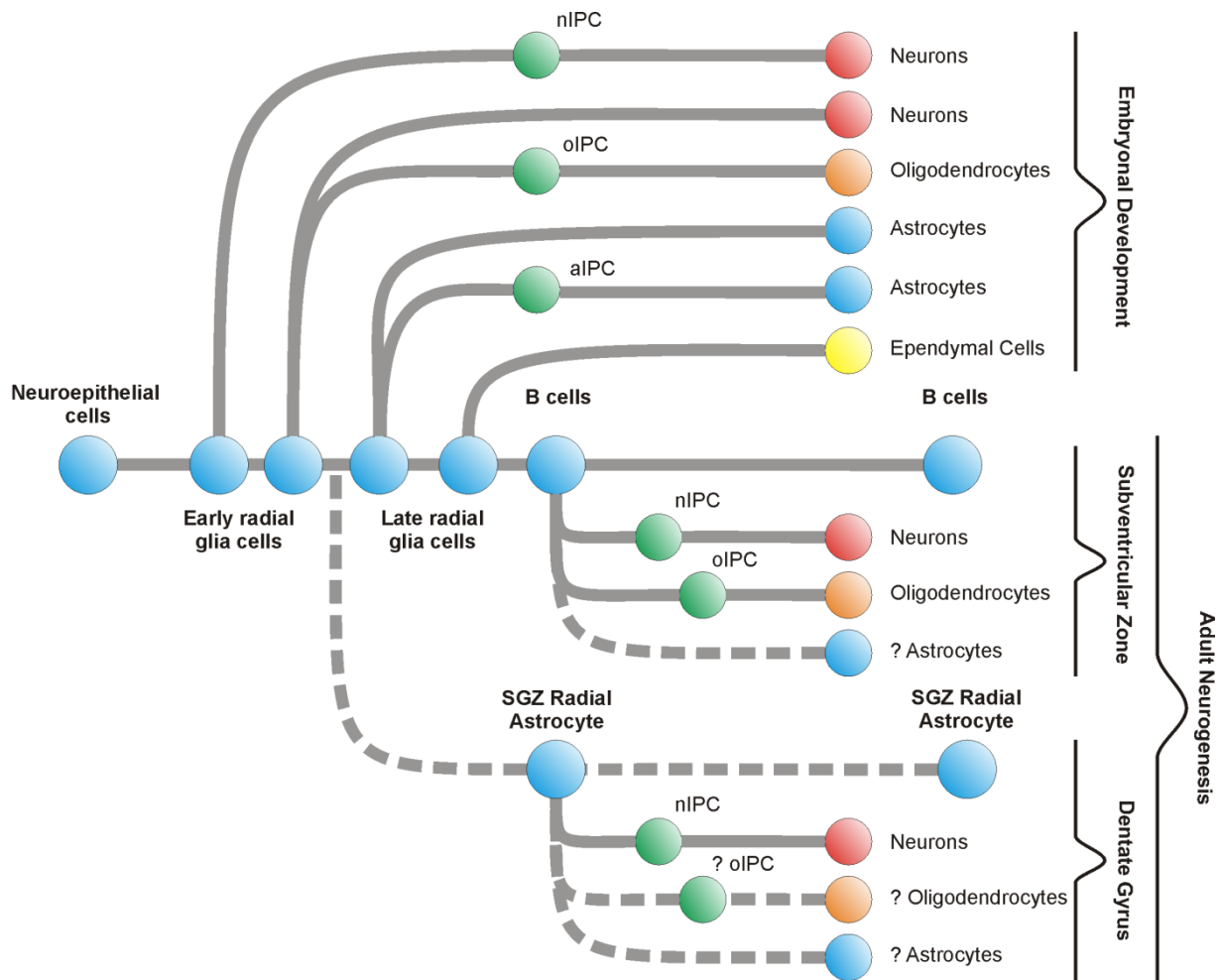
Figure 1: Neural cell lineage during neurogenesis (adapted from [9])

2.1.1 Subventricular zone (SVZ)

In the subventricular zone neurogenic processes occur most prominently in the walls of the lateral ventricles which most likely resemble the embryonic SVZ. Neurogenesis in the SVZ emanates from B cells which show astrocytic marker expression and resemble a radial glia cell-like morphology even though they show a less prominent basal-apical morphology and are also referred as to be SVZ-astrocytes [9, 11]. Even though the cell bodies of B cells are located under the ependymal cell layer these cells are equipped with small apical processes standing in contact with the ventricle and extent one single cilium into it which is supposed to be important for signal reception [12]. With their long basal processes containing special end feet B cells also stand in contact with blood vessels [13]. Even IPCs are often found to have direct contact to blood vessels. According to their special morphology it is assumed that B cells and IPCs receive signaling also from the vasculature regulating neurogenic functions. Anyway these B cells give rise to intermediate progenitor cells which are also known as C

cells [14]. The C cells or IPCs are highly proliferative and develop into neuroblasts or A cells which are neuronal committed precursor cells and migrate through the rostral migratory stream (RMS) to the olfactory bulb [15]. When arrived at the olfactory bulb these A cells differentiate into divers subtypes of interneurons [16]. Most of the cells become GABAergic granule neurons lacking axonal processes and form dendro-dendritic synapses. A very small part of the cells become either dopaminergic or glutamatergic neurons [17].
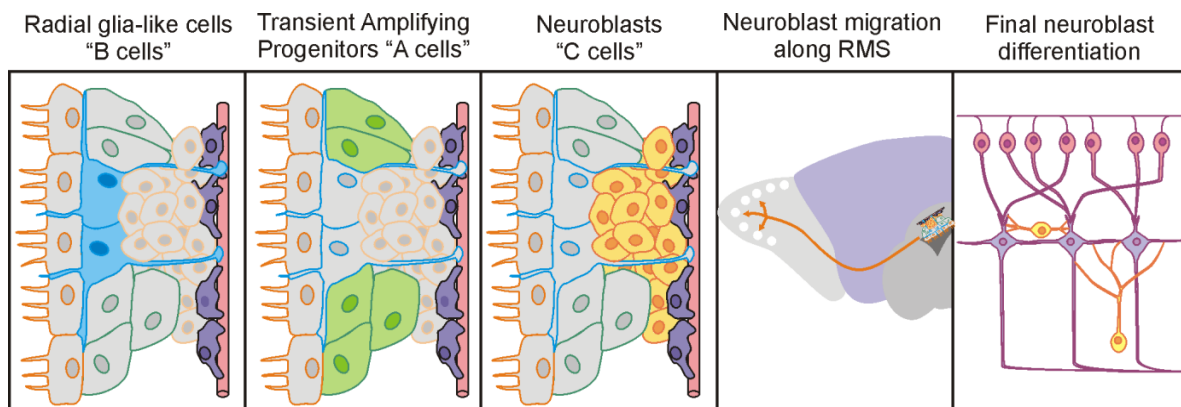
Figure 2: Process of subventricular neurogenesis (adapted from [11])

2.1.2   Subgranular zone of the dentate gyrus (SGZ)

The dentate gyrus of the hippocampus is the other main region of neurogenic processes in the adult mammalian brain. In contrast to neurogenesis in the SVZ, hippocampal neurogenesis has been directly linked to cognitive functions like learning and memory functions while impairments were found in patients suffering for example from epilepsy or depression (reviewed in [18]).

 Similar to the situation in the SVZ, also in the dentate gyrus special cells with astrocytic features function as neural stem cells. These neural stem cells resemble a radial glia like morphology with long processes leading through the granular cell layer and having contact to the vascular system and small processes horizontal to the subgranular zone [19]. According to the direct neighborhood of hippocampal neural stem cells and the vasculature even here a possible regulation of neurogenesis by soluble factors from the vascular system is presumed. Unlike ordinary astrocytes the hippocampal neural stem cells are characterized by simultaneously expression of GFAP and Nestin and are referred to as type-1 progenitors [10]. Type-1 cells give rise to neural intermediate progenitors known as type-2 progenitors [20] or D cells [21] which are characterized by transient expression of e.g. PSA-NCAM, NeuroD or DCX amongst others according to state of differentiation. Interestingly radial type-1 cells and

type-2 progenitors form clusters where a number of type-2 progenitors are bundled along the radial processes which led to the presumption that type-1 cells also somehow regulate the further development of the surrounding D cells. A lot of stimuli like adrenal steroids, exercise, environmental enrichment or inflammation and antidepressant drugs have influence on neurogenesis (see [9]). Soluble factors from the vasculature or electrophysiological activity from the surrounding granule cells may influence the radial glia cell which in turn might regulate D cell functions.
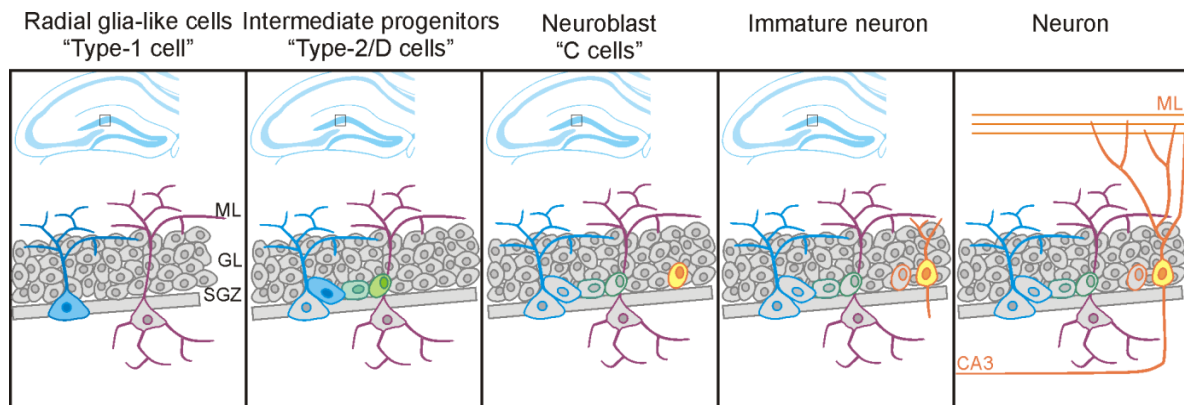
Figure 3: Process of hippocampal neurogenesis (adapted from [11])

Immature neurons differentiated from D cells migrate into the inner granule cell layer and become dentate granule cells. The immature neurons begin to integrate into neuronal circuitry by extending dendrites to the molecular layer and growing axons toward CA3. During neuron maturation new neurons are tonically activated as a result from nearby GABA release from neighboring interneurons, later getting synaptic GABAergic inputs finally followed by glutamatergic synaptic inputs. Newborn neurons are initially hyperexcitable and were observed to have an increased synaptic plasticity compared to adult granule cells (reviewed in [11]). Neurons generated during adult neurogenesis show basically similar electrophysiological properties while it is still unclear by which amount adult generated neurons contribute to general neuronal circuitry.

2.2 ABC Transporters

ATP binding cassette (ABC) transporters are proteins which are expressed ubiquitous throughout the three kingdoms of life: archaea, eubacteria and eukarya. Its members constitute one of the largest known superfamilies of genes. These transport proteins are expressed in cellular membranes and utilize chemical energy from ATP dephosphorylation for translocation of a wide range of metabolites and ions across cellular membranes. The

transport is always of unidirectional nature. Apart of some exceptions, mostly found in prokaryotes, these transporters carry out export functions. According to their functional properties and occurrence, these transporters are mostly divided into three different subclasses. The first group of import proteins is found only in prokaryotic cells where these transporters manage the incorporation of nutrients and ions [22, 23]. The second group, which is of interest in this study, is involved in export functions like secreting dietary agents or exposing cytotoxic metabolites across biological membranes (reviewed in [24], and even transporting signaling molecules [25]. The third group is more involved in nuclear processes like DNA repair and chromatin reorganization and also RNA trafficking and telomere maintenance [26-28].

Of this large group of genes, there are 49 members currently known to be expressed in humans, which are further classified into subgroups according to the phylogeny based on amino acid sequence similarities. These 7 subgroups are named ABCA to ABCG [29, 30]. ABC transporters show overlapping transport capacities for a wide range of peptides, hydrophobic compounds as well as drugs and drug conjugates. According to those features they also form an effective chemo-defense network against all sorts of xenobiotics [31]. Actually ABC transporters were first discovered in chemoresistant cancer cells [32, 33], and were since a scientific subject in cancer-related research. Based on that research, many ABC transporters were even found being expressed in stem cells due to the high resemblance in gene expression profiles of stem and cancer cells.

Apart from that ABC transporters are mostly found expressed at biological membranes which are defining different tissues or compartments against each other. A prominent example is the blood brain barrier which functions as a barrier between the brain parenchyma and the rest of the body which is impenetrable by undirected diffusion to secure the brain from xenobiotics and pathogens in general. Here, mostly all metabolite transport is regulated by ABC transport proteins. According to that, ABC transporter malfunctions have been recently found to be linked to proteopathies of the brain like Alzheimer's disease [34, 35]. Here, ABC transporters are responsible for the clearance of Aβ peptides across the blood brain barrier while lack of transport capacity for those peptides results in accumulation of Aβ and thereby in plaque formation. Recent studies underlined the overlapping transport capacities of ABC transporters of different subclasses for β-amyloid and most importantly evidenced the transporter ABCC1 to be most critical in the pathology of Alzheimer's disease by having the highest transport capacity for Aβ [36].

2.2.1   Structure and function of ABC transporters

The common structure of all ABC transport proteins is comprised of two TMDs (transmembrane domain) and two cytosolic ABCs (ATP binding cassettes) or NBDs (nucleotide binding domain). The TMDs contain multiple hydrophobic segments which span the membrane as α–helices multiple times. In general a TMD consist of 6-11 transmembrane-spanning α-helices. The TMDs are needed to form the transmembrane channel and are thought to contain the substrate binding sites. In contrast to the various TMD sequences the NBDs are highly conserved. They contain the Walker A and Walker B motifs for ATP binding as well as the so-called 'LSGGQ' motif which forms the diagnostic signature of all ABC transporters and is assumed to be responsible for triggering the interaction between different domains [37]. These NBDs function as molecular motors, transforming the chemical energy from ATP dephosphorylation into mechanical energy for initiating the conformational change of the ABC transport protein during substrate translocation. The most common form of ABC transporter is the full-transporter in which all single domains are aligned in the sequence TMD-NBD-TMD-NBD (full transporter). Other arrangements like NBD-TMD-NBD-TMD, TMD-NBD and NBD-TMD (half transporter) are possible as well.

The course of the ABC-transporter mediated efflux of substrates across the plasma membrane is still only insufficiently understood. Three different models of possible transport mechanism should be mentioned at the example of ABCB1 as one of the most studied members of the ABC transporter family [38].

The first and classical model assumes the two TMDs of ABCB1simply being arranged in a way forming a pore within the plasma membrane, letting the transporter actively expel metabolites from the cytoplasm into the extracellular compartment [39].

In contrast to that the "vacuum cleaner model" assumes that ABCB1is able to expel substrates into the extracellular space while the substrate is either within the intracellular medium or even when it is still located within the lipid bilayer of the plasma membrane. According to that assumption the transporter would function as a hydrophobic vacuum cleaner, floating across the plasma membrane and clean hydrophobic substrates from the membrane even before being able to enter the cytoplasm [38, 40].

Another model which was initially introduced by Higgins and Gottesman in 1992 and which is still the most favored explanation is the so-called flippase model [41]. The model assumes the substrate binding site of the TMDs to be located in the inner leaflet of the plasma

membrane. The substrate has to diffuse laterally in the direction of the binding site while being orientated hydrophobic side facing the inner leaflet of the membrane while the charged hydrophilic site is faced towards the cytoplasm. In the moment the substrate is bound to its binding site faced correctly, the TMDs flip the substrate to the outer membrane leaflet under consumption of the energy provided by ATP dephosphorylation at the NBDs. Once the substrate is flipped to the outer membrane leaflet, the substrate diffuses into the aquatic phase of the extracellular medium [41]. Actually genetic homology between ABCB1 and ABCB4, both proteins with flippase activity, supports this model of action [38].

Even with the flippase model given as the most likely possible transport mechanism, it is still unclear in which way the TMDs are capable to bind such a massively varying portfolio of substrates. Studies on transcriptional regulators revealed them to contain binding sites for specific drugs which are composed as hydrophobic pockets. While larger compounds completely fit into these pockets, smaller substrates are surrounded by water molecules, filling the gap between the substrate and the surrounding binding site. Hence it is postulated that even the multidrug binding sites of ABC transporters are characterized by an architecture similar to that of these transcriptional regulators. Due to the fact that large loop-domains are bound intra- and extracellular at the TMDs it is presumed that the actual substrate binding sites are sculpted by these domains [42]. By using antibodies to locate the substrate binding sites, the large intracytoplasmic domain separating TMD1 and TMD2, the linker domain between TMD2 and TMD3 and the last two transmembrane segments were identified as possible binding sites in ABCC1 [43]. This kind of adapting hydrophobic basket could sufficiently explain the variability of binding capacities for various compounds and the largely overlapping transport capacities of ABC transporters.

2.2.2   ABCB1

The group of human ABC transporters of the ABCB-family consists of 11 members. The full-transporters of this group contain 12 transmembrane domains. ABCB1 is with 1280 amino acids one of the largest proteins of this group (Figure 4).
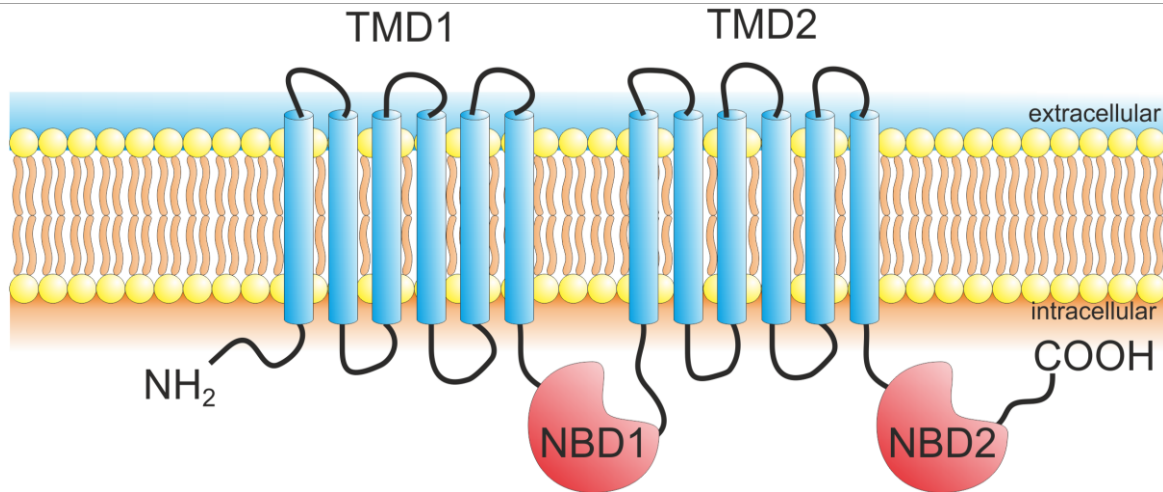
Figure 4: 2-dimensional representation of ABCB1 (adapted from [44]).

ABCB1, which was primarily called P-glycoprotein, was identified first in a hamster cell line, where it was found to maintain cell membrane permeability [32]. Further studies on multidrug resistant Chinese hamster ovary cell lines could link chemoresistance to the expression of ABCB1 [33]. Later it was found being expressed in several kinds of cancers. Since then substantial effort was undertaken to elucidate the physiological role of ABCB1. Hence, ABCB1 was found to be expressed in a variety of different tissues which include the small and large intestine, adrenal gland, kidney, placenta and the endothelial cells in the blood brain barrier and blood testis barrier where it seems to have export functions to maintain homeostasis of these body compartments (reviewed in [45]). ABCB1 was actually the first ABC transporter that was identified in the human blood brain barrier [46]. Here it was found to secure the brain from intoxication with passively diffusing lipophilic compounds [47]. To do so, it is located at the luminal side of the cerebral endothelial cells where it can expel the transported substrates directly into the blood stream. It was also recently linked to Alzheimer's disease when Aβ was identified as a substrate of ABCB1 [48-50]. Beside its role in Alzheimer's disease pathology it is also found expressed in stem cells of various tissues (reviewed in [51]). This is very comprehensible because cancer cells, in which it is involved in drug resistance, show a gene expression profile largely overlapping with that of stem cells [52]. Also ABCB1 was recently found expressed in neuronal stem cells *in vitro*. It was also observed that transient ABCB1 expression vanished when cell differentiation proceeded [53,

54]. Hence it was presumed that ABC transporters might play a crucial role in the maintenance of "stemcellness" in NSPCs [55].

2.2.3 ABCG2

The transporter ABCG2 was first isolated from multidrug resistant breast cancer cells which explains its synonymous designation BCRP1 (breast cancer related protein 1) [56]. In contrast to ABCB1, ABCG2 is essentially a so-called half transporter due to its composition out of only one TMD comprised of 6 transmembrane α-helices and one NBD (Figure 5). It is therefore assumed to build homodimers for achieving full functionality as an ABC transporter [57, 58]. ABCG2 is also highly expressed in tissues of toxicological relevance, comparable with that of ABCB1 or even ABCC1 (reviewed in [59]).
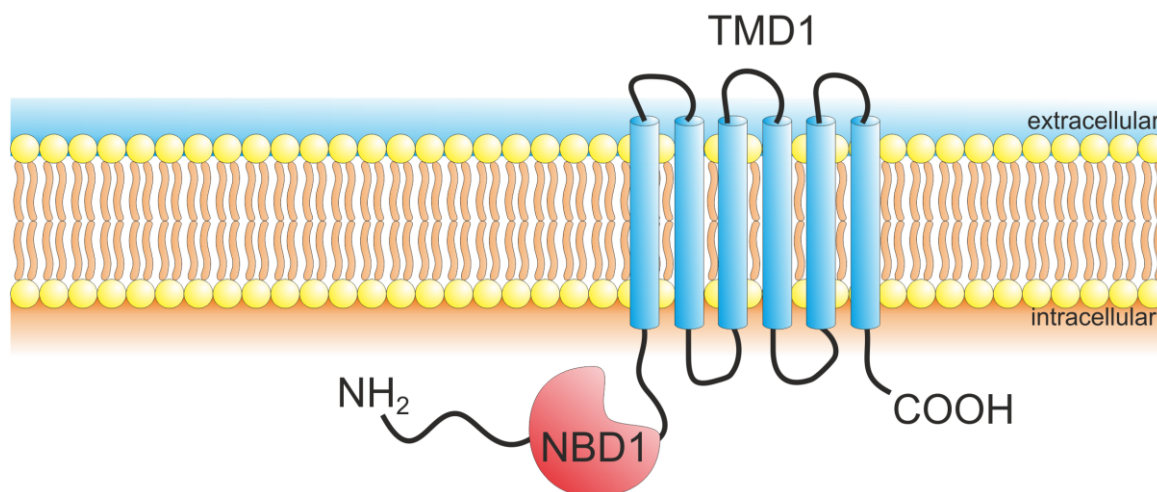
Figure 5: 2-dimensional representation of ABCG2 (adapted from [44]).

A structural precursor of heme (pheophorbide) was found to be a substrate of ABCG2 due to decreased intracellular accumulation of heme precursor proteins after the beginning of ABCG2 expression. Therefore it was suggested that the ability of stem cells to survive hypoxic conditions could be linked to abundant ABCG2 expression which prevents the accumulation of toxic heme, naturally occurring under such conditions [60]. Hence ABCG2 is expressed in various stem cell lines [60] and is abundantly expressed in various kinds of human malignancies like digestive tumors, genito-urinary tumors, female reproductive tumors, lung tumors and others [61]. Comparable to ABCB1 also ABCG2 was found transiently expressed in NSPCs prior to cell differentiation [62]. Hence even also ABCG2 was suggested to be responsible for maintenance of stem cell functions [55].

2.2.4   ABCC1

In contrast to other full transporters, 5 of the C-family ABC transporters (ABCC1, ABCC2, ABCC3, ABCC6 and ABCC10) show an atypical structure. These proteins are comprised of rather 5 than 4 domains. Here another TMD (TMD0) containing 5 transmembrane α-helices is added at the NH_2-terminal (Figure 6). Another main characteristic of all transporters of the C-family is the relatively low sequence homology between the two NBDs. Here NBD1 lacks 13 amino acids between the Walker A and Walker B motifs which are comprised in NBD2 as in mostly all NBDs of every other ABC subclass' members. Further studies also evidenced functional differences between the two nucleotide binding domains (reviewed in [63]).
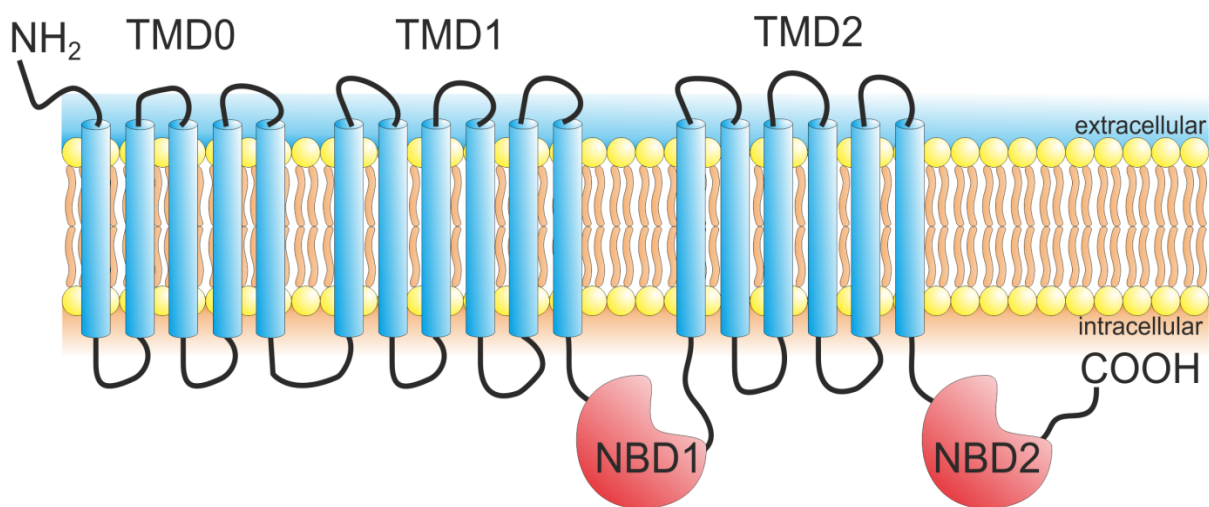
Figure 6: 2-dimensional representation of ABCC1 (adapted from [44]).

Even ABCC1 was initially identified in a lung tumor [64] but was as well found to be robustly expressed in other cancer cells like for example in a group of hematological and solid tumors (reviewed in [59]). Analog to other ABC transporters also ABCC1 is found in various tissue types like lung, small intestine, testis, kidney, muscle, heart, peripheral blood mononuclear cells, the choroid plexus and the placenta. ABCC1 shows a wide range of substrate specificity. Typical substrates of ABCC1 are free and conjugated bilirubin, oxidized glutathione and a number of xenobiotic substrates including many chemotherapeutic agents (reviewed in [65]). ABCC1 was also found to be expressed in the choroid plexus [66] where it was recently found to be the major ABC transporter involved in Aβ efflux from the brain [36].

2.2.5   ABC transporters in stem cells

While ABC transporters were found highly expressed in the diverse cancer cells, it was not surprisingly to find them also expressed in stem cells of various tissues. ABCB1 was the first

of the ABC transporter family which was observed in CD34$^+$ human hematopoietic stem cells as a result of their increased efflux capacity for the dye Rhodamine123 which is known to be a substrate of ABCB1 [67]. Using Rhodamine123 and the dye Hoechst3342, which is another ABC-transporter substrate, for analyzes of bone marrow cells in fluorescence activated cell sorters, a small subset of cells positive for phenotypic markers of hematopoietic stem cells was revealed [68]. After administration of ABC transporter inhibitors, this cell population was lost [68]. Staining for incorporation of Hoechst3342 was found to be useful for isolating cell populations which are highly enriched with stem cells [69]. According to the distinct staining profile of these cells with their high efflux capacity for Hoechst 3342, those were called side population (SP) and according cell populations were since found also in other tissues [70]. Other cell populations in which the SP cells were observed are mesenchymal, heart, liver and pancreatic stem cells (reviewed in [55]). Beside the initial ABC transporters ABCB1 and ABCG2 also ABCA3 was found expressed in the primitive stem cells of different tissues [71]. While these transporters are found robustly expressed in stem cells again and again and were therefore suspected to possibly have regulating functions on stem cell fate (reviewed in [55]), in a distinct SP of hepatocellular carcinoma moreover other transporters like ABCB2, ABCC7 and ABCA5 were found to be up regulated several fold compared to none SP cells [72]. These findings might suggest overlapping functions and co-regulation between ABC transporters distinct for specific cell populations.

Accordingly it was found that for example ABCG2 expression was highly regulated with the highest expression found in primitive cells followed by subsequent down regulation following commitment to differentiation. Accordingly forced expression of ABCG2 hindered in less hematopoietic development and resulted in less progeny in the bone marrow and peripheral blood after transplantation experiments of ABCG2 overexpressing progenitor cells [73]. Hence it was presumed that ABCG2 for instance might be capable of expelling substrates needed for differentiation or that ABCG2 is involved in stem cell interactions with their microenvironment by mediating extracellular signals. Therefore comparable experiments with ABCB1 overexpressing cells resulted in prolonged survival rates in vitro and increased repopulation capacity in vivo [74]. Together these findings might indicate specific functions for ABCB1 and ABCG2 in different types of stem cells, proliferating and quiescent ones.

Beside the expression of ABCB1 and ABCG2 widely known from other stem cell populations also ABCA2 was found expressed in early neural stem cells when derived from hematopoietic stem cells in vitro. Even though, the expression of ABCA2 seems to be region-dependent and

specific for oligodendrocytic progenitors, a subset of cortical GABAergic interneurons and pyramidal glutamatergic neurons [75]. Recent *in vitro* studies showed robust expression of ABCB1 and ABCG2 in neurosphere forming NSPCs. It was also shown that the high abundance of these transporters decreases at the stage of lineage commitment together with the down regulation of Nestin and up regulation of GFAP. Therefore it was proposed that both ABCB1 and ABCG2 may be seen as markers of NSPCs and may have a functional role in upholding the stem cell status [53, 62].
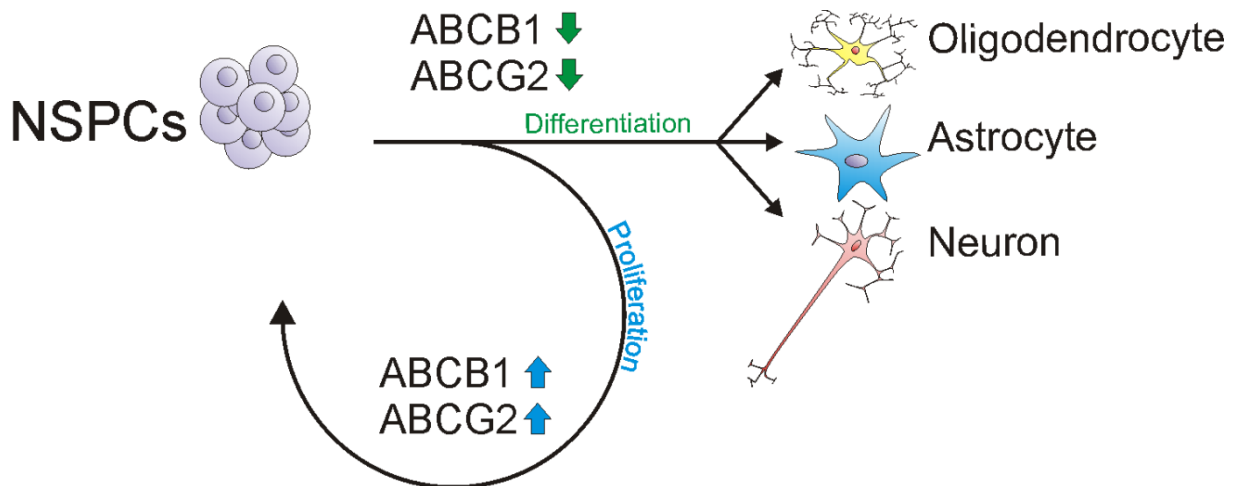
Figure 7: Presumed effects of ABC transporter function on NSPCs (adapted from [55])

2.3 Alzheimer's disease (AD)

Since Alzheimer's disease was described first by Alois Alzheimer in 1906 when he found characteristically intra- and extracellular protein deposits in the brain of one of his former patients suffering from dementia, Alzheimer's disease soon became the most frequently cited cause of dementing cerebral cortex pathologies [76].

The pathology of AD is a slow progress starting most often years before first clinical symptoms are observable. The pathology can be divided into stages with increasing severity of clinical symptoms. Initially patients at least start noticing disturbances in their short-term memory accompanied by unexplainable mood-shifts, impairments of language and first mild effects of spatial disorientation. The intermediate state, when dementia has become certified, organizing and performing all-day tasks like for example shopping, cooking or even dressing become increasingly difficult while patients also get more emotionally instable or even undergo personality changes. They become unable to differentiate between past and presence

and to recognize even near relatives. During the last stage, patients become bedridden and completely dependent from long-term-nursing. In most cases death results from infections as secondary and final pathologies (pneumonia, influenza, nephritis, etc.)

Beside the intracellular neurofibrillary tangles comprised of hyperphosphorylated Tau protein, the most prominent hallmark of AD is the occurrence of extracellular protein deposits or neuritic plaques which are composed of aggregated Aβ peptides. These Aβ peptides are generated as cleavage products of the amyloid precursor protein (APP) after cleavage by three different secretases. Their interplay defines the nature of APP cleavage resulting in either the amyloidogenic or non-amyloidogenic pathway [77, 78]. While the role of APP itself is still under discussion and assumed to be related to neuronal differentiation, survival and neurite outgrowth [79, 80], along with its soluble cleavage product sAPP [79], the short Aβ peptides resulting from the amyloidogenic cleavage pathway have been shown to be clearly of pathogenic nature.
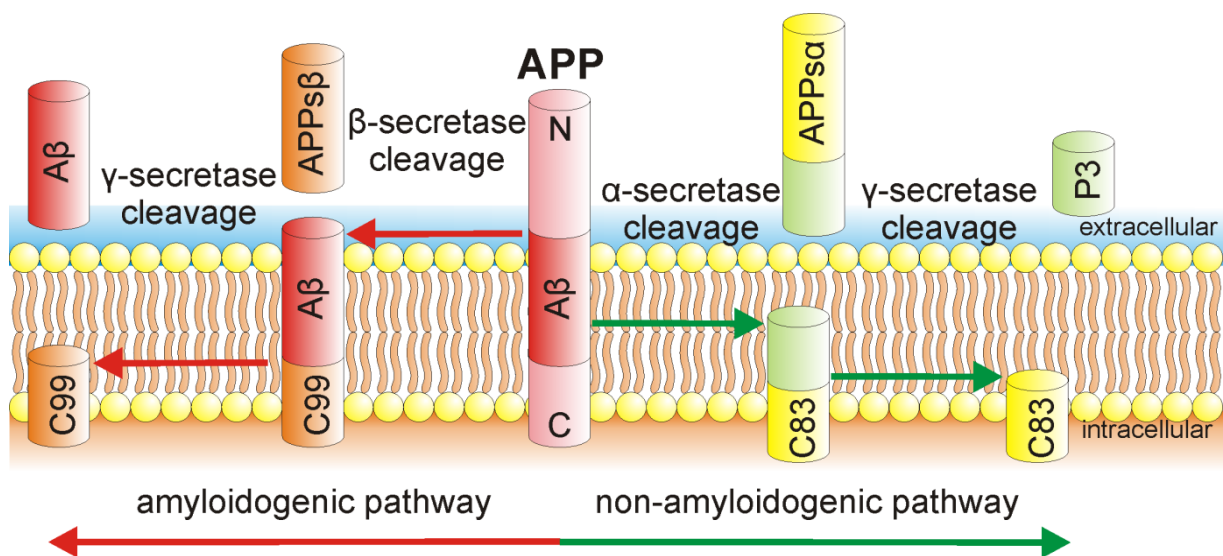
Figure 8: APP cleavage adapted from [81]

The three secretase families involved in APP cleavage are the α-, β- and γ-secretase group each cleaving the APP at distinct positions. The activity of these secretases dictates the fate of APP cleavage. The initial cleavage of APP by the β-secretase (beta-side APP-cleaving enzyme-1, BACE-1) followed by γ-secretase, which is a multi-protein complex composed of Presenelins 1 and 2 (PS1, PS2), Nicastrin, Pen2 and Aph [82], results in the generation of toxic Aβ peptides. If in contrast APP is first cleaved by one of the α-secretases (a disintegrin and metalloproteinase domain-containing protein –ADAM- 10 9, and 17), further cleavage of γ-secretase cannot lead to generation of Aβ.

But as long as the equilibrium of APP cleavage is shifted towards the amyloidogenic pathway, the toxic Aβ peptides are generated. As a result of a certain inaccuracy of secretase cleavage Aβ peptides have lengths between 38, 40 and 42 amino acids. Thereby the most prominent Aβ species is the $A\beta_{42}$ which also seems to be the most toxic variant and is most prone to fibril formations since it is the major Aβ species found in plaques [83]. Today it is relatively clear that not the beta-amyloid plaques are the main cause of neurodegeneration but more likely the neurodegenerative effect of soluble Aβ contributes to neurodegeneration much earlier than plaque formation has even begun. Accordingly studies revealed that neurodegeneration, or indirectly cognitive decline, much more correlates to concentration of soluble Aβ than plaque load [84, 85]. Much more than its shorter siblings $A\beta_{38}$, and $A\beta_{40}$, $A\beta_{42}$ has a very high tendency to form small soluble oligomers. Hence, $A\beta_{42}$ spontaneously assembles to trimeric or tetrameric complexes very early [86] followed by larger oligomers of pentameric or hexameric conformation which themselves are able to aggregate forming oligomers of higher order [87]. During the process of Aβ oligomerization fibrils are finally generated and begin to deposit in form of neuritic plaques.

Still only less than 1% of all AD cases [88] could be linked to genetic variants and contribute to the so called familial form of AD [83]. In contrast the vast majority of AD patients seem to suffer from the so-called sporadic form of AD. Until now only three genes are known to bear mutated variants contributing to AD pathology. These three are the two presenelin genes 1 and 2 which code for essential proteins of the γ–secretase complex and the APP gene itself which bears several mutations which are more prone to β-secretase cleavage. The mutations lead to enhanced amyloidogenic APP processing and thereby to AD pathology. While pathology of the sporadic form of AD does not develop before advanced age, forms of familial AD tend to develop before the age of 65 and in some individuals even at an age of 30 years.

Beside the enhanced Aβ peptide generation as a result of increased amyloidogenic APP cleavage, also malfunctions in transport processes across the blood-brain-barrier contribute to AD pathology. It is already known that Aβ is a substrate for certain ABC transporters like ABCB1 or ABCC1 [36, 49]. A recent study found impairments in ABC transport activity significantly severs AD pathology as a result of insufficient Aβ clearance in ABC deficient mouse models of Alzheimer's disease [36]. Due to the fact that lot of drugs chronically subscribed in elderly significantly impair ABC transporter function, these drugs could possibly also increase the risk of developing AD pathology.
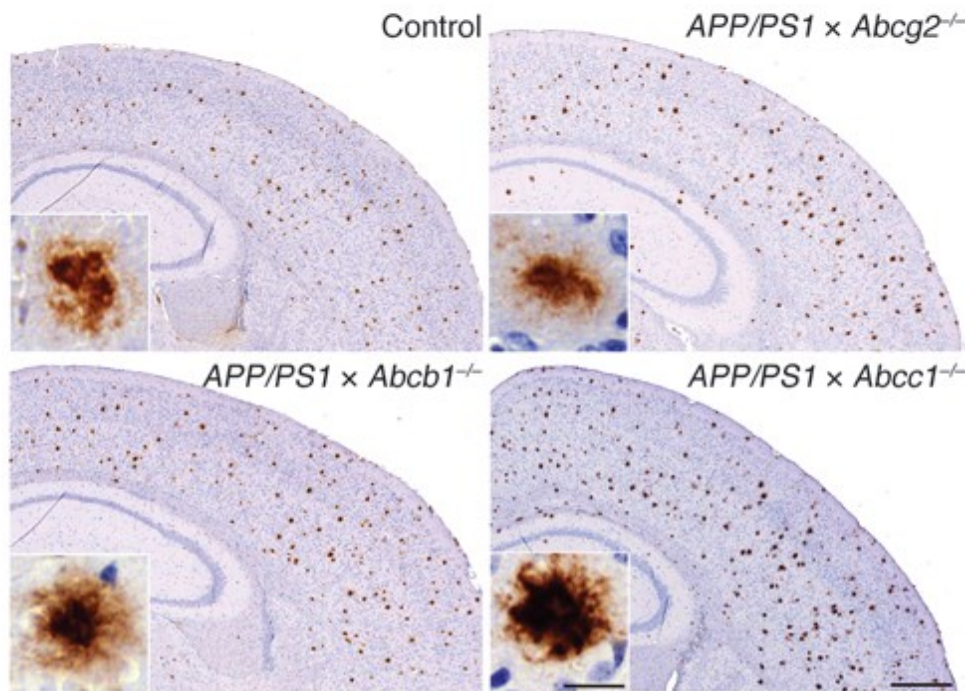
Figure 9: Cortical tissue samples from ABC transporter deficient AD mice reveal the significance of ABC transporter-mediated Aβ-clearance out of the brain parenchyma. ABCB1$^{0/0}$ (lower left) and ABCC1$^{0/0}$ (lower right) transgenic mice show significantly increased plaque load compared to transgenic control mice (upper left) from [36]

2.3.1 Neurogenesis in Alzheimer's disease

During the pathogenesis of AD, the hippocampus as one of the two major sites of neurogenesis is affected very early. Even though the effect of AD pathogenesis on neurogenic functions remains very controversial due to the fact that, somehow depending on the techniques used for the respective study, there were either impairment, enhancement or even no changes in neurogenesis observed at all. Postmortem studies on human brain samples of AD patients utilizing Western blot analyzes, revealed increased amounts of neurogenic markers [89]. For example proteins like TUC-4, PSA-NCAM, DCX and NeuroD, which are all proteins expressed at different stages of neuronal differentiation whose expression levels were observed to be increased in comparison to age-matched control samples in histological analyzes [90, 91]. In contrast, another study found no significant alteration in the number of DCX expressing neuroblasts. There was also found no evidence for altered cell proliferation when quantifying for the expression of the proliferation marker Ki67, at least in the neurogenic niche of the dentate gyrus. At least Ki67 was found to be expressed in a number of cells located in the CA1 and CA3 regions of the hippocampus. Here cell proliferation was therefore assumed to be related to glia cell proliferation which should be resulted from the gliosis occurring during AD pathology [92]. Studies focusing on the early stem cell

compartment also revealed intriguing results. While the level of Musashi1 expression, a posttranscriptional regulator highly expressed in proliferating stem and progenitor cells, was heavily decreased in AD brains, the number of GFAP and Nestin positive cells was significantly increased. These results imply severe impairments in NSC functionality, a hypothesis which is also supported by findings of primary SVZ-NSPCs isolated from AD brains that showed impaired viability and earlier senescence exhibition [93]. Studies of human AD infected brains also showed that SVZ and SGZ seem to be differentially affected by AD pathology due to findings of decreased numbers of SVZ-progenitors [94] and increased numbers of SGZ progenitors [89].

Since rodents do not suffer from pathologies like Alzheimer's disease, research depends on animal models which can only model distinct aspects of AD. These aspects are β–amyloid deposition or Tau pathology. Here human genes have to be introduced to generate transgenic animal models. Accordingly a lot of mouse models expressing different human genes under the control of several, mostly neuron-specific promoters exist today which significantly impedes comparative studies on neurogenesis in AD.

	Authors	Subject	markers
Increased neurogenesis	[89]	Human postmortem samples	TUC4, DCX
	[95]	PDGF-APP$_{(swed, indian)}$ mice	DCX, NeuroD, BrdU
	[96]	PDAPP mutant mice (SGZ)	DCX, BrdU
	[97]	APP23 mutant mice	DCX, BrdU, GFAP NeuN
No changes	[92]	Human postmortem samples	Ki67, DCX, GFAP
	[98]	PS1-mutant mice	TUC4, PSA-NCAM
Impaired neurogenesis	[99]	APP/PS1 mutant mice	BrdU, NeuN
	[96]	PDAPP mutant mice (SVZ)	DCX
	[100]	APP/PS1 mutant mice	MCM2, DCX
	[97]	Nestin-GFP x APP/PS1 mutant mice	Nestin-GFP
	[101]	APP mutant mice and NSPC experiments *in vitro*	BrdU, E-NCAM, GFAP

Table 1: AD pathology's effects on adult neurogenesis are highly discussed

Increased neurogenic activity was observed in a double-mutant AD mouse model with human APP (Swedish and Indian mutation) under the control of platelet derived growth factor. There it was found that BrdU incorporation and DCX positive cells were both increased in SVZ and SGZ though these observations were made at an age prior to significant plaque deposition [95]. Another AD model (APP23 mutant mice) did not show alterations in neurogenesis prior

to plaque deposition while at an age of 25 months neurogenesis was significantly increased compared to control mice as revealed by histological analyzes after staining for neurogenic markers [97]. No alteration of adult neurogenesis was therefore found in an AD mouse model based on overexpression of PS1 which is known to be somehow involved in embryonic development [98]. Actually much more studies implied a negative influence of AD-pathology on neurogenesis. By utilizing immunohistological methods several studies on different single human APP transgenic [96] or combined PS1 overexpressing and human mutant APP mouse models found decreased numbers of neuronal progenitors at different stages of differentiation [97, 99, 100].

2.4 Overall motivation and aims

ABC transporters, as part of one of the oldest and most ubiquitously expressed protein families throughout life, have recently been known for their relevance in the pathology of neurodegenerative disorders like especially Alzheimer's disease. They were also often discussed regarding their relevance in stem cell functions and in particular in neuronal stem cells. It was therefore assumed that expression of ABCB1 and ABCG2 in particular might be necessary for the maintenance of the NSPC's stem cell character.

This study was performed in order to contribute more understanding to the basic functional relevance of ABC transporters in neurogenic functions like adult neurogenesis in general and especially with relevance to brain pathology in form of cortical injury and neurodegenerative diseases like Alzheimer's disease. With regard to ABC transporter involvement in AD as also in stem cell functions, the study sought to answer the question whether functional impairments of ABC transporters also contribute to AD pathology in the sense of impairments of neurogenic functions.

The following questions were to answer:

1. Does ABC transporter deficiency alter neurogenic functions in general?
2. Are possible alterations in stem cell functions of cell intrinsic nature?
3. Does ABC deficiency lead to further alterations in brain ontogenesis and do such alterations result in a distinct behavioral phenotype?
4. How do pathogenic effects like injury or neurodegenerative disorders affect neurogenic functions?

To analyze the functional relevance of ABC transporters for neurogenic functions *in vivo*, ABC deficient mouse strains were comparatively analyzed by quantification of neuronal progenitor cells and cell proliferation capacity on cryogenic brain slices. In order to assess the question whether the ABC deficiency-induced alterations in NSPC functions were of cell intrinsic nature, NSPCs were isolated from the ABC deficient mouse strains and analyzed *in vitro* for proliferation and neuronal differentiation capacity. To find possible ABC deficiency-dependent deficits during brain ontogenesis, the different mouse strain's brains were comparatively analyzed for cortical morphology. Behavioral assessment was performed to find distinct behavioral phenotypes as possible results of presumed impairments during ontogenesis. To find out whether pathogenic events contribute to adult neurogenesis in

dependency of ABC transporter equipment, a CCI model was used to model cortical injury and sub-sequentially quantifying neurogenesis. Additionally a transgenic AD mouse model was crossbred with ABC-deficient mouse strains to analyze neurogenesis during Aβ deposition in dependency of ABC transporter function. The function of Aβ on proliferating and differentiating NSPCs was also determined *in vitro*.

3   Experimental procedures

3.1   Chemicals

Agarose	Biozym Diagnostik GmbH
Bond-MaxTM Bond Polymer Refine Detection-Kit	Leica
BrdU	Sigma-Aldrich
$CaCl_2*(2H_2O)$	Carl Roth
Chicken serum	Vector Labs
Chloroform	Carl Roth
Cresyl violet	Leica
Culture flask T-25cm²	Greiner-Bio One
DAPI	Invitrogen
DePex	Serva Electrophoresis
D-Glucose	Sigma
Dimethylsulfoxide (DMSO)	Sigma-Aldrich
EGF	PeproTech
Ethanol 96%	Carl Roth
Ethidium bomide	Invitrogen
FGF	PeproTech
Glacial acetic acid	Carl Roth
sterile centrifuge tubes 15mL/50mL	Greiner-Bio One
HCl	Carl Roth
Heparin	Sigma-Aldrich
Hexafluoroispropanol (HFIP)	Sigma-Aldrich
Igepal A630	Fluka Biochemika
KCl	Carl Roth
Ketamin (Ketanest)	Pfizer
Matrigel	BD Bioscience
$MgCl_2*(6H_2O)$	Carl Roth
microcentrifuge tubes 1.5mL	Eppendorf
microcentrifuge tubes 2mL	Eppendorf
NaCl	Carl Roth GmbH
NaH_3	Carl Roth
$NaHCO_3$	Carl Roth
NeuroCult Basal media	StemCell
NeuroCult differentiation supplements	StemCell Inc.

NeuroCult proliferation supplements	StemCell Inc.
OCT-compound	Leica
Paraffin	Leica/Menarini
PBS (10x)	Sigma-Aldrich
Pen/Strep 10x	PAA
petri dish 100mm	Greiner-Bio One
petri dish 50mm	Greiner-Bio One
PFA (4% in PBS)	Formafix Switzerland AG
Proteinase K	Carl Roth
RNAlater	Applied Biosystems
Succrose	Carl Roth
TaqPCR kit	Qiagen
Tris-HCl	Carl Roth
Triton X-100	Carl roth
TRIzol	Invitrogen
Trypan Blue	Carl Roth
Trypsin/EDTA	Invitrogen Corp.
Tween 20	Merck
Xylazine (Rompun)	Bayer
Xylene	Carl Roth

3.2   Equipment

Bond-Max staining system	Leica
Centrifuge	Hermle Z 400 K
CO2 incubator	Binder
Cryostat CM350S	Leica
Elevated Plus-maze	TSE Systems
Gel documentation system	DeconScience Tec
Light/Dark-box	TSE Systems
LSM 700	Zeiss
Microscope Stemi	Zeiss
Mirax Desk	Zeiss
Rotorgene Q	Qiagen
Stereotactic frame	Stoelting
Thermocycler Tprofessional Basic	Biometra
Videotracking system TSE VideoMot2	TSE Systems
Y-maze	TSE Systems

3.3   Software

AxioVision	Zeiss
MS Office	Microsoft
Prism 5	GraphPad Software

3.4 Animal procedures

Mice were bred in the animal care facility of the Neurodegeneration Research Lab (NRL) and were housed under a 12h/12h light/dark cycle at a mean temperature of 22°C. All animals had access to food (Sniff, Germany) and water *ad libitum*.

All protocols involving the use of animals were approved by the local authorities (LALLF M-V TSD 7221.3-1.1-035/10 and LALLF M-V TSD 7221.3-1.1-024/11).

3.4.1 ABC knockout mice

FVB.129P2-Abcg2^{tm1Ahs} N7 (ABCG2$^{0/0}$), FVB.129P2-Abcb1a^{tm1Bor}Abcb1b^{tm1Bor} N12 (ABCB1$^{0/0}$), and FVB.129P2-Abcc1^{atm1Bor} N12 (ABCC1$^{0/0}$) mice were purchased from Taconic Farms (Denmark) [102-104] including a breeding permission. Accordingly animals were bred as required in the NRL's animal care facility.

3.4.2 APP/PS1-, ABC knockout- and combined mouse models

A combination of the human transgenes Thy-1-APPKM670/671 and Thy1-PS1L166P, from here on referred to as APP/PS1, was introduced into C57BL/6J mice resulting in a mouse model of Alzheimer's disease [105] which was kindly provided by M. Herzig, R. Radde and M. Jucker (University of Tübingen, Germany).

APP/PS1 transgenic mice had to be crossbred in a way to only generate heterozygous APP/PS1$^{+/0}$ mice. Due to the fact that homozygous mice showed decreased viability as a result of excessive transgene expression and because of zygosity is not assessable by means of PCR technique, APP/PS1 breeding was always performed by mating ♂APP/PS1$^{+/0}$ with ♀APP/PS1$^{0/0}$.

Due to the different background strains of APP/PS1 (C57BL/6J) and ABCko strains (FVB), the APP/PS1 transgene had to be introduced by crossbreeding the APP/PS1-C57BL/6J with the respective ABCko-FVB mice for at least 9 generations to ensure maximum background homogeneity. To do so, male APP/PS1$^{+/0}$ mice were bred to female FVB mice. The resulting male APP/PS1$^{+/0}$ mixed C57BL/6J/FVB offspring were each repeatedly bred to female homogeneous FVB mice for at least another 8 generations. Thereby the APP/PS1 transgene could be transferred from the C57BL/6J into the FVB background. Further crossbreeding with the respective ABC knockout strains only needed two generations to introduce the FVB-APP/PS1 transgene into the FVB-ABC knockout strains (F$_0$ ♂APP/PS1$^{+/0}$ x F$_0$ ♀ABC$^{0/0}$ →

F_1 ♂APP/PS1$^{+/0}$-ABC$^{+/0}$ x F_1 ♀APP/PS1$^{0/0}$-ABC$^{+/0}$ → F_2 APP/PS1$^{+/0}$-ABC$^{0/0}$). The individual mice's genotypes were analyzed by means of PCR techniques as described in 3.9.1.2.

3.4.3   BrdU application

5'-bromo-deoxyurodine (BrdU) is a bromine-labeled thymidine-analog. If present, BrdU is incorporated instead of thymidine into newly synthesized DNA during the cell cycle's S-phase. The detection of DNA-incorporated BrdU, by means of immunological techniques, allows the detection of newly synthesized DNA and thereby proliferative activity [106]. For the histological detection of proliferative activity in the neurogenic zone of the hippocampus, BrdU was applied to the animals for 7 days prior to sacrifice.

To all animals, used for histological experiments, BrdU was administered daily in form of an intraperitoneal injection of 50μg/g body weight (Table 2). BrdU was therefore diluted in sterile saline (NaCl 0.9%, Bayer) to a concentration 10mg/mL.

	FVB	ABCB1$^{0/0}$	ABCG2$^{0/0}$	ABCC1$^{0/0}$
Controls	3♀ / 3♂	3♀ / 3♂	3♀ / 3♂	3♀ / 3♂
CCI	3♀ / 3♂	3♀ / 3♂	3♀ / 3♂	3♀ / 3♂

Table 2: Animals which have received BrdU administrations

3.4.4   Controlled cortical impact

Resident NSPCs of the neurogenic brain regions are known to be able to compensate loss of neurons during neurodegenerative processes in limited amounts. Traumatic brain injury for example is a neurogenic effect, able to activate proliferation and differentiation of NSPCs [107]. The controlled cortical impact (CCI) is a conventional model of traumatic brain injury commonly used for studies of adult neurogenesis [107, 108].

For each group (FVB controls, ABCB1$^{0/0}$, ABCG2$^{0/0}$, ABCC1$^{0/0}$), 6 mice (3 males, 3 females) were used for controlled cortical impact-surgery at the age of 90 days (Table 2).

The animals were anesthetized using a ketamine (Ketanest, Pfizer Pharma)/xylazin (Rompun, Bayer) mixture. Both injectable solutions were diluted in sterile saline (NaCl 0.9%, Bayer) to a final concentration of 1.9mg/mL ketamin and 0.5mg/mL xylazine. The mixture was administered intraperitoneal with a volume of 20μg/g bodyweight. Within 5 minutes the animals were anesthetized and ready for surgery. Anesthesia lasted for ca. 20 minutes. After further 30 minutes animals were fully awakened.

The animals were put into a stereotactic frame (Motorized standard lab stereotaxic, Stoelting Co). After sanitizing the scalp with ethanol (70%) a midline incision exposed the skull. A drill (ø 2mm, Dremel) was used to open the skull at position bregma -2.0mm anterior and bregma -2.0mm lateral. A steel cannula of 1.2mm in diameter (B. Braun) with a manually deformed tip was used as impact device for the CCI. The impact device was driven 2.2mm into the cortex right above the hippocampus. The wound was closed using suture clips after surgery. The animals were positioned under an infrared lamp until fully awakened to prevent hypothermia.

3.5 Biopsy

3.5.1 Sample preparation for histological and molecular biological experiments

Materials needed for sample preparation:

- Dissecting set
- Micro-tubes
- Paraformaldehyde (PFA 4% in PBS)
- Liquid nitrogen

Animals were killed by cervical dislocation. Animals were transcardially perfused with 20mL PBS (10x: 0.137 mM NaCl, 2.7 mM KCl, 8.0mM Na_2HPO_4, in dH_2O, pH 7.4, Sigma-Aldrich). If whole brains were used for histological analyzes, animals were perfused additionally with 20mL PFA (paraformaldehyde 4% in PBS, Formafix Switzerland AG). Scalp was cut using small scissors and the skull was opened by use of forceps at the commissure between the parietal and interparietal bone fragments. The interparietal bone fragment was extracted first, before elevating both parietal and frontal bone fragments with great care to expose the brain. A small and flat spatula is used to lift the brain out of the opened skull. The brains were cut sagittal to use each hemisphere for further processing for either molecular biological experiments (snap frozen in liquid nitrogen) or histological experiments (put into paraformaldehyde for tissue fixation).

3.5.2 Sample preparation for cell culturing experiments

Material needed for tissue preparation:

- Dissecting set (sterile)
- Sterile centrifuge tubes 50mL / 15 mL (sterile)
- Culture dishes 50mm / 100 mm (sterile)
- ice box

- Microscope (Stemi D4, Zeiss)
- Ethanol (70%) for disinfection
- aCSF media pH: 7.4 (sterile and ice cold)

Components	MW	C [mM]
NaCl	58.44	124
KCl	74.56	5
$MgCl_2*(6H_20)$	203.3	3.2
$CaCl_2*(2H_2O)$	147.02	0.1
NaHCO3	84.01	26
D-glucose	180.16	100
Pen/Strep		

Table 3: Artificial CSF-media

3.6 Histology

3.6.1 Sample preparation

For paraffin embedded tissue.

Tissue samples were post-fixed in PFA for 14 days. After fixation, tissue samples were dehydrated before embedding in paraffin (Table 2).

Step	Reagent	Duration [min]
1	PFA 4%	5
2	Ethanol 70%	180
3	Ethanol 80%	60
4	Ethanol 80%	120
5	Ethanol 90%	60
6	Ethanol 90%	60
7	Ethanol abs.	120
8	Ethanol abs.	120
9	Xylene	120
10	Xylene	120
11	Paraffin 60°C	120
12	Paraffin 60°C	120

Table 4: Tissue dehydration and paraffin embedding

Embedding tissue for cryo-slices

Tissue samples were post-fixed for 24 hours in PFA. After fixation, tissue was immersed sequentially in 15% and 25% sucrose (in PBS) at 4°C for 2 hours each. Brain hemispheres were put on cork plates and completely covered with OCT-compound (LEICA, Germany) and snap-frozen with liquid nitrogen. Samples were stored at -20°C.

3.6.2 Immunohistochemistry on paraffin slices

Coronal sections (5µm thick) were cut from paraffin embedded brains and mounted on glass slides. Sections had to be deparaffinized prior to immunohistochemical protocols (Table 5).

Step	Reagent	Duration [min]
1	Xylene	10
2	Xylene	10
3	Ethanol abs.	2
4	Ethanol 95%	1
5	Ethanol 70%	1
6	Ethanol 50%	1
7	Ethanol 30%	1
8	NaCl 0.85%	2
9	PBS	2

Table 5: Deparaffinization protocol

Immunostaining was initiated after blocking endogenous peroxidase (5min). Primary antibodies against NeuN were incubated routinely for 30min at room temperature with a dilution of 1:200. Primary antibodies were detected with the Bond-Max^{TM} Bond Polymer Refine Detection-Kit and standard protocol DABR30 (Leica, Germany). The stained slides were dried and covered with coverslips using Pertex mounting media (Leica, Germany).

3.6.3 Immunofluorescence on cryo section

Cryo sections (16µm thick) were cut using a cryostat (CM 350S, Leica). Cryo-slices were stained free-floating. Prior to incubation with antibodies, DNA had to be denatured by incubating slices for 30min in 1.5M HCl at 37°C. The DNA denaturation step was followed by three subsequent washing steps, incubating the slices for 10min each in PBS. To block unspecific protein bindings, the slices were incubated for 1h in blocking buffer containing 5% chicken serum (vector labs) and Triton X-100 (0.05%), for blocking unspecific antigen binding and membrane permeabilization, diluted in PBS. Slices were incubated overnight at 4°C with the appropriate primary antibody combinations (Table 6) diluted in blocking buffer. Primary antibody incubation was followed by three subsequent washing steps in PBS for

10min each. The slices were incubated with the appropriate secondary antibodies (Table 6), diluted in PBS, for 1h in the dark. Incubation with secondary antibodies was followed again by 3 subsequent washing steps with PBS for 10min each in the dark. To stain nuclear DNA, slices were rinsed for 10sec in DAPI solution (1µg DAPI/1mL PBS) before the final washing step in PBS. The slices were mounted on glass slides and dried for 30min in the dark. After drying the slices were embedded in DePex (Serva) and covered with glass coverslips.

Combination	Primary antibody	Secondary antibody
Sox2	Anti-BrdU	Anti-mouse-Cy2
	Anti-Sox2	Anti-goat-Cy3
DCX	Anti-Brdu	Anti-mouse-Cy2
	Anti-DCX	Anti-goat-Cy3
Calretinin	Anti-Brdu	Anti-mouse-Cy2
	Anti-Calretinin	Anti-goat-Cy3

Table 6: Antibody combinations

3.6.4 Nissl staining on cryo slices

The Nissl stain is a classical histological staining technique which is used to stain nucleotide rich parts of the cell (nucleus, endoplasmic reticulum). The Nissl bodies, named after the german neurologist Franz Nissl (1860-1919), are rough endoplasmic reticulum with lots of free ribosomes. A common Nissl stain is obtained by the thiazine stain cresyl violett.

Cryo slices were mounted on glass slides and were than further processed for Nissl staining. Needed materials:

- Staining dishes and slide racks
- Glass slides and cover slips
- Deionized H_2O
- Ethanol 100%
- Glacial acetic acid
- Cresyl violet (add 1.25g cresyl violet and 0.75mL glacial acetic acid to 250mL deionized H_2O)
- Acid 70% ethanol (2mL glacial acetic acid in 200mL 70% ethanol)
- Mounting media (DePex)

The slices were prepared as explained in Table 7.

Washing out lipids and fatty acids	95% ethanol	15min
	70% ethanol	1min
	50% ethanol	1min
Rehydration	Deionized H_2O	2min
	Deionized H_2O	1min
	Cresyl violet stain	2min
Staining	Deionized H_2O	1min
Dehydration	50% ethanol	1min
	70% acid ethanol	1min
	95% ethanol	1min
	95% ethanol	A few dips
	100% ethanol	1min
Mounting	Mounting in DePex	

Table 7: Nissl staining protocol using cresyl violet

Microphotographs of the stained slices were prepared using a bright field microscope with a digital camera mount. The images were processed using the AxioVision software package (Zeiss). An area of the hippocampal granular zone of at least 500µm length was measured and cells within this area were counted. The cell number was normalized to [n cells/500µm] based on the measured area length.

3.7   Microscopy techniques

3.7.1   Bright field microscopy

Bright field microscopy was performed using a computerized semi-automated Mirax Desk microscope (Zeiss, Germany). The Mirax Desk system allowed the digitization of whole tissue sections. The tissue was digitized at a resolution of 0.23µm/pixel. Further processing was achieved with the Axiovision software suite (Zeiss, Germany).

3.7.2   Confocal laser scanning microscopy

Microphotographs of fluoresecence labeled cryo-slices were achieved by using the confocal laser scanning microscope LSM700 (Zeiss, Germany) equipped with solid state lasers emitting at wavelengths of 405nm, 488nm, 555nm and 639nm. Microphotographs were taken using a 63x oil emersion objective (Zeiss) at a resolution of 1024 x 1024pixel.

3.8   Cell culture

3.8.1   *Isolation of neuronal stem and progenitor cells from the subgranular zone*

Neural stem and progenitor cells were isolated according to established protocols from the hippocampi of young adult mice (around 50d of age) from all of the studied mouse strains (FVB, ABCB1$^{0/0}$, ABCG2$^{0/0}$, ABCC1$^{0/0}$) [109].

Animals were sacrificed by cervical dislocation. Animal's heads were sterilized afterwards by rinsing with 70% ethanol. Scalp was cut sagittal to expose the skull. The skull was cut along the sagittal suture and the interparietal, parietal and frontal bones were dissected to expose the brain. The brains were scooped into petri dishes containing ice-cold and sterile aCSF media (Table 3). The brains were positioned flat on their ventral surfaces. A scalpel was used to make a coronal cut 6-8mm from the olfactory bulbs. A second coronal cut is used to dissect a ca. 2mm thick slice embodying the lateral ventricles. A fine curved scissor was used to isolate the lateral ventricles from the surrounding tissue. The isolated ventricular tissue was placed into a new petri dish containing aCSF media and was thoroughly minced using a scalpel.

3.8.2   *Culture and passage of neurosphere cultures*

Minced tissue was transferred into a 15mL sterile centrifuge tube. After centrifuging at 200g for 8min (centrifuge Hermle Z 400 K), the supernatant was discarded and the tissue was dissociated for 15min at 37°C under repeated agitation using 2mL warm Trypsin/EDTA solution (Invitrogen Corp.). After dissociation process, 10mL NeuroCult Basal media was added and tissue samples were centrifuged for 8min at 200g. After discarding the supernatant, an additional washing step was performed using 10mL NeuroCult Basal media. After resuspending the pellet in 1mL NeuroCult Basal media, cells were mechanically dissociated by pipetting the cell suspension in and out for 50 times. Cell concentration was analyzed with a hemocytometer (Fuchs-Rosenthal). To discriminate vital cells from dead cells and debris, cell suspension was mixed 1:2 with Trypan Blue. Trypan blue allows the discrimination of bright living cells from blue stained dead cells due to its trait of being expelled in living cells but being accumulated in dead cells. Only bright cells with a clearly round shape were counted within the grid area corresponding to 0.2µl were counted and used to extrapolate the overall cell concentration of the cell suspension.

NeuroCult™ Basal medium, StemCell Inc.	90mL
NeuroCult™ proliferation supplements, StemCell Inc.	10mL
EGF	100µl [10µg/mL]
FGF	50µl [10µg/mL]
Heparin	50µl [0.2%]

Table 8: Complete proliferation medium (100mL)

Cells were seeded at a concentration of 1.9 x 10^5 cells per 10mL complete proliferation medium (Table 8) in T-25cm² flasks and incubated at 37°C and 5% CO_2 (Incubator CO_2, Binder). Cells were allowed to proliferate until neurospheres were grown to a size of 100-150µm. Thus, cultures were passaged every 7 to 10 days. Therefore cultures were transferred into 15mL flasks and centrifuged at 200g for 8min. The supernatant was discarded. The cell pellet was resuspended in 1mL complete proliferation medium and the neurospheres were mechanically dissociated using a pipette. The cell concentration was counted using a hemocytometer and cells were re-cultured at a concentration of 1 x 10^5 cells in 10mL medium. Cell lines were passaged at least 4 times prior to usage for further experiments.

3.8.3   Proliferation experiments

To determine the proliferation capacity of NSPCs, cells were seeded on matrigel coated coverslips and incubated for 24h at 37°C and 5% CO_2. BrdU incorporation was quantified via immunofluorescence. The relative amount of BrdU labeled cells reflects the proliferative activity of the cell culture.

Sterile coverslips were put into 24-well culture plates. Coverslips were coated by adding 500µL ice-cold NeuroCult Basal medium with Matrigel (2mg/24mL Basal medium). Matrigel was allowed to coagulate over night at 4°C. NSPCs were seeded at a concentration of 5 x 10^4 cells/well in complete proliferation medium for 24h. Half an hour prior to fixation BrdU (10µM final concentration) was added to the cell cultures. Cells were fixated for 20min using PFA (4% in PBS). After three washing steps with PBS, DNA was denatured with 1.5M HCl at 37°C for 30min. After three additional washing steps with PBS, cells were incubated in blocking buffer (10% chicken serum, 0.05% Triton X-100 in PBS) for 1h. Anti-BrdU antibody (1:500) was incubated overnight in blocking solution. After 3 additional washing steps with PBS, anti-mouse Cy3 (1:1000 in PBS) was incubated 1h to label anti-BrdU antibodies bound to BrdU incorporated into DNA of newly proliferated cells. Coverslips were washed three times with PBS and were incubated in DAPI solution (1µg/mL in distilled water) for 5sec prior to a final washing step in PBS. Coverslips were dried in the dark for 3min at 37°C before embedding in DePex on glass slides.

3.8.4 Differentiation experiments

To determine the neuronal differentiation capacity, NSPCs were seeded on matrigel coated coverslips under differentiation conditions. The amount of Tuj1$^+$ cells (neurons) in relation to the overall cell number reflects the capability for neuronal differentiation of NSPCs.

NeuroCult™ Basal medium, StemCell Inc.	90mL
NeuroCult™ differentiation supplements, StemCell Inc.	10mL

Table 9: Complete differentiation medium (100mL)

Sterile coverslips were put into 24-well culture plates. Coverslips were coated by adding 500µL ice-cold NeuroCult Basal medium with Matrigel (2mg/24mL Basal medium) to the coverslip filled wells. Matrigel was allowed to coagulate over night at 4°C. NSPCs were seeded at a concentration of 1 x 10^5 cells/well in complete differentiation medium (Table 9). After 24h the medium was replaced by fresh differentiation medium. The cells were allowed to differentiate for 72h. Thereafter cells were fixated for 20min using PFA (4% in PBS). After three washing steps with PBS, cells were incubated in blocking buffer (10% chicken serum, 0.05% Triton X-100 in PBS) for 1h. Than the cells were incubated with the primary antibodies against β-III-tubulin (Tuj1, Covance, 1:500) and glial fibrilary acid protein (anti-GFAP, DAKO, 1:2000) diluted in blocking buffer overnight at 4°C. Three subsequent washing steps with PBS for 10min each followed the primary antibody incubation. The secondary antibodies against GFAP (anti-rabbit Cy2, Dianova, 1:1000) and β-III-tubulin (anti-mouse Cy3, Dianova, 1:1000) were diluted in PBS. The cells were incubated with the secondary antibodies at room temperature for 1h in the dark. After three additional washing steps (in PBS for 10min each) in the dark, the cells were rinsed for ca. 10sec in DAPI (1µg/mL in water) and finally rinsed in PBS before drying for 30min in the dark. The coverslips containing the labeled cell cultures were mounted on glass-slides using DePex.

3.9 Molecular biological experiments

3.9.1 Nucleic acid based methods

3.9.1.1 <u>DNA extraction</u>

DNA extraction was needed for genotyping purpose in order to organize the breeding procedures after determining the actual state of transgene or knock out inheritance by each animal.

For genotyping, the sample material had to be retrieved. Therefore, the tail was cut ca. 4mm from the tip to retrieve a tissue sample from all animals, which were bred in house. The tissue samples were digested overnight in DNA extraction buffer (Table 10) at 55°C under vigorous agitation in a thermo block to let the proteinase k digest all the proteins and expose the nucleic acids. Samples were incubated at 95°C for additional 30min to denature the proteinase k and were than stored at 4°C until further use.

DNA extraction buffer	
Tris-HCl, pH9.0	10mM
KCl	1M
Igepal A630	0.4%
Tween 20	0.1%
Proteinase K	1.5%

Table 10: DNA extraction buffer

3.9.1.2 <u>Polymerase-chain-reaction (PCR)</u>

The PCR technique allows the amplification of distinct DNA sequences by using a DNA polymerase and adequate primer pairs, enclosing the sequence of interest, *in vitro*. The PCR is characterized by three distinct steps of action. First, the DNA has to be denatured into two single strands at a temperature of 95°C. In the second step the primer pairs have to bind their complementary target positions at the 3' ends of the target sequence on both sense- and anti-sense strand at a primer sequence depending annealing temperature which is suitable for the annealing of both primers. In the last step the DNA polymerase binds the "primed" DNA positions and starts the elongation of the primer DNA in 3' direction according to the complementary strand's DNA sequence. These three steps have to be repeated several times depending on the initial concentration of the template DNA to obtain sufficient amounts of target DNA [110].

To perform PCRs, a commercially available PCR kit (Taq PCR kit, Qiagen) was used. One microliter DNA extract was used as template for polymerase chain reaction (Table 13 - Table 16). Amplification reaction was performed using a thermocycler (TProfessional Basic, Biometra). 10µl amplificate was used for agarose gel electrophoresis (2% agarose in TAE-Buffer [Table 11], containing 3µl ethidium bromide/100mL). After electrophoretic separation of different sized DNA fragments, gels were illuminated by an ultraviolet illuminator and photographed for documentary means (Gel documentation System, DeconScience Tec).

TAE-Buffer (50x)	
Tris-base	242g
Acetic acid (glacial)	57.1mL
EDTA	100mL 0.5M EDTA

Table 11: TAE-buffer (50x)

ABCB1		N192	wt	5'-GAGAAACCATGTCCTTCCAG-3'
	wt (600bp)	N193	wt	5'-AAGCTGTGCATGATTCTGGG-3'
	ko (540bp)	N194	Ko	5'-GCCTTCTATCGCCTTCTTGA-3'
ABCG2		N218	wt for	5'-CTTCTCCATTCATCAGCCTCG-3'
	wt (368bp)	N219	wt rev	5'-CAGTCGATGGATCCACTTAGG-3'
	ko (595bp)	N207	ko rev	5'-GGAGCAAAGCTGCTATTGGC-3'
ABCC1		N131	wt rev	5'-AAGACAAGGGCTTGGGATGC-3'
	wt (900bp)	N221	wt for	5'-CCATCTCTGAGATCTTGCCG-3'
	ko (600bp)	N207	ko rev	5'-GGAGCAAAGCTGCTATTGGC-3'
APP/PS1 transgene		N205	for	5'-GAATTCCGACATGACTCAGG 3'
	(246bp)	N206	rev	5'-GTTCTGCTGCATCTTGGACA-3'
Actin as internal control		N278	for	5' CCTCATGAAGATCCTGACCG 3'
	(400bp)	N279	rev	5' GCACTGTGTTGGCATAGAGG 3'

Table 12: PCR primers for genotyping analyzes

ABCB1	C_{stock}	C_{final}	V
H_2O			2.7μL
Taq mastermix			5.5μL
Primer N192	10μM	1.15μM	1.3μL
Primer N193	10μM	0.7μM	0.7μL
Primer N194	10μM	0.7μM	0.7μL
$V_{mastermix}$			10.9μL
V_{DNA}			1μL
V_{total}			11.9μL
Thermocycler program			
ABCB1		Initial denaturation	5min 95°C
	Cycle 35x	DNA denaturation	30sec 95°C
		Primer annealing	60sec 58°C
		Elongation	60sec 72°C
		Final elongation	5min 72°C
		Storage	∞ 4°C

Table 13: ABCB1 PCR mastermix and thermocycler protocol

ABCG2	C_{stock}	C_{final}	V
H_2O			5.1μL
Taq mastermix			5.5μL
Primer N218	25μM	0.28μM	0.1μL
Primer N219	25μM	0.28μM	0.1μL
Primer N207	25μM	0.28μM	0.1μL
$V_{mastermix}$			10.9μL
V_{DNA}			1μL
V_{total}			11.9μL
Thermocycler program			
ABCG2		Initial denaturation	5min 95°C
	Cycle 35x	DNA denaturation	45sec 95°C
		Primer annealing	60sec 62°C
		Elongation	90sec 72°C
		Final elongation	5min 72°C
		Storage	∞ 4°C

Table 14: ABCG2 PCR mastermix and thermocycler protocol

ABCC1	C_{stock}	C_{final}	V
H_2O			4.7μL
Taq mastermix			5.5μL
Primer N131	25μM	1μM	0.4μL
Primer N221	25μM	0.55μM	0.2μL
Primer N207	25μM	0.25μM	0.1μL
$V_{mastermix}$			10.9μL
V_{DNA}			1μL
V_{total}			11.9μL
Thermocycler program			
ABCC1		Initial denaturation	5min 95°C
	Cycle 35x	DNA denaturation	45sec 95°C
		Primer annealing	60sec 62°C
		Elongation	90sec 72°C
		Final elongation	5min 72°C
		Storage	∞ 4°C

Table 15: ABCC1 PCR mastermix and thermocycler protocol

APP/PS1	C_{stock}	C_{final}	V
H_2O			3.5μL
Taq mastermix			5.5μL
Primer N205 (APP/PS1)	10μM	0.45μM	0.5μL
Primer N206 (APP/PS1)	10μM	0.45μM	0.5μL
Primer N278 (Actin)	10μM	0.45μM	0.5μL
Primer N279 (Actin)	10μM	0.45μM	0.5μL
$V_{mastermix}$			11μL
V_{DNA}			1μL
V_{total}			12μL
Thermocycler program			
APP/PS1		Initial denaturation	5min 95°C
	Cycle 35x	DNA denaturation	45sec 95°C
		Primer annealing	45sec 62°C
		Elongation	45sec 72°C
		Final elongation	5min 72°C
		Storage	∞ 4°C

Table 16: APP/PS1 PCR mastermix and thermocycler protocol

3.9.1.3 <u>RNA-extraction</u>

RNA extraction was performed according to the technique initially established by Chomczynski and Sacchi in 1987 [111]. The TRIzol (Invitrogen product name) method combines the advantages of the acid phenol and guanidine isothiocyanate extraction methods leading to powerful protein denaturation, inactivating RNases (guanidine isothiocyanate) and enabling RNA separation into the aqueous supernatant phase (acidic phenol/chloroform) for easy RNA extraction. The method is widely considered as to deliver best quality RNA yield.

Tissue samples were incubated in TRIzol (Invitrogen) for protein denaturation and RNase inactivation using 1mL/100mg tissue. The samples were homogenized at 5000rpm for 15sec using a cell homogenizer (Precellys24, Bertin Technologies). The mixture was incubated with chloroform 100µl/1mL TRIzol for DNA precipitation for 3min at room temperature. The upper aqueous phase was carefully aspirated for further processing into a sterile microfuge tube (1.5mL). RNA was precipitated incubating aqueous phase with 500µL/mL TRIzol for 15min at room temperature. The samples were centrifuged at 12.000g for 15min at 4°C. The supernatant was discarded and the RNA pellet was washed twice with 1mL RNase free ethanol (75%) after vigorous vortexing and subsequent centrifugation at 12.000g for 5min at 4°C. After discarding the ethanol, pellets were dried for 15min at room temperature. The dried RNA pellets were solubilized in RNase free water (1µl/1mg tissue sample). The solubilized RNA was stored to -80°C until further use.

To analyze mRNA expression in NSPCs, tissue samples from the neurosphere cultures were taken 3 days after their last passage. The neurosphere cultures were aspirated from the culture flasks and transferred into 15ml sterile centrifuge tubes. Adhering cells were scraped off the flask using a sterile cell scraper and also transferred to the according sterile micro-centrifuge tube. The cultures were centrifuged at 200g for 8min at 4°C. The culture medium was discarded and the RNA was extracted using the TRIzol method as described above.

RNA extraction from dissected hippocampi

The mRNA samples were obtained from brain hemispheres, which were submersed in the RNA-preservative RNAlater (Applied Biosystems) to restore the RNA expression profile. The hippocampus was dissected for long-term storage or RNA preparation at the latest 48h after harvesting the tissue samples. The preservative denatured the tissue samples, making the dissection of the hippocampus easy manageable. Therefore the brain hemispheres were put under a stereo microscope into a 50mm petri dish containing RNAlater. Using fine forceps

and micro-scissors the hippocampus was dissected. The RNA was prepared from the hippocampus and stored as described in above.

3.9.1.4 Quantitative real-time PCR (qRT-PCR)

For quantification of mRNA expression of distinct genes, the mRNA sample has to be transcribed into DNA first, using a reverse transcriptase. To quantify the expression of the target gene, the mRNA, transcribed into DNA, has to be amplified and its increasing concentration has to be detected in real-time. While early approaches to qRT-PCR used fluorescence probes like ethidium bromide, simply intercalating with amplified DNA and intensifying fluorescence activity with increasing DNA concentration [112], more recent and highly sophisticated approaches use an additional probe sequence that fluoresces upon hybridization (LightCycler, Roche) or hydrolysis (TaqMan, Applied Biosystems) [113]. In the case of TaqMan chemistry, additionally to the primer pair, needed for DNA amplification, a DNA probe (TaqMan probe) is used, binding the DNA sequence between the two primer positions. The additional TaqMan probe contains a fluorophore (5'-end) and a quencher (3'-end). As long as the TaqMan probe is intact, the quencher suppresses the fluorophore's fluorescence activity. During amplification the Taq polymerase is decomposing the TaqMan probe due to its 5' to 3' exonuclease activity and releases the fluorophore and quencher, thereby separation of the fluorophore from its quencher is leading to increased fluorescence activity. Here, the amplitude of the fluorescence signal is directly related to the concentration of newly amplified DNA. Measuring the fluorescence signal in relation to the number of amplification cycles allows conclusions about the initial RNA concentration.

An integrated Reverse Transcriptase and TaqMan reaction protocol was used to perform reverse transcriptase and quantitative real-time PCR in the same reaction tube as subsequent reactions. The One-Step RT-PCR kit (Applied Biosystems) allows both, the reverse transcription and polymerase chain reaction in one buffer system by utilization of a recombinant Moloney Murine Leukemia Virus Reverse Transcriptase (Applied Biosystems) and thermal stable DNA polymerase (AmpliTaq Gold, Applied Biosystems). TaqMan probes were purchased from Applied Biosystems (Table 17). For qRT-PCR 10pg RNA were used as template. Therefore RNA samples were diluted to a concentration of 5pg RNA/µl.

Gene of interest	Label	ID
GAPDH (reference)	FAM	Mm99999915_g1
ABCB1a	VIC	Mm00440761_m1
ABCB1b	VIC	Mm00440736_m1
ABCG2	VIC	Mm00496364_m1
ABCC1	VIC	Mm00456156_m1

Table 17: TaqMan probes

The mastermix for RT-PCR was provided according to Table 18. All samples were analyzed in triplicates plus two additional blank samples containing only mastermix without RNA samples. Analyzes were performed as multiplex measurements simultaneously measuring a Vic- and FAM- labeled TaqMan assay in each well. A Rotor-Gene Q (Qiagen) was used for lightcycling and analyzes.

qRT-PCR mastermix			
		$H2O$	3.625µl
		MM	7.500µl
		RT-MM	0.375µl
		Assay-VIC	0.750µl
		Assay-FAM	0.750µl
		$V_{Mastermix}$	13.000µl
		V_{RNA}	2.000µl
		V_{Total}	15µl
Lightcycler program			
RT reaction		reverse transcription	30min @ 48°C
		RT inactivation	10min @ 95°C
PCR-reaction	40x	DNA denaturation	15sec @ 95°C
		annealing and elongation	60sec @ 95°C

Table 18: qRT-PCR mastermix and lightcycling program

The fluorescence intensities of the target genes were compared to those of the according internal control (GAPDH) using the $\Delta\Delta C_T$ method [114] and were described as fold-changes compared to the control.

3.10 Oligomeric Aβ$_{42}$ preparation

Monomerization and storage of Aβ$_{42}$

HPLC purified and lyophilized Aβ$_{42}$ (Sigma-Aldrich, USA) was dissolved in hexafluoroisopropanol (HFIP) to obtain a concentration of 1mM Aβ$_{42}$ in HFIP in microcentrifuge tubes. The solution was incubated for 60min at room temperature. Afterwards the solution is set back on ice for 5-10min. The HFIP was allowed to evaporate until the

microcentrifuge tubes were completely dried leaving a film of monomeric $A\beta_{42}$. The monomeric $A\beta_{42}$ was stored at -80°C until further use [115].

Oligomeric $A\beta_{42}$ incubation protocol

Dry monomeric $A\beta_{42}$ films were dissolved in fresh DMSO (Sigma-Aldrich, USA) to a final concentration of 5mM. The solution was further diluted in DMEM/F12 media to a final concentration of 100µM. The solution was incubated for 24h at 4°C. The oligomeric $A\beta_{42}$ solution was afterwards directly used for cell culture experiments at a concentration of 1µM [116].

3.11 Behavioral experiments

3.11.1 Y-maze

The y-maze testing apparatus consist of a y-shaped maze with three arms at a 120° angle from each other. The dimensions of each of the walled arms are 325mm (length), 85mm (width) and 150mm (height). The test is used to assess the willingness of mice to explore new environments. Due to the explorative nature of rodents, the mice will rather investigate a new arm, than entering a previously visited arm. A normally behaving mouse should show a tendency to enter the less recently visited arm. The proper function of several parts of the brain (hippocampus, basal forebrain, prefrontal cortex) is needed to achieve normally in this task.

Animals were tested once in the y-maze setup. The mice were put in the middle of the maze and were allowed to move freely within the maze. The movement was automatically tracked with an infrared camera and analyzed with the *Video Mot* software package (TSE Systems). The following parameters were assessed: running distance, number of arm entries, and percentage of alternating entries [117].

3.11.2 Elevated plus-maze

With the elevated plus maze (EPM) the overall anxiety level of the different mouse strains was assessed. The EPM is based on a simple principle, which says that the exploratory drive to examine a given arm is equal to each arm, while the anxiety driven avoidance to enter an unknown area is lower in enclosed arms compared to open arms, which results in increased exploration of the enclosed arms [118].

Each mouse was tested once without prior training in the EPM apparatus (TSE Systems). The EPM consisted of plus-shaped platform 50cm above the ground consisting of 4 equal arms (300mm x 50mm) of which 2 confronting arms were enclosed by walls (150mm high) while the other two were open. Again, the mice were set in the middle of the maze and were allowed to move freely within the maze, while being recorded by an infrared camera for 5min. The following parameters were analyzed using the *Video Mot* software package (TSE Systems): number of closed arm entries, open arm entries, speed in each compartment, time spent in each set of arms and time spent in the central area [119].

3.11.3 Light/Dark-box

The light/dark box (LDB) test incorporates the feature of light and open-space avoidance of the open field test, but its setup additionally allows one to monitor mice behavior within the dark (non-stress) compartment.

All mice were tested once in the LDB setup. The box-shaped maze (500mm x 500mm x 400mm) consisted of a darkened area ($1/3^{rd}$) and an illuminated (~400Lux) compartment ($2/3^{rd}$) which are connected by a door (60mm x 60mm). The experiments began by putting the animals in the middle of the open compartment, facing away from the door. The animals were allowed to move freely for 5min while being recorded by an infrared camera, even in the darkened compartment, throughout the test. The following parameters were analyzed using the *Video Mot* software package (TSE Systems): duration of stay per compartment, distance travelled per compartment, transitions between compartments, and number of rearing in each compartment [120].

3.12 Statistical Analysis

Data were analyzed using the software package Prism5 (Graph-Pad Software). All data are presented as arithmetic means (here referred to as "mean") with their respective standard error of the mean (SEM). The unpaired, two-tailed Student's t-Test was performed to assess for statistical significance. Data were deemed statistically significant with $p \leq 0.05$ (*$p \leq 0.05$; **$p \leq 0.01$; ***$p \leq 0.001$).

4 Results

4.1 Comparative quantification of hippocampal neurogenesis

4.1.1 Neurogenesis under normal conditions

Molecular markers of neurogenic progenitors in the subgranular zone of the dentate gyrus were analyzed to assess the ABC transporter's influence in adult neurogenesis. To do so, NSPC's at different states of differentiation were comparatively quantified in ABC deficient and control mouse strains. Earliest stem and progenitor cells were quantified by labeling with antibodies against Sox2, a transcription factor only expressed in early NSPCs making it a reliable marker of undifferentiated NSPCs [121, 122]. Beside the earliest NSPCs, also neuronal committed progenitors were quantified by labeling for the cytoskeletal protein Doublecortin (DCX) [123, 124]. Newly generated postmitotic neurons were quantified as well by labeling for the Calcium binding protein Calretinin which is only transiently expressed and is substituted by Calbindin during cellular maturation. [125].

The Sox2 positive NSPC pool was observed to be significantly altered as a result of distinct ABC transporter deficiency. In fact the Sox2$^+$ cell pool was significantly increased (+17%) in mice lacking expression of ABCC1 compared to control mice. Therefore alterations were observed in neither ABCB1$^{0/0}$ nor ABCG2$^{0/0}$ mice (Figure 10A, Table 19). In contrast, quantification of the DCX$^+$ early neuronal progenitor pool revealed a significant decrease of neuronal differentiation in mice lacking either expression of ABCB1 (-36%) or ABCG2 (-23%) while no significant alterations were observed in ABCC1$^{0/0}$ mice (Figure 10B, Table 19). Quantification of Calretinin$^+$ neurons revealed a similar result. In animals lacking expression of ABCB1 neuronal differentiation was decreased on the basis of significantly reduced numbers of Calretinin$^+$ cells (-37%). No significant alterations were observed in mice lacking the expression of either ABCG2 or ABCC1 (Figure 10C, Table 19). Therefore quantification of BrdU incorporation did not show ABC deficiency-dependent impairments of cell proliferation (Figure 10D, Table 19)
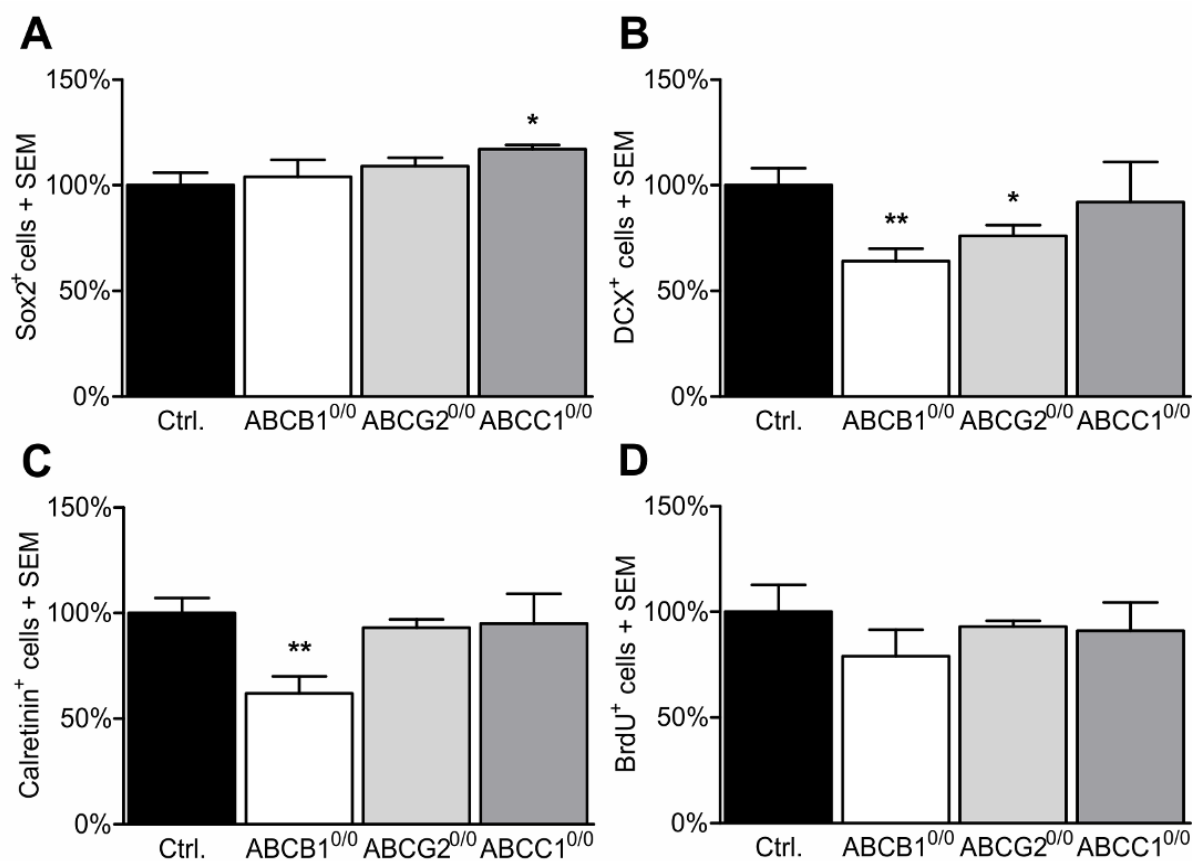
Figure 10: ABCB1 deficiency impairs neuronal differentiation in the dentate gyrus. Shown are the relative quantities of cells positive for Sox2, DCX, Calretinin and BrdU in the SGZ of the dentate gyrus in ABC-deficient mice as compared to the FVB controls. Error bar: SEM; Significance vs. Ctrl: * $p<0.05$; **$p<0.01$

NSPC cell counts						
	Strain	MEAN	rel MEAN	±SEM	tTest vs. Ctrl	n
Sox2	Ctrl	162,7	100,0%	6,4%		6
	ABCB1$^{0/0}$	169,5	104,2%	7,6%	p=0,689	6
	ABCG2$^{0/0}$	177,4	109,0%	3,6%	p=0,266	6
	ABCC1$^{0/0}$	190,8	117,3%	2,5%	p=0,049	4
DCX	Ctrl	47,7	100,0%	7,5%		6
	ABCB1$^{0/0}$	30,4	63,7%	6,4%	p=0,004	5
	ABCG2$^{0/0}$	36,3	76,2%	5,0%	p=0,026	6
	ABCC1$^{0/0}$	44,0	92,3%	18,6%	p=0,697	6
Calretinin	Ctrl	20,5	100,0%	6,9%		6
	ABCB1$^{0/0}$	12,8	62,5%	7,8%	p=0,002	5
	ABCG2$^{0/0}$	19,1	92,8%	4,5%	p=0,390	6
	ABCC1$^{0/0}$	19,6	95,3%	14,2%	p=0,769	6
BrdU	Ctrl	18,0	100,0%	10,6%		5
	ABCB1$^{0/0}$	14,8	81,8%	12,5%	p=0,246	**5**
	ABCG2$^{0/0}$	17,3	95,8%	2,7%	p=0,619	6
	ABCC1$^{0/0}$	16,8	93,3%	13,4%	p=0,605	6

Table 19: NSPC cell counts

BrdU incorporation experiments revealed ABC transporter deficiency leading to altered rates of NSPC differentiation.

Proliferation activity in the NSPC pool was assessed by quantifying the relative number of BrdU$^+$ cell numbers in the poll of Sox2$^+$, DCX$^+$ and Calretinin$^+$ cells. Therefore, BrdU was administered to the mice 7 days prior to harvesting the brain tissue. The absence of either one of the three analyzed ABC transporters led to significant decline of proliferating Sox2$^+$ cells (-25% ABCB1$^{0/0}$; -28% ABCG2$^{0/0}$; -37% ABCC1$^{0/0}$; Figure 11A/D, Table 20). In contrast, there were no significant changes in proliferation capacity observed in the DCX$^+$ cell pool (Figure 11B/E). Therefore, BrdU uptake was significantly increased in ABCG2$^{0/0}$ (+43%) and ABCC1$^{0/0}$ (+51%) mice while there was no changed observed in ABCB1 deficient animals (Figure 11C/F, Table 20).

NSPC cell counts, BrdU positive cell fractions					
	Strain	MEAN	±SEM	tTest vs. Ctrl	n
Sox2$^+$/BrdU$^+$	Ctrl	6,7%	0,5%		4
	ABCB1$^{0/0}$	5,0%	0,6%	p=0,045	5
	ABCG2$^{0/0}$	4,8%	0,2%	p=0,012	6
	ABCC1$^{0/0}$	4,2%	0,4%	p=0,011	6
DCX$^+$/BrdU$^+$	Ctrl	27,4%	6,9%		4
	ABCB1$^{0/0}$	21,3%	2,6%	p=0,472	5
	ABCG2$^{0/0}$	25,2%	4,4%	p=0,803	6
	ABCC1$^{0/0}$	24,7%	3,7%	p=0,747	6
Calretinin$^+$/Brdu$^+$	Ctrl	19,6%	1,5%		4
	ABCB1$^{0/0}$	23,3%	1,7%	p=0,152	5
	ABCG2$^{0/0}$	28,0%	3,0%	p=0,039	6
	ABCC1$^{0/0}$	29,5%	0,9%	p=0,002	6

Table 20: NSPC cell counts, BrdU positive cell fractions
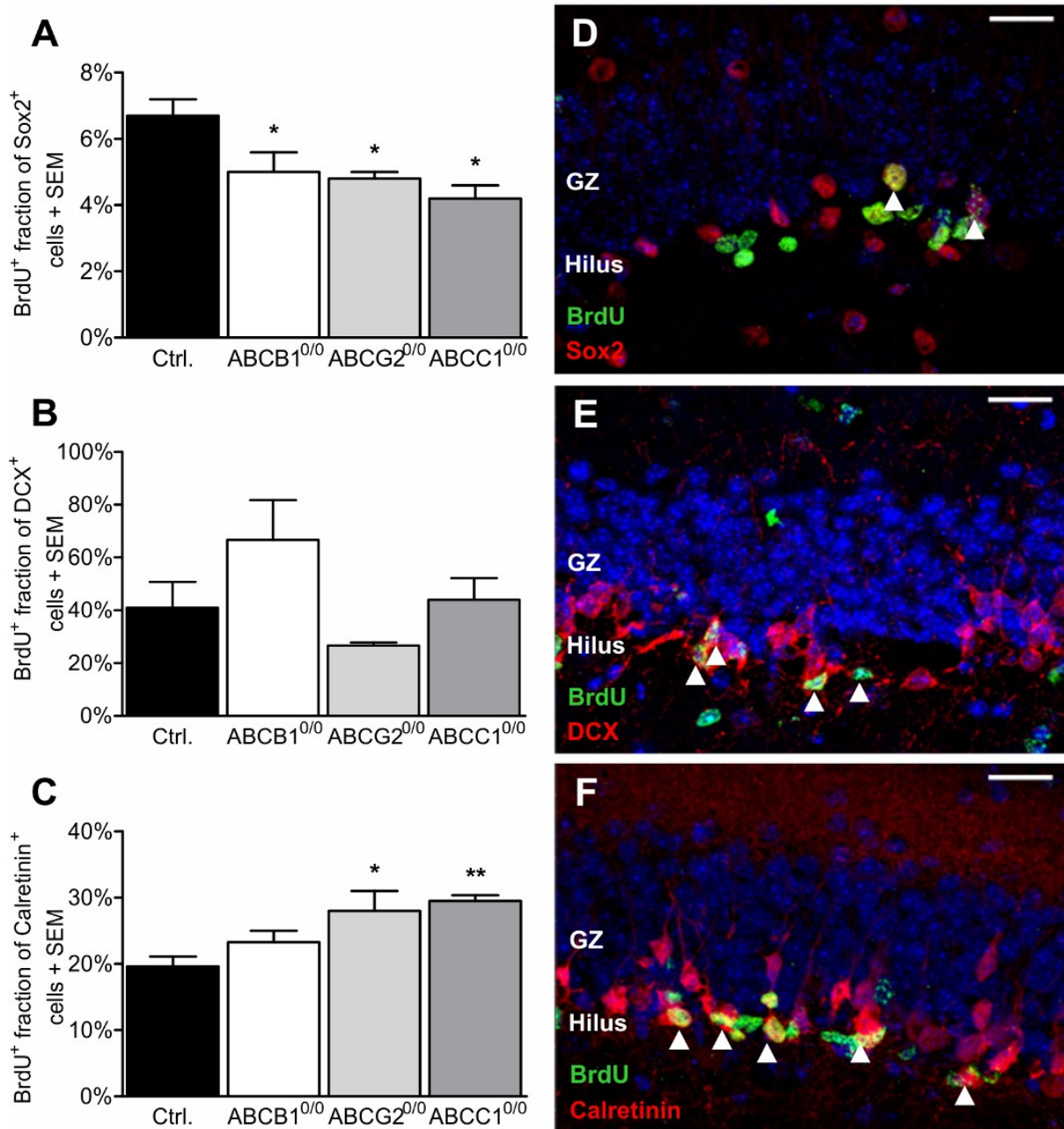
Figure 11: ABCC1 deficiency impairs stem cell proliferation and accelerates late neuronal differentiation. The graphs show the newly generated population (BrdU incorporation) of $Sox2^+$ (A), DCX^+ (B) and $Calretinin^+$ (C) cells in the SGZ of the DG. The photomicrographs display expression examples for marker combinations: Sox2/BrdU (D), DCX/BrdU (E) and Calretinin/BrdU (F). Arrowheads indicate double-labeled cells. Error bar: SEM; Significance vs. Ctrl: * $p<0.05$; **$p<0.01$; Scale bar: 20µm

4.1.2 Neurogenesis after controlled cortical impact

Since traumatic brain injury is known to trigger neurogenesis [107], the controlled cortical injury model was utilized for analyzing the involvement of ABC transporters in neuroregenerative functions. Because ABC transporter depletion might only affect neurogenesis during disease state, the CCI paradigm [108] was chosen to amplify NSPC

proliferation and differentiation. As a result of the CCI surgery 7 days prior to analysis, neurogenesis was according to the literature [107, 108, 126] significantly increased in the dentate gyrus of the ipsilateral hemispheres in all analyzed mouse strains compared to the respective contralateral hemisphere (Figure 12).
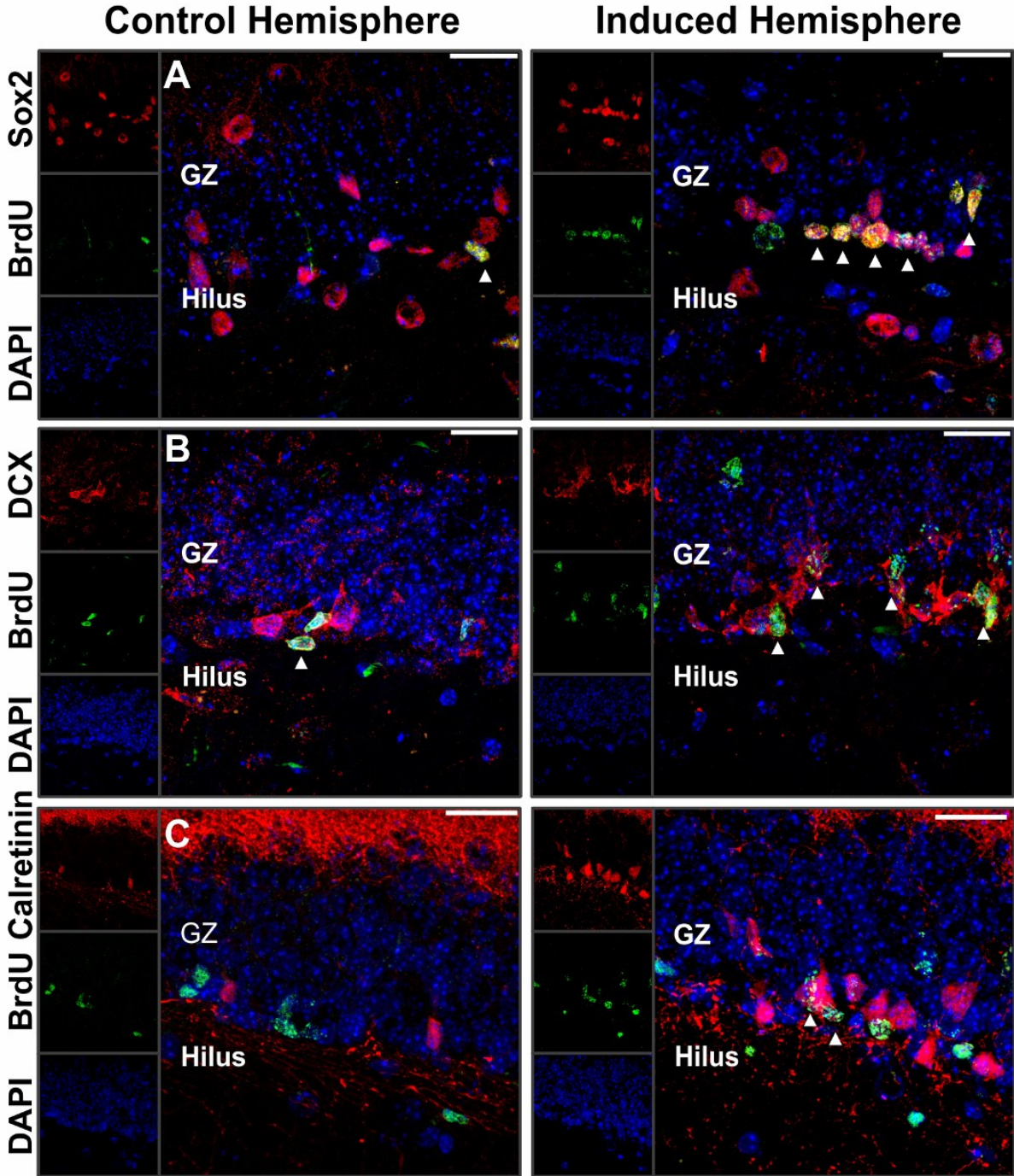
Figure 12: Neurogenesis is induced by controlled cortical impact (CCI) trauma. The photomicrographs show the SGZ of the DG after CCI (LEFT: Control hemispheres; RIGHT: hemispheres after CCI). Shown are the marker combinations Sox2/BrdU (A), DCX/BrdU (B) and Calretinin/BrdU (C). Arrowheads indicate double labeled cells. Scale bar: 20μm

As a result of CCI surgery, neurogenesis was significantly increased in ipsilateral hemispheres compared to the non-affected control hemispheres of all analyzed mice (FVB, ABCB1$^{0/0}$, ABCG2$^{0/0}$, ABCC1$^{0/0}$). Beside cell proliferation also the number of Sox2^{+} early NSPCs, DCX^{+} neuronal progenitors and newly generated Calretinin^{+} neurons was significantly increased in the ipsilateral hemisphere compared to the contralateral control hemispheres (Table 21).

		NSPC cell counts CCI								
		contralateral				ipsilateral				
	Strain	Mean	rel Mean	±SEM	tTest vs. Ctrl	Mean	rel Mean	±SEM	tTest vs. Ctrl	n
Sox2	Ctrl	180.7	100.0%	2.7%		216.7	120.0%	10.3%		5
	ABCB1$^{0/0}$	153.8	85.1%	7.0%	p=0.063	177.7	98.4%	3.8%	p=0.042	6
	ABCG2$^{0/0}$	171.7	95.0%	3.5%	p=0.171	198.1	109.7%	3.6%	p=0.414	6
	ABCC1$^{0/0}$	162.2	89.8%	2.9%	p=0.024	187.3	103.7%	2.8%	p=0.048	6
DCX	Ctrl	33.7	100.0%	5.3%		73.8	218.9%	4.5%		6
	ABCB1$^{0/0}$	31.3	93.0%	6.8%	p=0.215	47.5	140.9%	8.7%	p=0.001	6
	ABCG2$^{0/0}$	35.9	106.5%	12.6%	p=0.663	64.5	191.2%	10.5%	p=0.242	6
	ABCC1$^{0/0}$	34.1	101.1%	4.3%	p=0.874	49.6	147.2%	6.5%	p=0.000	6
Calretinin	Ctrl	14.6	100.0%	12.4%		31.2	212.9%	9.1%		5
	ABCB1$^{0/0}$	14.5	99.4%	10.3%	p=0.972	22.2	151.6%	11.2%	p=0.045	5
	ABCG2$^{0/0}$	17.9	120.6%	8.8%	p=0.225	32.3	220.5%	10.1%	p=0.804	6
	ABCC1$^{0/0}$	15.3	104.5%	4.8%	p=0.726	23.7	162.1%	6.6%	p=0.039	6
BrdU	Ctrl	19.6	100.0%	12.9%		76.6	390.1%	5.9%		6
	ABCB1$^{0/0}$	16.3	83.0%	4.4%	p=0.273	40.5	206.3%	15.3%	p=0.001	5
	ABCG2$^{0/0}$	15.7	80.1%	4.9%	p=0.170	52.7	268.6%	18.5%	p=0.049	6
	ABCC1$^{0/0}$	17.0	100.0%	3.4%	p=0.335	35.7	181.9%	5.5%	p=0.000	6

Table 21: NSPC cell counts CCI

According to the results, ABC transporter expression influenced the amount of altered cell proliferation. In all ABC deficient strains the proliferation capacity, as observed in the ipsilateral hemispheres, was significantly reduced in comparison to the control strain (-47% ABCB1$^{0/0}$; -31% ABCG2$^{0/0}$; -53% ABCC1$^{0/0}$, Figure 13A, Table 21). As the increased proliferation index implied, results indicated a significant increase in the Sox2^{+} cell pool in the CCI-affected brain hemispheres. Independently of ABC transporter expression status the Sox2+ cell pool was significantly increased in the ispilateral hemisphere compared to the respective contralateral control hemispheres (Figure 13B, Table 21). Even more affected by CCI treatment were the pools of DCX and Calretinin positive cells. CCI treatment led to a significant increase in neuronal differentiation due to extended numbers of DCX positive neuronal progenitors compared to the cell numbers in the control hemispheres. Still, ABC transporter deficiency affected the relative increase in neuronal differentiation of induced vs. control hemispheres when compared to the control mice. In comparison to the control mice, only ABCB1$^{0/0}$ and ABCC1$^{0/0}$ strains revealed a significant decrease of neuronal progenitors

(-36% ABCB1$^{0/0}$; -33% ABCC1$^{0/0}$), while ABCG2$^{0/0}$ mice showed no impairments (Figure 13C, Table 21). According to the quantification of DCX^{+} progenitors also Calretinin^{+} newly generated neurons were decreased in numbers in ABCB1$^{0/0}$ (-29%) and ABCC1$^{0/0}$ (-29%) while there was no deficit observed in mice lacking expression of ABCG2 (Figure 13D, Table

21).
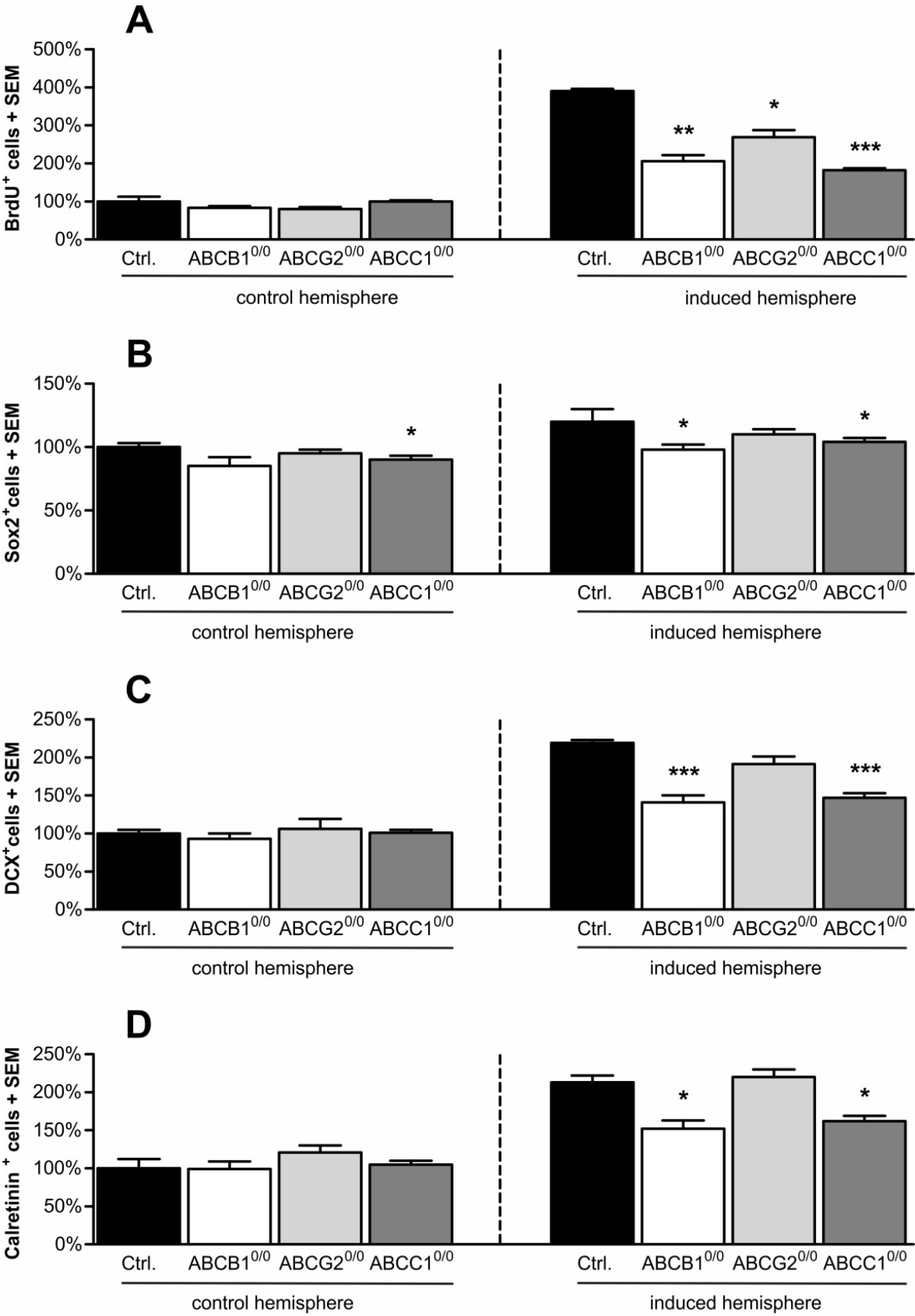
Figure 13: CCI paradigm reveals ABC transporter's significance in neurogenesis. Error bars: SEM; Significance vs. Ctrl: *p<0.05; **p<0.01; ***p<0.001

NSPC cell counts CCI. BrdU positive cell fraction								
		contralateral			ipsilateral			
	Strain	rel Mean	±SEM	tTest vs. Ctrl	rel Mean	SEM	tTest vs. Ctrl	n
Sox2$^+$/BrdU$^+$	Ctrl	3.8%	0.7%		16.1%	1.1%		5
	ABCB1$^{0/0}$	6.0%	0.6%	p=0.039	11.6%	2.1%	p=0.095	5
	ABCG2$^{0/0}$	4.8%	0.3%	p=0.181	10.4%	2.0%	p=0.042	6
	ABCC1$^{0/0}$	6.4%	0.6%	p=0.016	9.1%	1.0%	p=0.001	6
DCX$^+$/BrdU$^+$	Ctrl	29.9%	2.9%		51.5%	5.3%		6
	ABCB1$^{0/0}$	25.0%	4.3%	p=0.355	32.5%	6.4%	p=0.001	5
	ABCG2$^{0/0}$	28.7%	9.0%	p=0.895	36.1%	4.4%	p=0.050	6
	ABCC1$^{0/0}$	27.4%	3.2%	p=0.577	34.8%	5.2%	p=0.048	6
Calretinin$^+$/ BrdU$^+$	Ctrl	35.1%	7.5%		38.4%	6.4%		5
	ABCB1$^{0/0}$	40.6%	3.9%	p=0.570	42.9%	8.0%	p=0.671	4
	ABCG2$^{0/0}$	25.5%	4.9%	p=0.235	29.5%	4.4%	p=0.284	5
	ABCC1$^{0/0}$	42.4%	2.0%	p=0.726	42.2%	3.3%	p=0.590	6

Table 22: NSPC cell counts CCI, BrdU positive cell fraction

4.1.3 Impact of ABC transport deficiency on neurogenic functions in a mouse model of Alzheimer's disease
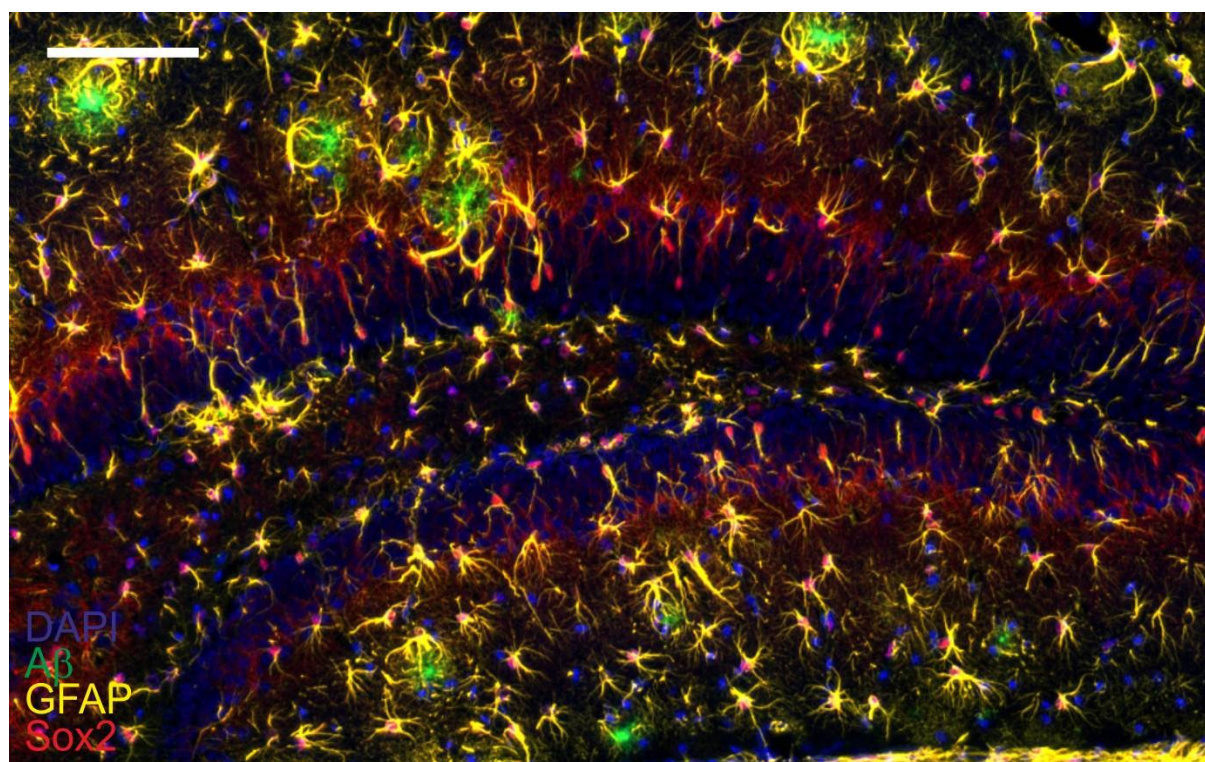
Figure 14: β-amyloid deposition enhances neurogenic functions in the hippocampus. The photomicrograph shows a tissue section stained for nuclear DNA (DAPI, blue), Aβ deposition (green), glial fibrillary acid protein (yellow) and Sox2 (red). Scale bar: 100µm

Quantification of NSPCs in different states of differentiation was performed on cryo slices of transgenic ABC transporter deficient mice to assess the influence of the β-amyloid pathology on neurogenic processes within the hippocampal dentate gyrus.

Analyzes revealed significant effects of ABC deficiency in transgenic APP/PS1$^{+/0}$ mice. Lack of expression of ABCB1 led to a significant increase in the number of Sox2 positive cells by 16% while the difference in cell number was even greater in mice deficient for ABCG2 (+19%) and ABCC1 (+22%) (Figure 15A, Table 23). While even non transgenic ABC deficient animals showed at least a trend towards increased NSPC cell number, which became only significant in ABCC$^{0/0}$ mice, the differences were not yet significantly different in comparison to the respective transgenic AD model mice.
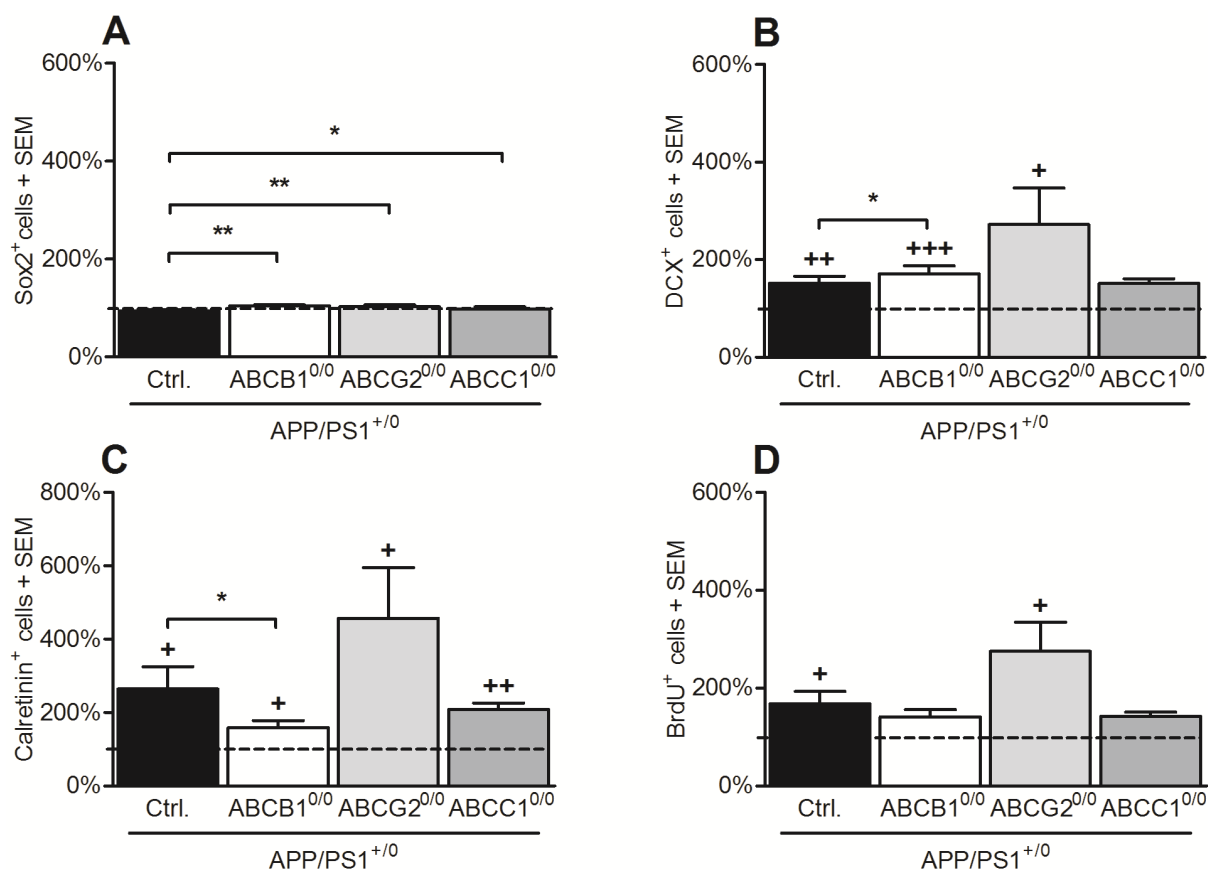
Figure 15: AD pathology affects adult neurogenesis in dependency of ABC expression. The diagram indicates the relative change of cell counts in ABC deficient transgenic mice in comparison to their respective non-transgenic counterparts. The respective non-transgenic counterparts were set as hundred percent each. Error bars: SEM; Significance vs. APP/PS1$^{+/0}$ Ctrl: *$p<0.05$; **$p<0.01$; ***$p<0.001$; Significance vs. respective APP/PS1$^{0/0}$ strain: +$p<0.05$; ++$p<0.01$; +++$p<0.001$

The influence of β-amyloid deposition on the number of DCX^{+} neuronal progenitors appeared more significant. By comparing the ABC deficient transgenic mouse strains with the transgenic control group, only ABCB1$^{0/0}$-APP/PS1$^{+/0}$ mice revealed a significantly impaired number (-28%) of DCX^{+} neuronal progenitors (Figure 15B, Table 23). Interestingly, β-amyloid deposition led to increased numbers of DCX positive progenitors in APP/PS1$^{+/0}$ controls (+52%) as like in ABCB1$^{0/0}$ (+71%) and ABCG2$^{0/0}$ (+172%) mice. Only in ABCC1$^{0/0}$ transgenic mice the increase of the DCX positive progenitor pool did not become

statistically significant while at least indicating a trend towards the same direction (Figure 15B, Table 23).

	Strain	rel Mean	±SEM	tTest vs.Ctrl	tTest vs non transgenic littermates	n
NSPC cell counts of transgenic strains compared to non-transgenic strains						
Sox2	Ctrl	93%	3.4%		p=0.352	6
	ABCB1$^{0/0}$	104%	2.4%	p=0.005	p=0.628	6
	ABCG2$^{0/0}$	102%	4.0%	p=0.009	p=0.769	6
	ABCC1$^{0/0}$	97%	5.1%	p=0.012	p=0.558	4
DCX	Ctrl	152%	14.0%		p=0.008	.6
	ABCB1$^{0/0}$	171%	15.8%	p=0.032	p=0.004	6
	ABCG2$^{0/0}$	272%	74.6%	p=0.372	p=0.045	6
	ABCC1$^{0/0}$	151%	10.2%	p=0.505	p=0.064	4
Calretinin	Ctrl	264%	60.7%		p=0.023	6
	ABCB1$^{0/0}$	159%	18.9%	p=0.039	p=0.012	5
	ABCG2$^{0/0}$	457%	137.7%	p=0.284	p=0.027	6
	ABCC1$^{0/0}$	209%	17.1%	p=0.425	p=0.001	4
BrdU	Ctrl	168%	25.3%		p=0.046	6
	ABCB1$^{0/0}$	141%	15.5%	p=0.090	p=0.079	6
	ABCG2$^{0/0}$	275%	59.1%	p=0.155	p=0.014	6
	ABCC1$^{0/0}$	142%	8.7%	p=0.295	p=0.051	4

Table 23: Transgene NSPC count relative to non-transgenic strains

AD related β–amyloid pathology altered the Calretinin positive cell pool in a fashion comparable to that shown for DCX positive neuronal progenitors. As like shown for the non-transgenic mouse groups, even the transgenic mice deficient for ABCB1 showed an impaired (-62%) cell number within the pool of Calretinin^{+} newly generated neurons compared to the APP/PS1$^{+/0}$ control mice. But even here, all transgenic mice showed a significantly increased number of Calretinin^{+} cells in dependency of the β-amyloid deposition compared to their respective non-transgenic counterparts. In numbers the increase was +68% for APP/PS1$^{+/0}$ controls, +41% for ABCB deficient transgenic mice, +175% in ABCG2 deficient transgenic mice and +42% in ABCC1 deficient transgenic mice (Figure 15C, Table 23).

BrdU positive cell counts of transgenic strains					
	Strain	rel Mean	±SEM	tTest vs FVB	n
Sox2$^+$/BrdU$^+$	Ctrl	11.2%	2.3%		6
	ABCB1$^{0/0}$	5.9%	1.2%	p=0.064	6
	ABCG2$^{0/0}$	11.3%	2.4%	p=0.982	6
	ABCC1$^{0/0}$	5.8%	0.9%	p=0.100	4
DCX$^+$/BrdU$^+$	Ctrl	27.0%	2.9%		6
	ABCB1$^{0/0}$	24.8%	5.5%	p=0.720	5
	ABCG2$^{0/0}$	26.7%	5.8%	p=0.962	6
	ABCC1$^{0/0}$	23.5%	3.7%	p=0.465	4
Calretinin$^+$/ BrdU$^+$	Ctrl	17.0%	1.9%		6
	ABCB1$^{0/0}$	22.1%	4.5%	p=0.255	3
	ABCG2$^{0/0}$	20.4%	4.2%	p=0.477	6
	ABCC1$^{0/0}$	28.2%	2.8%	p=0.010	4

Table 24: BrdU positive progenitor cell fractions in APP/PS1 transgenic mouse strains

As expected also the overall cell proliferation was affected by Aβ deposition. While the proliferation rate was not significantly affected by ABC deficiency when compared to transgenic control mice, the differences between transgenic and non-transgenic control respectively ABCG2$^{0/0}$ mice were significant. Transgenic control mice showed an increased cell count of BrdU positive cells of +68% when compared to their non-trangenic counterpart, while the cell number of BrdU$^+$ cells was even more drastically increased by +175% in ABCG2$^{0/0}$ transgenic mice when compared with ABCG2$^{0/0}$ non-transgenic mice (Figure 15D, Table 24).

4.2 Proliferation and differentiation of NSPCs *in vitro*

4.2.1 Proliferation capacity with regard to ABC expression

To analyze the proliferation capacity of ABC transporter-deficient NSPCs, primary NSPC lines from the subventricular zone of control and ABC transporter-deficient animals were used. Primary NSPC cultures were generated by isolating NSPC from the subventricular zone of control and ABC deficient mouse strains. BrdU incorporation into newly amplified DNA was used as an indicator for comparative assessment of cell proliferation capacity in the different cell lines. Thirty minutes prior analysis BrdU was added and allowed to be incorporated into the DNA during cell proliferation. Comparative analyzes only revealed significantly increased proliferation capacity (+62%) in cells lacking expression of ABCG2. In neither ABCB1$^{0/0}$ nor ABCC1$^{0/0}$ cell lines the difference in cell proliferation did reach significance (Figure 16 A/B, Table 25).

4.2.2   Differentiation capacity with regard to ABC expression

Also the capability for neuronal differentiation was comparatively analyzed *in vitro* by quantifying the relative amount of neuronal cells after 3 days under proliferating conditions. Neuronal cells were identified by use of immunofluorescence methods labeling the neuron-specific β-III-tubulin with a Tuj1 antibody. The results of the differentiation assays did not reveal any impairment in neuronal differentiation as a result of single ABC transporter deficiency (Figure 16 C/D; Table 26).
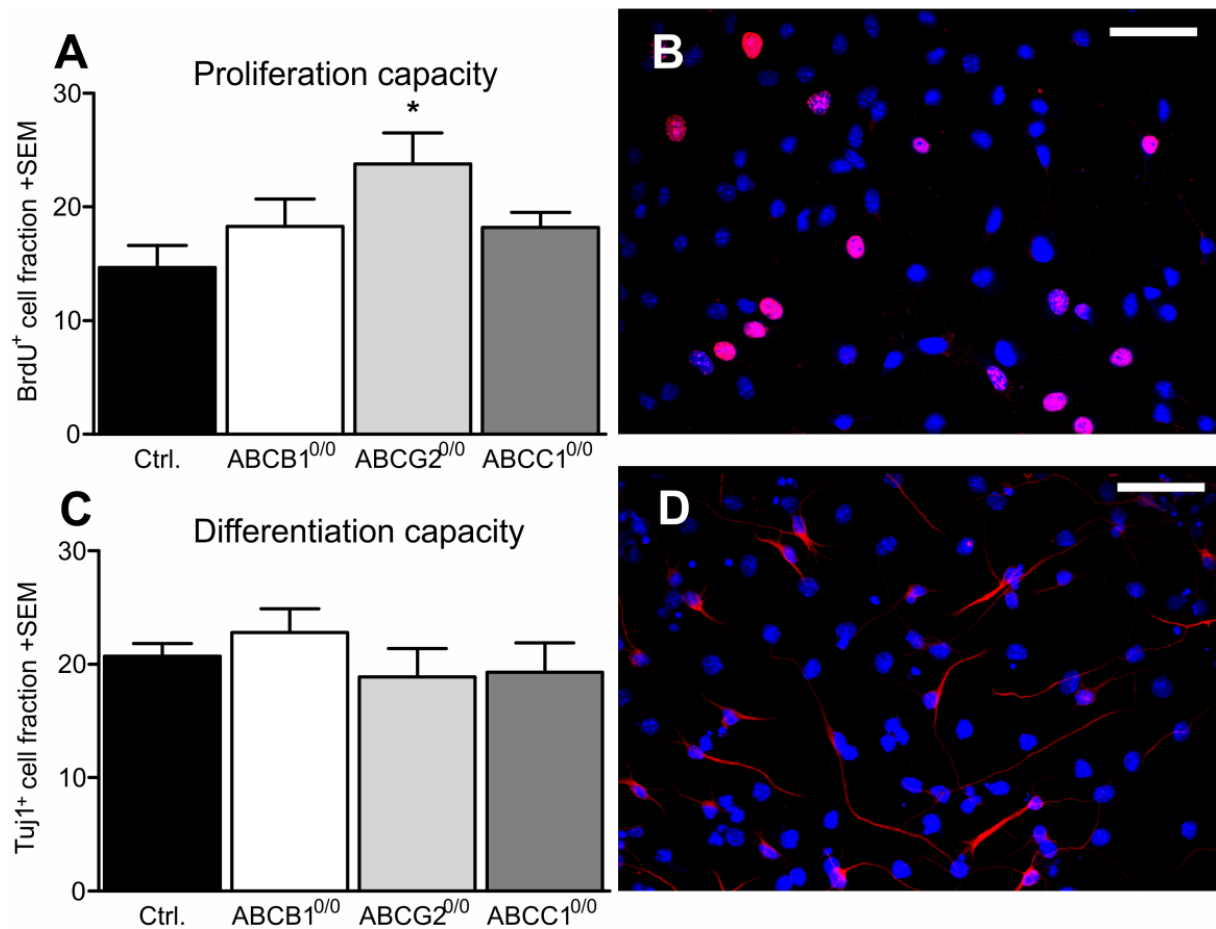
Figure 16: ABC transporter-deficiency did not impair neuronal differentiation in vitro. ABCG2$^{0/0}$ cells showed a significant increase in proliferation capacity (+62%, A) quantified by detection of BrdU uptake using immunofluorescence (B). The differentiation capacity was not impaired by loss of ABC expression (C) as revealed by quantification of neuronal cells positive for Tuj1 (D). Error bar: SEM; Significance vs. Ctrl: *p<0.05; Scale bar: 50μm

4.2.3   Effects of β-amyloid on proliferation and differentiation of NSPCs in vitro

To test whether Aβ administration affects on NSPC proliferation and differentiation processes in a cell-intrinsic manner, we administered 1μM synthetic Aβ$_{42}$ to NSPC cultures during proliferation and differentiation experiments.

According to the experiments with the non-transgenic cell lines, cell proliferation was tested after 24 hours post-passage with a 30min BrdU incubation protocol. $A\beta_{42}$ was administered at a concentration of $1\mu M$ directly at the beginning of the 24 hour experiment. Quantification of the BrdU-labeled newly proliferated cells revealed results very comparable to those without $A\beta_{42}$ administration. Only $ABCG2^{0/0}$ cells showed a significant increase (+24%) in proliferation capacity compared to the controls after $A\beta_{42}$ treatment. No significant effects of $A\beta_{42}$ treatment were observed when comparing the proliferation capacity without and after $A\beta_{42}$ administration in none of the analyzed NSPC cultures (Figure 17, Table 25).
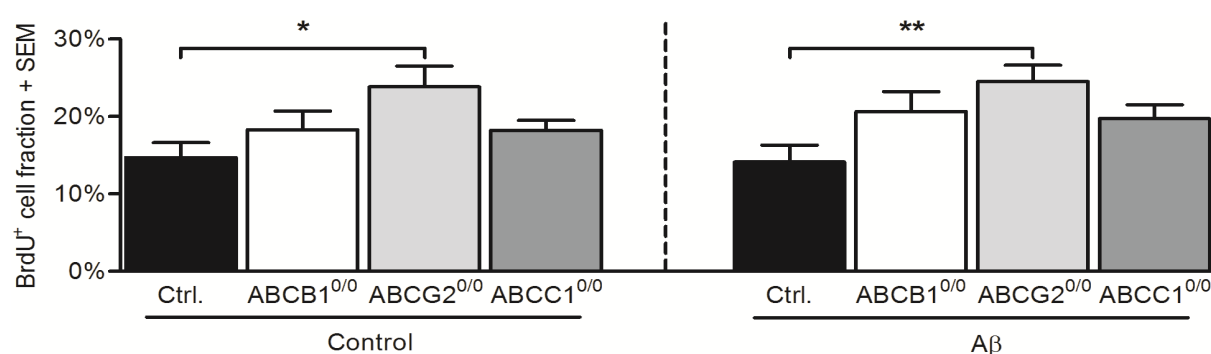
Figure 17: $A\beta$ administration did not significantly affect NSPC proliferation. Significance: *$p<0.05$; **$p<0.01$

While $A\beta_{42}$ did not seem to affect cell proliferation capacity in NSPCs, still the question remains whether it is able to induce alterations in NSPC maturation. The experiments were performed as for the untreated NSPC cultures unless the needed administration of $1\mu M$ $A\beta_{42}$ at the beginning of the 72 hour differentiation experiment. The following quantification the NSPC's ability for neuronal differentiation revealed an $A\beta_{42}$-dependent increase in neuronal differentiation capacity in NSPCs of the FVB control strain. The control strain showed an increase in the proportion of neuronal cells in culture by 23% as a result of $A\beta_{42}$ treatment (Figure 18, Table 26). There were no significant ABC-dependent effects observed.
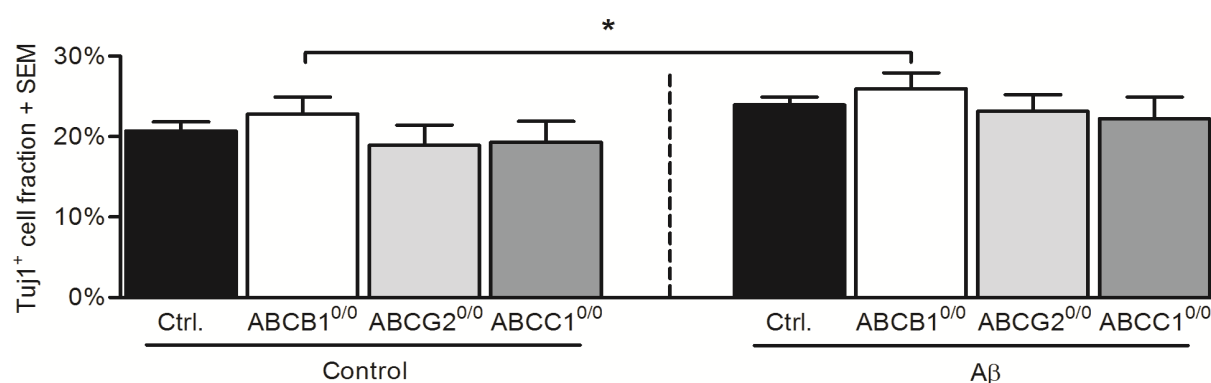
Figure 18: Administration of $A\beta$ increased pro-neuronal cell differentiation in FVB NSPC strains. Significance: *$p<0.05$

BrdU positive cell fraction in NSPC proliferation assay									
	Control				Aβ Administration				tTest Ctrl vs. Aβ
Strain	MEAN	±SEM	tTest vs. Ctrl	n	MEAN	±SEM	tTest vs. Ctrl	n	
Ctrl	14.7%	1.9%		11	14.1%	2.2%		12	p=0.845
ABCB1$^{0/0}$	18.3%	2.4%	p=0.257	13	20.6%	2.6%	p=0.072	13	p=0.528
ABCG2$^{0/0}$	23.8%	2.7%	p=0.017	15	24.5%	2.1%	p=0.002	17	p=0.840
ABCC1$^{0/0}$	18.2%	1.3%	p=0.126	18	19.7%	1.8%	p=0.056	18	p=0.493

Table 25: BrdU positive cell fraction in NSPC proliferation assay

Tuj1 positive cell fraction in NSPC differentiation assay									
	Control				Aβ Administration				tTest Ctrl vs. Aβ
Strain	MEAN	±SEM	tTest vs. Ctrl	n	MEAN	±SEM	tTest vs. Ctrl	n	
Ctrl	20.7%	1.1%		18	23.9%	1.0%		15	p=0.0496
ABCB1$^{0/0}$	22.8%	2.1%	p=0.361	14	25.9%	2.0%	p=0.343	12	p=0.283
ABCG2$^{0/0}$	18.9%	2.5%	p=0.500	16	23.1%	2.1%	p=0.750	16	p=0.211
ABCC1$^{0/0}$	19.3%	2.6%	p=0.588	15	22.2%	2.7%	p=0.560	14	p=0.430

Table 26: Tuj1 positive cell fraction in NSPC differentiation assay

4.3 RNA analyzes

4.3.1 Expression of ABC transporters in NSPCs

To justify any conclusions about ABC transporter involvement in stem cell functions, the actual expression of the questioned ABC transporters had to be verified. Therefore mRNA was isolated from the different NSPC lines and the relative expression levels for ABCB1a, ABCB1b, ABCG2 and ABCC1 were quantified by utilizing quantitative real-time PCR. These analyzes confirmed all three transport proteins (ABCB1, ABCG2, ABCC1) to be expressed by revealing also a possible co-regulation between ABCB1 and ABCG2.

Interestingly, these analyzes showed that only one of the two murine isoforms of ABCB1 (ABCB1a and ABCB1b) were actually expressed in NSPCs. Only ABCB1b was found to be expressed while NSPCs completely lack the expression of ABCB1a. A possible co-regulation between ABCG2 and ABCB1 was implicated by the finding that ABCB1b mRNA expression was significantly decreased (-28%) in NSPCs lacking the expression of ABCG2 (Figure 19A, Table 27). Vice versa, expression levels of ABCG2 mRNA were found to be increased (+71%) in ABCB1$^{0/0}$ NSPCs. Even the lack of ABCC1 expression led to an increase of ABCG2 mRNA expression (+73%) without reaching statistical significance (Figure 19B;

Table 27). In contrast neither expression of ABCB1 or ABCG2 was significantly altered as a result of lacking expression of ABCC1. Appropriately, in neither ABCB1$^{0/0}$ nor ABCG2$^{0/0}$ NSPCs the expression of ABCC1 was significantly impaired (Figure 19C; Table 27).
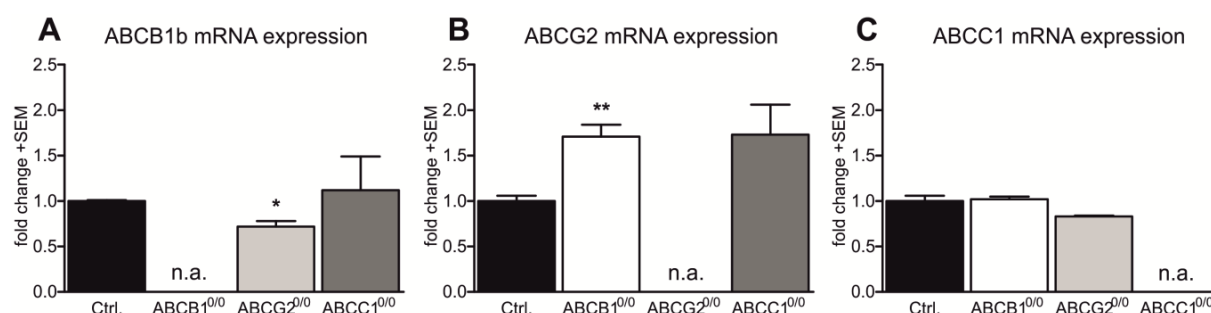
Figure 19: Expression of ABCB1b and ABCG2 are co-regulated in NSPCs in vitro. Relative mRNA expression of ABCB1b, ABCG2 and ABCC1 was measured against mRNA expression of GAPDH using TaqMan assays. Expression of ABCB1b was significantly impaired (-28%) in ABCG2$^{0/0}$ cells (A). In reverse, expression of ABCG2 was increased significantly (+71%) in animals lacking ABCB1 expression, while a comparable effect on ABCC1$^{0/0}$ cells did not reach statistical significance (B). For ABCC1 mRNA expression, no significant changes were observed in the other cell lines (C). Error bar: SEM; Significance vs. Ctrl: * p<0.05; **p<0.01

ABC transporter mRNA expression					
Gene	Strain	Fold change	±SEM	tTest vs FVB	n
ABCB1b	Ctrl	1.00	0.01		3
	ABCB1$^{0/0}$	-	-	-	-
	ABCG2$^{0/0}$	0.72	0.06	p=0.053	3
	ABCC1$^{0/0}$	1.12	0.05	p=0.001	3
ABCG2	Ctrl	1.00	0.06		3
	ABCB1$^{0/0}$	1.71	0.13	p=0.008	3
	ABCG2$^{0/0}$	-	-	-	-
	ABCC1$^{0/0}$	1.73	0.33	p=0.099	3
ABCC1	Ctrl	1.00	0.06		3
	ABCB1$^{0/0}$	1.02	0.03	p=0.821	3
	ABCG2$^{0/0}$	0.83	0.01	p=0.054	3
	ABCC1$^{0/0}$	-	-	-	-

Table 27: ABC transporter mRNA expression

4.3.2 Expression of genes relevant to adult neurogenesis

In vitro

To analyze whether loss of ABC transporter expression has cell intrinsic effects on neuronal stem and progenitor cells, we used mRNA extracts from cell cultures for quantitative RT-PCR as described in 3.9.1.3 and 3.9.1.4. The results are described as fold-changes compared to the control strain. Analyzes were performed for the E3 ligase Mindbomb 1, the transcription factor Mash1, the Notch ligand Jagged1, the transmembrane receptor Notch1, the

intermediate filament Nestin and the microtubule-associated protein DCX. The results are plotted in Figure 20 and Table 28.

MibI

The results show that only loss of ABCB1 was able to significantly affect the expression level of distinct genes. The expression of MibI was increased significantly by 37% in comparison to the controls. The average increase of MibI expression in $ABCG2^{0/0}$ strains did not reach statistical significance due to high variation of the values. The expression of MibI was virtually not affected by loss of ABCC1 expression

Mash1

The analyzes of the mRNA expression of the Mash1 transcription factor did not show significant alterations due to loss of ABC transporter function.

Jagged1

The expression of Jagged1, a Notch1 ligand, was as well assessed using quantitative RT-PCR. Analyzes show a significant increase of Jagged1 expression in NSPCs lacking the ABC transporter ABCB1. Here the expression level was increased by 36%. While the average values for Jagged1 mRNA were even increased in $ABCG2^{0/0}$ and $ABCC1^{0/0}$ strains, the changes did not reach statistical significance due to high deviation of the single values.

Notch1

While the expression of the Notch ligand Jagged1 was at least significantly increased in $ABCB1^{0/0}$ NSPCs, there was no significant alteration in Notch1 mRNA expression observable for neither of the analyzed ABC deficient NSPC strains.

Nestin

Analyzes of mRNA expression levels of the NSPC-specific intermediate filament protein Nestin revealed no significant alterations in expression due to loss of ABC transporter functions.

DCX

Therefore, the microtubule-associated protein DCX, which is first expressed when NSPCs become neuronal committed, is surprisingly differentially expressed across the different ABC deficient NSPC strains. NSPCS deficient for ABCB1 show a significant increase in DCX

mRNA level by 32%. The increased expression in ABCG2$^{0/0}$ and ABCC1$^{0/0}$ did not reach statistical significance.

Figure 20: *In vitro* **Expression of genes relevant for neurogenic functions.** The diagrams show relative expression levels of target genes compared to GAPDH as fold-changes. Only loss of ABCB1 expression significantly increased the expression of MibI (A), Jagged1 (C) and DCX (F). All other genes were unaffected by loss of either ABCB1, ABCG2 or ABCC1. Error bar: SEM; Significance vs. Ctrl: *p<0.05

	In vitro mRNA expression				
	Strain	±SEM	SEM	tTest vs. Ctrl	n
MibI	Ctrl	1.0	0.1		3
	$ABCB1^{0/0}$	1.4	0.1	p=0.038	3
	$ABCG2^{0/0}$	1.9	1.3	p=0.508	3
	$ABCC1^{0/0}$	1.1	0.5	p=0.803	3
Mash1	Ctrl	1.0	0.0		3
	$ABCB1^{0/0}$	1.1	0.1	p=0.348	3
	$ABCG2^{0/0}$	1.0	0.1	p=0.904	3
	$ABCC1^{0/0}$	1.2	0.2	p=0.426	3
Jagged1	Ctrl	1.0	0.0		3
	$ABCB1^{0/0}$	1.4	0.1	p=0.036	3
	$ABCG2^{0/0}$	1.4	0.2	p=0.152	3
	$ABCC1^{0/0}$	1.9	0.8	p=0.296	3
Notch1	Ctrl	1.0	0.0		3
	$ABCB1^{0/0}$	1.0	0.1	p=0.908	3
	$ABCG2^{0/0}$	1.1	0.2	p=0.599	3
	$ABCC1^{0/0}$	1.2	0.1	p=0.175	3
Nestin	Ctrl	1.0	0.1		3
	$ABCB1^{0/0}$	1.0	0.1	p=0.795	3
	$ABCG2^{0/0}$	0.7	0.1	p=0.150	3
	$ABCC1^{0/0}$	1.2	0.3	p=0.487	3
DCX	Ctrl	1.0	0.1		3
	$ABCB1^{0/0}$	1.3	0.0	p=0.027	3
	$ABCG2^{0/0}$	1.9	1.3	p=0.508	3
	$ABCC1^{0/0}$	1.1	0.5	p=0.803	3

Table 28: In vitro mRNA expression

In vivo

To analyze whether expression of distinct proteins, involved in neurogenic processes, might be altered due to loss of ABC transporter expression, we used mRNA extracts from hippocampal tissue for quantitative RT-PCR as described in 3.9.1.3 and 3.9.1.4. The results are described as fold-changes compared to the control strain. Analyzes were performed for the E3 ligase Mindbomb1, the transcription factor Mash1, the Notch ligand Jagged1, the transmembrane receptor Notch1, the intermediate filament Nestin and the microtubule-associated protein DCX. The results are plotted in Figure 21 and Table 29.

MibI

Analyzes showed that the E3 ligase MibI, which is a major key member in Notch1 signaling is altered in its mRNA expression due to loss of distinct ABC transporter function. In $ABCB1^{0/0}$ mice the mRNA level is increased by 55% compared to the controls. In both $ABCG2^{0/0}$ and $ABCC1^{0/0}$ mice the increased mRNA expression did not reach statistical significance (Figure 21A).

Mash1

The expression of the NSPC specific transcription factor is only altered in mice lacking ABCC1 expression. Here the mRNA level is decreased by 39% compared to the controls. Instead, animals lacking the transporters ABCB1 or ABCG2 do not show significant alterations, while ABCG2$^{0/0}$ mice show at least a trend towards increased Mash1 levels without reaching statistical significance (Figure 21B).

Jagged1

The Notch ligand Jagged1 seems not to be altered in its mRNA expression with regard to ABC deficiency. In none of the ABC deficient animals the mRNA level was significantly changed in comparison to the controls (Figure 21C).

Notch1

The transmembrane receptor Notch1, which is significantly involved in stem cell differentiation processes, is altered in its mRNA expression by the status of ABC transporter expression. In animals lacking the expression of ABCB1, the Notch mRNA level is increased by 30%. In contrast to that, loss of ABCC1 expression instead results in decreased Notch expression by 33%. In ABCG2$^{0/0}$ mice only an insignificant trend towards increased Notch1 expression is observed (Figure 21D).

Nestin

The intermediate filament protein Nestin, expressed during neuronal differentiation of NSPCs, seemed to be increased in expression due to loss of ABCB1 and ABCC1 expression. While the expression of Nestin in ABCB1$^{0/0}$ mice was increased by 52%, the increase in ABCC1$^{0/0}$ did not reach statistical significance and represents only a trend (Figure 21E).

DCX

While the microtubule-associated protein DCX seem to be increased in mRNA expression due to loss of all analyzed ABC transporters, this increase only reaches statistical significance in ABCB1$^{0/0}$ (+50%) and ABCC1$^{0/0}$ (+90%) mice.
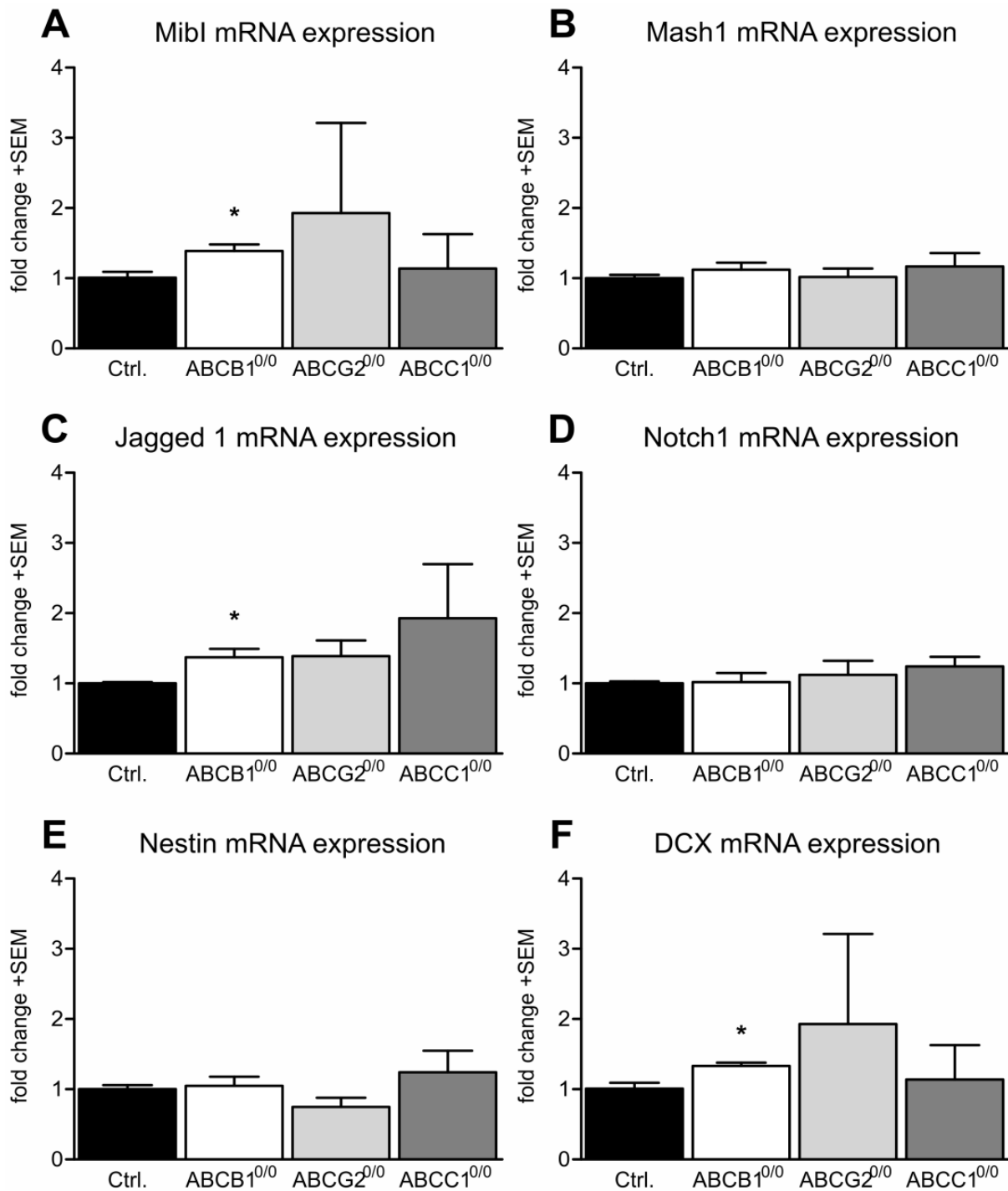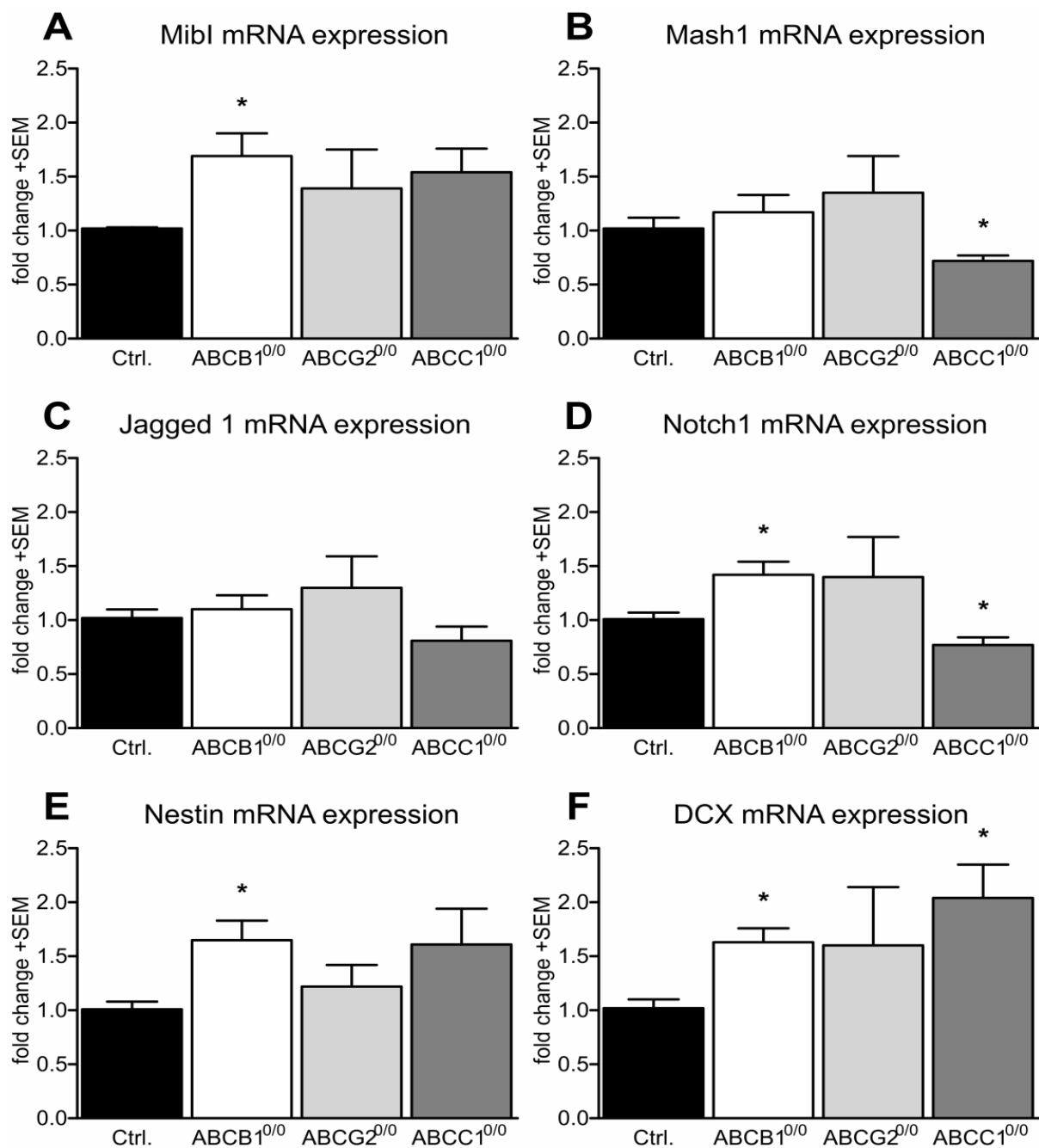
Figure 21: Hippocampal Expression of genes relevant for neurogenic functions. The diagrams show relative expression levels of target genes compared to GAPDH as fold-changes. Loss of ABCB1 expression significantly affected expression of MibI (A), Notch1(D), Nestin (E) and DCX (F), while it did not affect expression of Mash 1 (B) and Jagged1 (C). Therefore loss of ABCC1 expression significantly affected the expression of Mash 1 (B), Notch1 (D) and DCX (F). Lost expression of ABCG2 had no effects on the mRNA levels of the analyzed genes. Error bar: SEM; Significance vs. Ctrl: $*p < 0.05$

Hippocampal mRNA expression					
	Strain	MEAN	±SEM	tTest vs. Ctrl	n
MibI	Ctrl	1.02	0.10		n=6
	ABCB1$^{0/0}$	1.69	0.21	p=0.463	n=4
	ABCG2$^{0/0}$	1.39	0.36	p=0.369	n=7
	ABCC1$^{0/0}$	1.54	0.22	p=0.062	n=7
Mash1	Ctrl	1.02	0.10		n=6
	ABCB1$^{0/0}$	1.17	0.16	p=0.476	n=4
	ABCG2$^{0/0}$	1.35	0.34	p=0.387	n=7
	ABCC1$^{0/0}$	0.72	0.05	p=0.025	n=7
Jagged1	Ctrl	1.02	0.08		n=6
	ABCB1$^{0/0}$	1.10	0.13	p=0.612	n=4
	ABCG2$^{0/0}$	1.30	0.29	p=0.373	n=7
	ABCC1$^{0/0}$	0.81	0.13	p=0.074	n=7
Notch1	Ctrl	1.01	0.06		n=6
	ABCB1$^{0/0}$	1.42	0.12	p=0.034	n=4
	ABCG2$^{0/0}$	1.40	0.37	p=0.334	n=7
	ABCC1$^{0/0}$	0.77	0.07	p=0.041	n=7
Nestin	Ctrl	1.01	0.07		n=6
	ABCB1$^{0/0}$	1.65	0.18	p=0.045	n=4
	ABCG2$^{0/0}$	1.22	0.20	p=0.350	n=7
	ABCC1$^{0/0}$	1.61	0.33	p=0.123	n=7
DCX	Ctrl	1.02	0.08		n=6
	ABCB1$^{0/0}$	1.63	0.13	p=0.011	n=4
	ABCG2$^{0/0}$	1.60	0.54	p=0.320	n=7
	ABCC1$^{0/0}$	2.04	0.31	p=0.019	n=7

Table 29: Hippocampal mRNA expression

4.4 Histological analyzes

4.4.1 *Neuronal density and cortex layer cytoarchitecture within the frontal cortex*

To determine whether ABC deficiency also leads to deficits in cortical development, tissue was analyzed for changes in cortical neuronal density and alterations in cytoarchitecture. For each strain 5 to 7 brains were immunohistochemically stained for the neuronal marker NeuN. The digitized brain sections were computer-assisted analyzed for the proportional NeuN^{+} cortical area. Analyzes revealed a slight increase in neuronal Cortex area which was not yet significant (Figure 22B, Table 30).

To analyze whether ABC deficiency might result in developmental impairments of the neocortex, measurements of the proportional cortical layer sizes were performed on the digitized NeuN-labeled brain sections. These analyzes revealed changes in cortical layers I and VI for distinct ABC deficient strains, while layer II-IV (combined) and layer IV remained unaffected. Lack of ABCB1 expression resulted in a significant decrease by 12% in size of

layer I, while the other layers remained unaffected. Instead, animals deficient for ABCC1 showed a significantly increased size of layer VI (+15%) while all other layers were not significantly affected. Loss of ABCG2 expression did not seem to affect cortical cytoarchitecture due to unaffected sizes of the cortical layers (Figure 22C, Table 31).
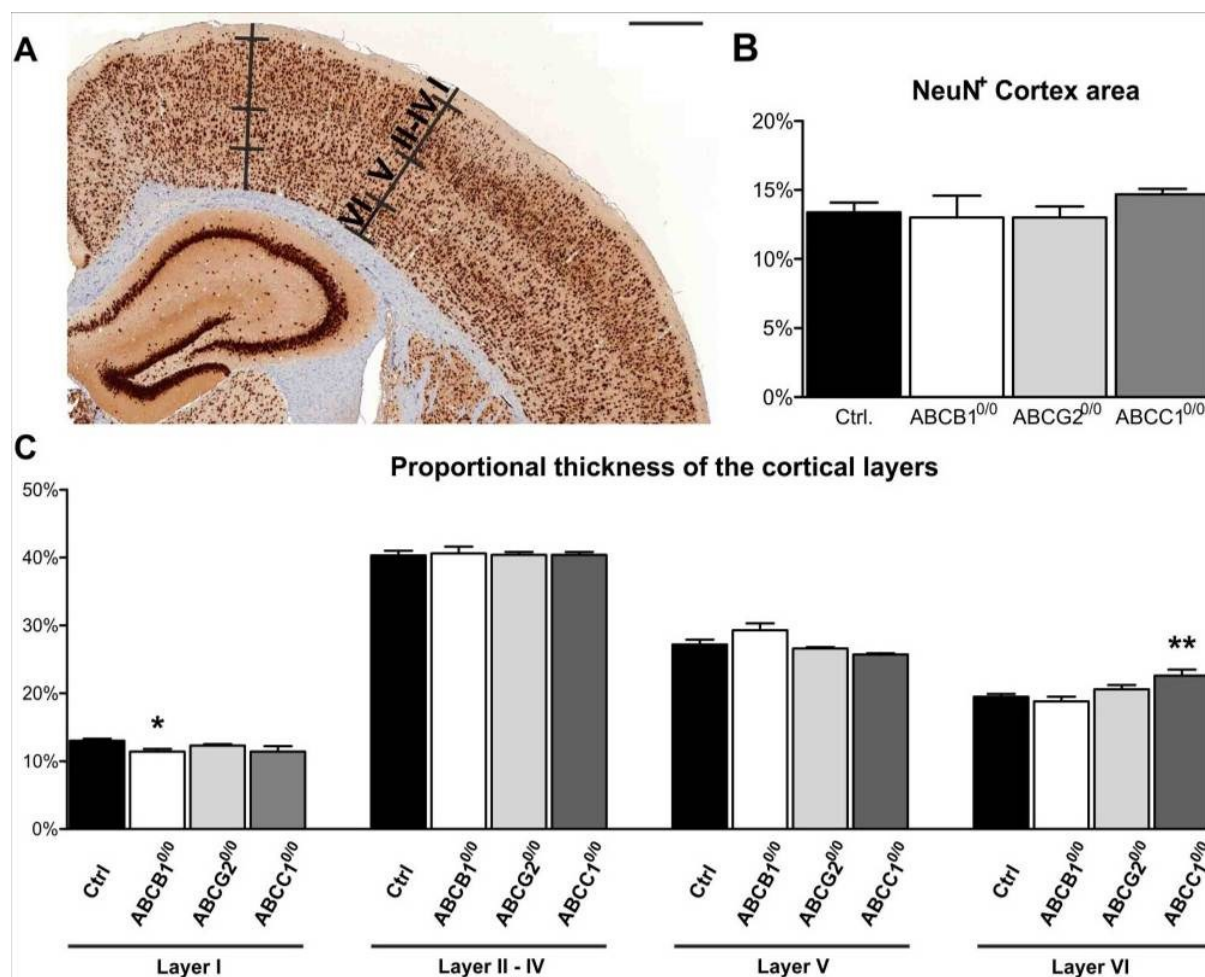
Figure 22: ABC deficiency alters neuronal cytoarchitecture but not neuronal density. Paraffin-embedded brain sections (A) were labeled with an antibody against NeuN, digitized, and the NeuN+ area was computer-assisted determined relative to the cortical area to quantify the neuronal density of the cortex (B). The thickness of the cortical layers I, II-IV (combined), V and VI were measured (A) and analyzed (C). The loss of ABCB1 expression significantly decreased the thickness of layer I (-12%) while loss of ABCC1 only affected the thickness of layer VI (+15%) Scale bars: 500µm (A); Error bars: SEM; Significance vs. Ctrl: *<p0.05, **<0.01

NeuN+ cortical area				
Strain	MEAN	±SEM	tTest vs. Ctrl	n
Ctrl	13%	0.7%		7
ABCB1$^{0/0}$	13%	1.9%	p=0.808	5
ABCG2$^{0/0}$	13%	0.8%	p=0.662	5
ABCC1$^{0/0}$	15%	0.4%	p=0.127	6

Table 30: NeuN$^+$ cortical area

Cortical layer distribution					
	Strain	Mean	±SEM	tTest vs. Ctrl	n
Layer I	Ctrl	13.0%	0.3%		7
	ABCB1$^{0/0}$	11.4%	0.4%	p=0.014	5
	ABCG2$^{0/0}$	12.3%	0.2%	p=0.131	7
	ABCC1$^{0/0}$	11.4%	0.8%	p=0.068	6
Layer II - IV	Ctrl	40.3%	0.7%		7
	ABCB1$^{0/0}$	40.6%	1.0%	p=0.845	5
	ABCG2$^{0/0}$	40.4%	0.4%	p=0.917	7
	ABCC1$^{0/0}$	40.4%	0.4%	p=0.983	6
Layer V	Ctrl	27.2%	0.7%		7
	ABCB1$^{0/0}$	29.3%	1.0%	p=0.108	5
	ABCG2$^{0/0}$	26.6%	0.2%	p=0.441	7
	ABCC1$^{0/0}$	25.7%	0.2%	p=0.068	6
Layer VI	Ctrl	19.5%	0.4%		7
	ABCB1$^{0/0}$	18.8%	0.7%	p=0.351	5
	ABCG2$^{0/0}$	20.6%	0.6%	p=0.140	7
	ABCC1$^{0/0}$	22.6%	0.9%	p=0.008	6

Table 31: Cortical layer distribution

4.4.2 Cellular density of the granular zone of the dentate gyrus

Impairments of neurogenic functions due to lack of ABC transporter function might be reflected in alterations of morphology of the dentate gyrus. To assess possible impairments, microphotographs of Nissl-stained cryo-slices were used to perform cell counts of the dentate gyrus' granular zone. The cell counts revealed a significant increase in the cell number of the granular zone in animals lacking the transporter ABCC1. In ABCC1$^{0/0}$ animals the cell number was increased by 22% compared to controls. Neither ABCB1$^{0/0}$ nor ABCG2$^{0/0}$ mice showed significantly altered cell density of the granular zone (Figure 23; Table 32).
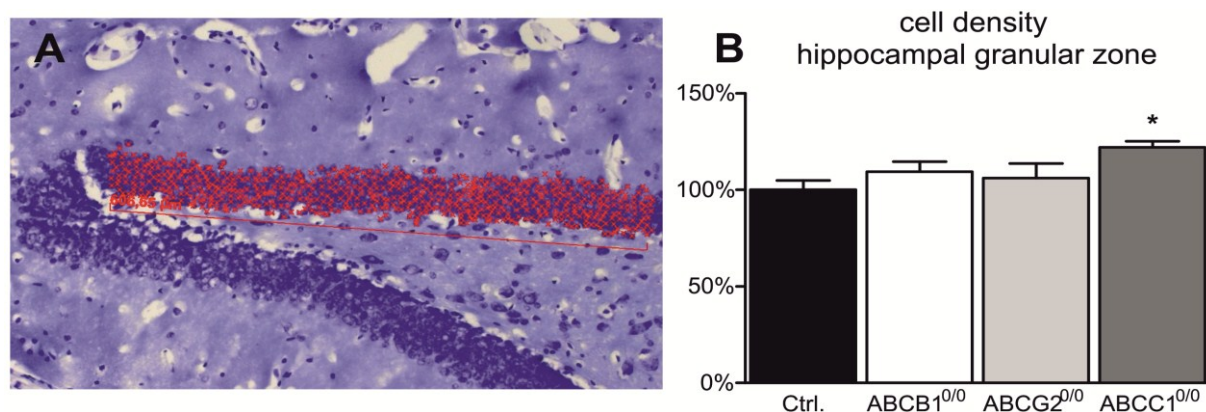
Figure 23: Loss of ABCC1 function results in altered cell density of the dentate gyrus. A fraction of the dentate gyrus of known length (606µm) was used for cell counting analyzes (A). The cell number was normalized to a fraction of 500µm in length and the measured cell counts were normalized to the controls (B) and revealed a significant increase in cell counts of ABCC1$^{0/0}$ animals (+22%). Error bar: SEM; Significance vs. Ctrl: *<p0.05

Mean number of cells per 500μm granular cell layer				
Strain	MEAN	±SEM	tTest vs. Ctrl	n
Ctrl	387	19		3
ABCB1$^{0/0}$	424	23	p=0.316	5
ABCG2$^{0/0}$	411	31	p=0.647	7
ABCC1$^{0/0}$	472	15	p=0.015	10

Table 32: Mean number of cells per 500μm granular cell layer

4.5   Behavioral experiments

Due to the fact that the hippocampus works as a main interface between cortical inputs and is involved in memory consolidation, it was of urgent importance to assess whether ABC deficiency is able to affect brain functions in a way impairing the behavioral phenotype. Standard behavioral assessments like y-maze, EPM and LDB experiments were utilized to evaluate levels of overall activity, anxious behavior and exploratory behavior [127-130].

4.5.1   Y-maze

The y-maze was used as experimental approach to analyze the overall activity and spontaneous alternation behavior. While spontaneous alternation behavior was not significantly altered as result of ABC transporter deficiency, overall activity was indeed significantly reduced in mice lacking expression of either ABCB1 or ABCG2 due to decreased overall running distance (Figure 25A, Table 33) and number of arm entries (Figure 24B; Table 33). In those mouse strains running distance was shortened by 13% (ABCB1$^{0/0}$) and 17% (ABCG2$^{0/0}$). The number of arm entries was as well significantly reduced in ABCB1$^{0/0}$ (-16%) and ABCG2$^{0/0}$ (-23%).
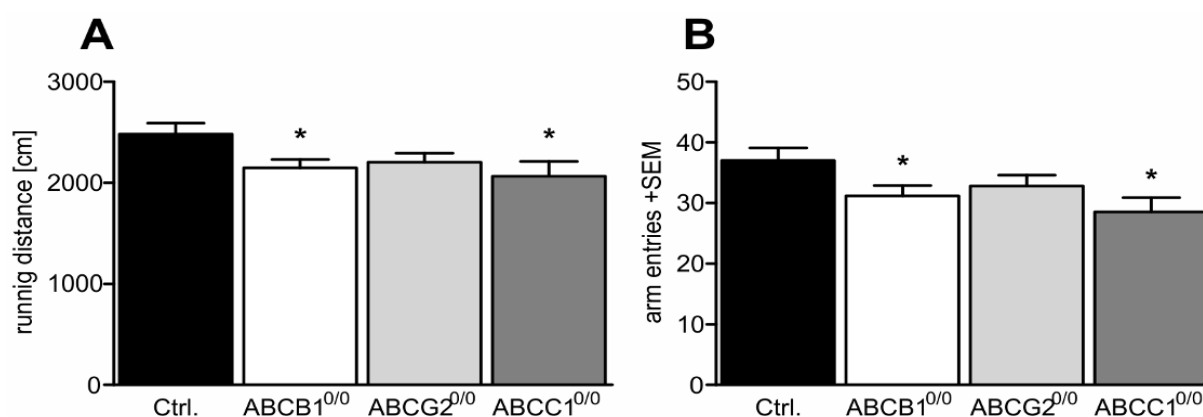
Figure 24: ABC deficiency leads to impaired exploratory activity. The diagrams show Y-maze-related parameters. Plotting the animals' course in the Y-maze, the running distance reveals a significant decrease in ABCB1- (-13%) and ABCC1- (-17%) deficient animals (A), while this parameter was only slightly, non-significantly decreased in ABCG2-deficient mice. The same behavioral pattern was detected for exploratory activity as assessed by the arm entries (ABCB1$^{0/0}$ -16%; ABCC1$^{0/0}$ -23%) (B). Error bar: SEM; Significance vs. Ctrl: *p<0.05

Y-maze Analysis					
	Strain	Mean	±SEM	t-Test	n
Running Distance	Ctrl	2480.4	110.3		19
	ABCB1$^{0/0}$	2149.6	82.0	p=0.022	16
	ABCG2$^{0/0}$	2204.3	89.0	p=0.059	23
	ABCC1$^{0/0}$	2066.9	144.7	p=0.034	11
Alterations	Ctrl	37.0	2.1		19
	ABCB1$^{0/0}$	31.2	1.7	p=0.040	16
	ABCG2$^{0/0}$	32.8	1.8	p=0.142	23
	ABCC1$^{0/0}$	28.5	2.4	p=0.013	11

Table 33: Y-maze Analysis

4.5.2 Elevated plus-maze

The elevated plus-maze is a standardized experimental approach to assess anxious behavior in rodents. This experimental setting is based on the principle of opposing motivations for exploring the environment on the one hand while avoiding open surroundings on the other. While exploratory drive is equal for each arm of the maze, open surroundings bear an anxiety driven aversion modulating the subjects entering probability of entering the open arms and resulting in less entries into the open arms [118].

The time spent in open arms was significantly decreased (-44% ABCB1$^{0/0}$; -31% ABCG2$^{0/0}$) in ABCB1 and ABCG2 deficient mice (Figure 25A, Table 34), while the decrease in ABCC1$^{0/0}$ mice did not reach statistical significance. In contrast all ABC deficient animals remained significantly longer in the enclosed compartments (+43% ABCB1$^{0/0}$, +24%

ABCG2$^{0/0}$, +32% ABCC1$^{0/0}$) than animals of the control strain (Figure 25B, Table 34). By comparing the running velocity in the open compartment no significant impairments were found in neither of the ABC deficient mouse strains (Figure 25C, Table 34). Therefore the parameter of running velocity was significantly altered in the enclosed compartment as a result of either ABCB1 or ABCC1 deficiency (Figure 25D, Table 34).
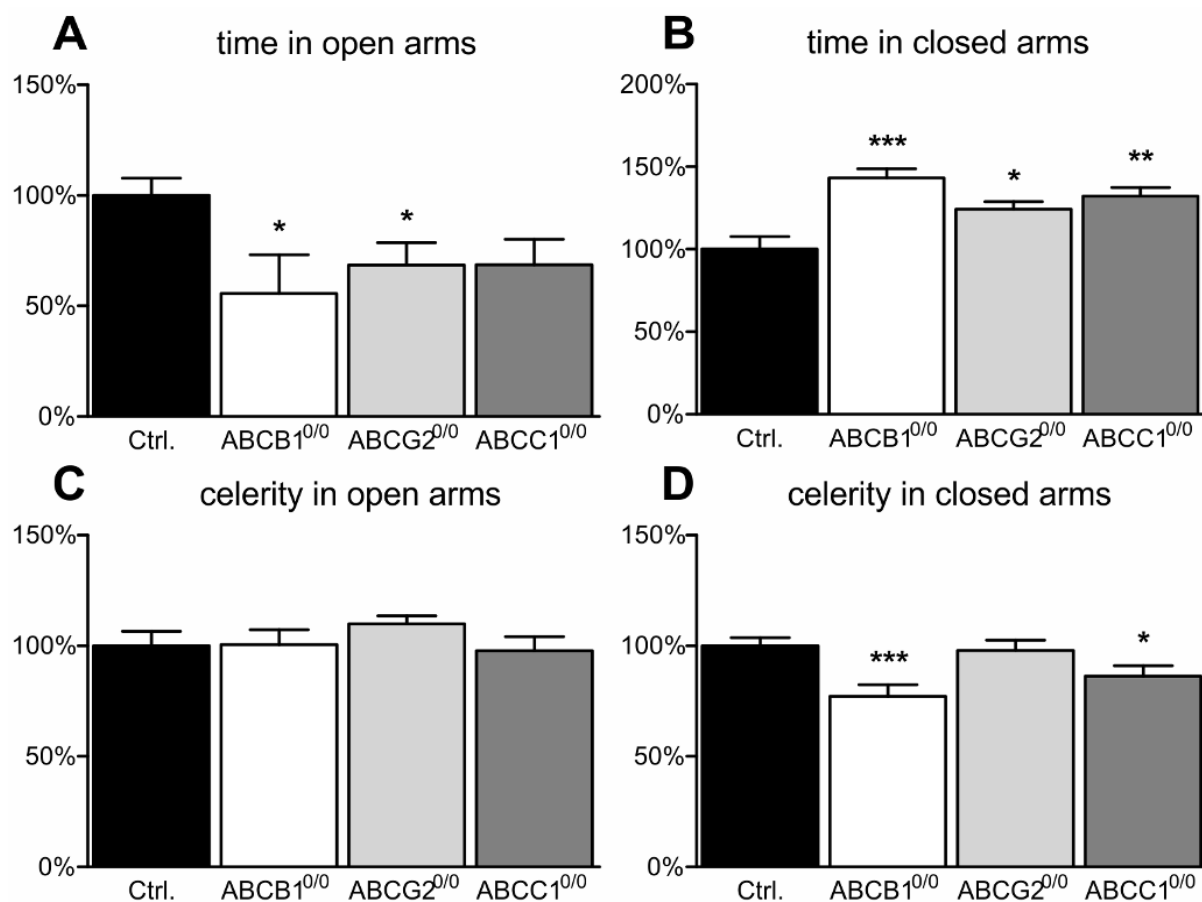
Figure 25: ABC transporter deficiency promotes anxiety. The diagrams show parameters assessed via the elevated plus maze. Mice deficient for ABCB1 (-44%) and ABCG2 (-32%) showed a significantly decreased presence in the open arms (A). The time of residence in the closed compartments was significantly increased in all ABC transporter-deficient mouse strains (ABCB1$^{0/0}$ +43%; ABCG2$^{0/0}$ +24%; ABCC1$^{0/0}$ +32%) (B). Running speed (celerity) in the open arms was not changed in any of the ABC transporter-deficient mice (C). ABCB1 (-23%) and ABCC1 (-14%) transporter-deficient mice showed significantly lower celerity values in the closed arms (D). Error bar: SEM; Significance vs. Ctrl *p<0.05; **p<0.01; ***p<0.001

EPM analysis					
Parameter	Strain	Mean	±SEM	tTest vs Ctrl	N
time in open parts	Ctrl	100%	13.0%		14
	ABCB1$^{0/0}$	56%	13.8%	p=0.007	18
	ABCG2$^{0/0}$	68%	10.2%	p=0.030	20
	ABCC1$^{0/0}$	72%	14.1%	p=0.149	13
time in closed parts	Ctrl	100%	7.8%		14
	ABCB1$^{0/0}$	141%	4.7%	p=0.000	18
	ABCG2$^{0/0}$	124%	4.6%	p=0.014	20
	ABCC1$^{0/0}$	132%	6.9%	p=0.015	13
celerity in open	Ctrl	100%	15.0%		14
	ABCB1$^{0/0}$	105%	19.6%	p=0.749	18
	ABCG2$^{0/0}$	146%	7.8%	p=0.182	20
	ABCC1$^{0/0}$	206%	3.3%	p=0.817	13
celerity in closed	Ctrl	100%	3.7%		14
	ABCB1$^{0/0}$	106%	5.2%	p=0.000	18
	ABCG2$^{0/0}$	80%	15.0%	p=0.730	20
	ABCC1$^{0/0}$	85%	18.6%	p=0.114	13

Table 34: EPM analysis

4.5.3 Light/Dark-box

As like in an open-field test the LD-box allows the assessment of overall exploratory behavior (running distance, rearing and compartment transition) in an open surrounding while also comprising an enclosed compartment which both in combination also allow the assessment of anxiety like behavior (light avoidance, differential activity in both compartments). With regard to activity within the open maze compartment, comparative analyzes of running speeds in ABC deficient animals showed no alterations compared to control mice (Figure 26A, Table 35).

In contrast, activity within the dark compartment was significantly altered as a result of ABC deficiency. In mice lacking expression of ABCB1 an increased activity was observed within the dark compartment due to longer running distance (+64%) in comparison to controls (Figure 26B, Table 35). Accordingly ABCB1$^{0/0}$ mice spent significantly more time within the dark compartment compared to controls (Figure 26C, Table 35). Both ABCB1 and ABCC1 deficient animals revealed impairments in exploratory behavior due to number of transitions between the two compartments. In both strains the number of transitions was significantly decreased compared to controls by 59% in ABCB1$^{0/0}$ and 49% in ABCC1$^{0/0}$ mice compared to controls (Figure 26D, Table 35). Rearing activity was also deemed as to be a characterizing parameter of exploratory behavior. Observations showed rearing activity in open-field compartment as to be decreased (-67%) in ABCC1$^{0/0}$ mice (Figure 26E, Table 35) while no differences were observed within the dark compartment (Figure 26F, Table 35). ABCB1$^{0/0}$

mice revealed no alterations in rearing activity in the open field area (Figure 26E, Table 35), though rearing activity is significantly increased in the dark compartment (+71%, Figure 26F; Table 35).
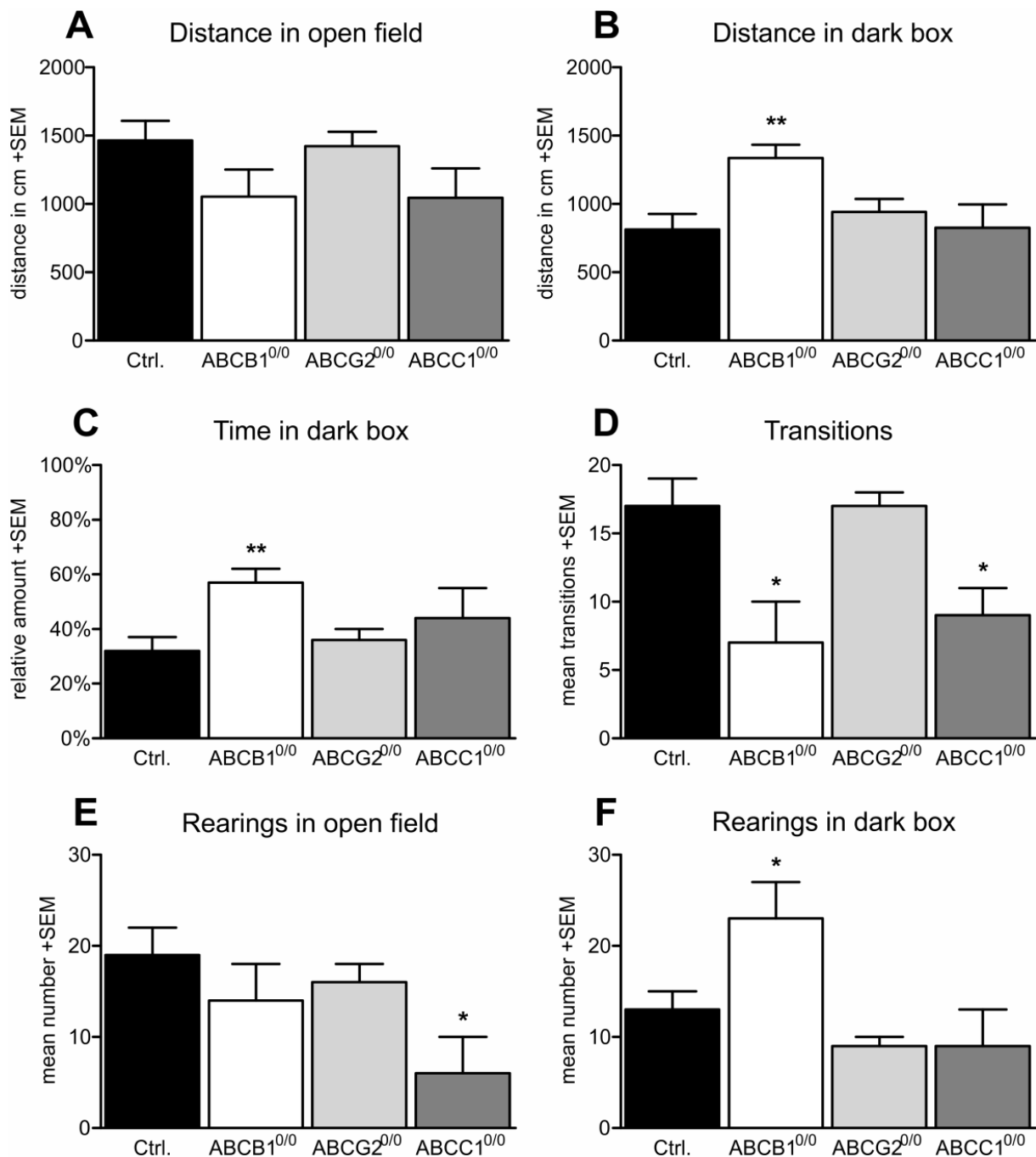
Figure 26: Light/dark box experiments verified altered anxiety and exploratory behavior. Comparing the running distance of the animals in the open field revealed no significant differences (A). However, the distance traveled by ABCB1-deficient mice (+64%) in the dark compartment (B) was significantly increased compared to the controls. Also, the time in the dark compartment (C) was significantly increased in ABCB1$^{0/0}$ mice (+78%) compared to controls. The mean number of transitions between the two compartments (D) was impaired in both ABCB1$^{0/0}$ (-59%) and ABCC$^{0/0}$ (-49%) mice. Comparing the rearing frequency in both compartments revealed a significant decrease for ABCC1$^{0/0}$ (-67%) mice in the open field (E), while the frequency was increased in the dark compartment (F) for ABCB1$^{0/0}$ (+71%) mice. Error bar: SEM; Significance vs. Ctrl: *$<$p0.05; **$<$p0.01

LDB analysis					
Parameter	Strain	Mean	±SEM	tTest vs. Ctrl	n
traveld in field	Ctrl	1466	141		9
	ABCB1$^{0/0}$	1054	199	p=0.109	10
	ABCG2$^{0/0}$	1423	106	p=0.809	9
	ABCC1$^{0/0}$	1046	215	p=0.128	21
traveled in box	Ctrl	812	116		9
	ABCB1$^{0/0}$	1335	97	p=0.003	10
	ABCG2$^{0/0}$	942	94	p=0.392	9
	ABCC1$^{0/0}$	825	170	p=0.950	21
time spend in dark	Ctrl	32	5		9
	ABCB1$^{0/0}$	57	5	p=0.002	10
	ABCG2$^{0/0}$	36	4	p=0.487	9
	ABCC1$^{0/0}$	44	11	p=0.351	21
transitions	Ctrl	17	2		9
	ABCB1$^{0/0}$	7	3	p=0.025	10
	ABCG2$^{0/0}$	17	1	p=0.900	9
	ABCC1$^{0/0}$	9	2	p=0.028	21
rearings in light	Ctrl	19	3		9
	ABCB1$^{0/0}$	14	4	p=0.337	10
	ABCG2$^{0/0}$	16	2	p=0.482	9
	ABCC1$^{0/0}$	6	4	p=0.036	21
rearings in dark	Ctrl	13	2		9
	ABCB1$^{0/0}$	23	4	p=0.048	10
	ABCG2$^{0/0}$	9	1	p=0.155	9
	ABCC1$^{0/0}$	9	4	p=0.410	21

Table 35: LDB analysis

4.5.4 *Effects of AD pathology on behavioral phenotypes in ABC deficient mice*

Due to the significant impact of Aβ-pathology on neurogenic functions in the hippocampal dentate gyrus and the pro-neuronal effect of Aβ-administration on differentiating NSPCs, possible effects on behavioral phenotypes had to be assessed in transgenic mice. The experiments were performed analogues to those performed with non-transgenic mouse strains.
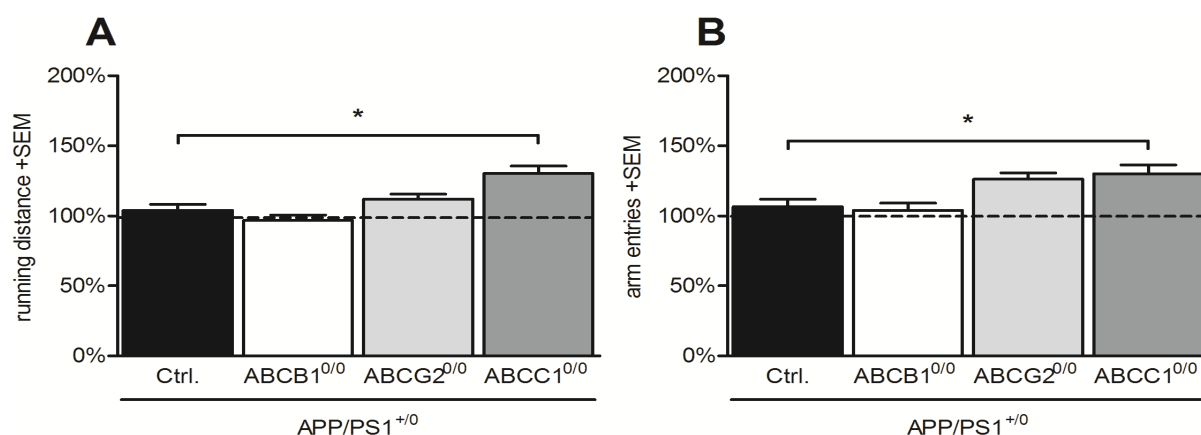
Figure 27: AD pathology significantly increases the activity in ABCC1$^{0/0}$ mice. The diagram indicates the relative change of behavioral parameters of ABC deficient transgenic mice in comparison to their respective non-transgenic counterparts. Shown are running distance and number of arm entries. Error bars: SEM; Significance vs. APP/PS1$^{+/0}$ transgenic control *p<0.05; Significance between transgenic and non-transgenic counterparts +p<0.05

Y-maze analysis in transgenic mouse strains						
Parameters	Strain	Mean	±SEM	tTest vs APP$^{+/0}$ Ctrl	tTest vs non-transgenic littermates	n
Running distance	Ctrl	2384.3	225.8		0.674	12
	ABCB1$^{0/0}$	2217.6	181.5	0.571	0.703	12
	ABCG2$^{0/0}$	1967.8	311.9	0.299	0.423	6
	ABCC1$^{0/0}$	1587.6	244.3	0.028	0.095	9
Arm entries	Ctrl	34.8	4.1		0.594	12
	ABCB1$^{0/0}$	30.0	3.7	0.396	0.739	12
	ABCG2$^{0/0}$	26.0	4.9	0.213	0.126	6
	ABCC1$^{0/0}$	21.9	4.4	0.046	0.181	9

Table 36: Y-maze analysis in transgenic mouse strains

While ABC deficiency clearly led to decreased activity and exploratory behavior as observed in ABCB1 and ABCC1 deficient animals, transgenic APP/PS1$^{+/0}$ mouse strains more likely showed a similar effect even though transgenic ABCB1$^{0/0}$ mice were mostly inconspicuous. The effect of Aβ-deposition on the behavioral phenotype was most obvious in ABCC1$^{0/0}$ transgenic mice. While the running activity (-29%, Figure 27A, Table 36) and the overall number of arm entries (-37%, Figure 27B, Table 36) was still decreased in ABCC1$^{0/0}$ transgenic mice compared to those parameters in APP/PS1$^{+/0}$ control mice. Therefore no significant differences were observed in transgenic mouse strains compared to their non-transgenic counterparts (Figure 27, Table 36).
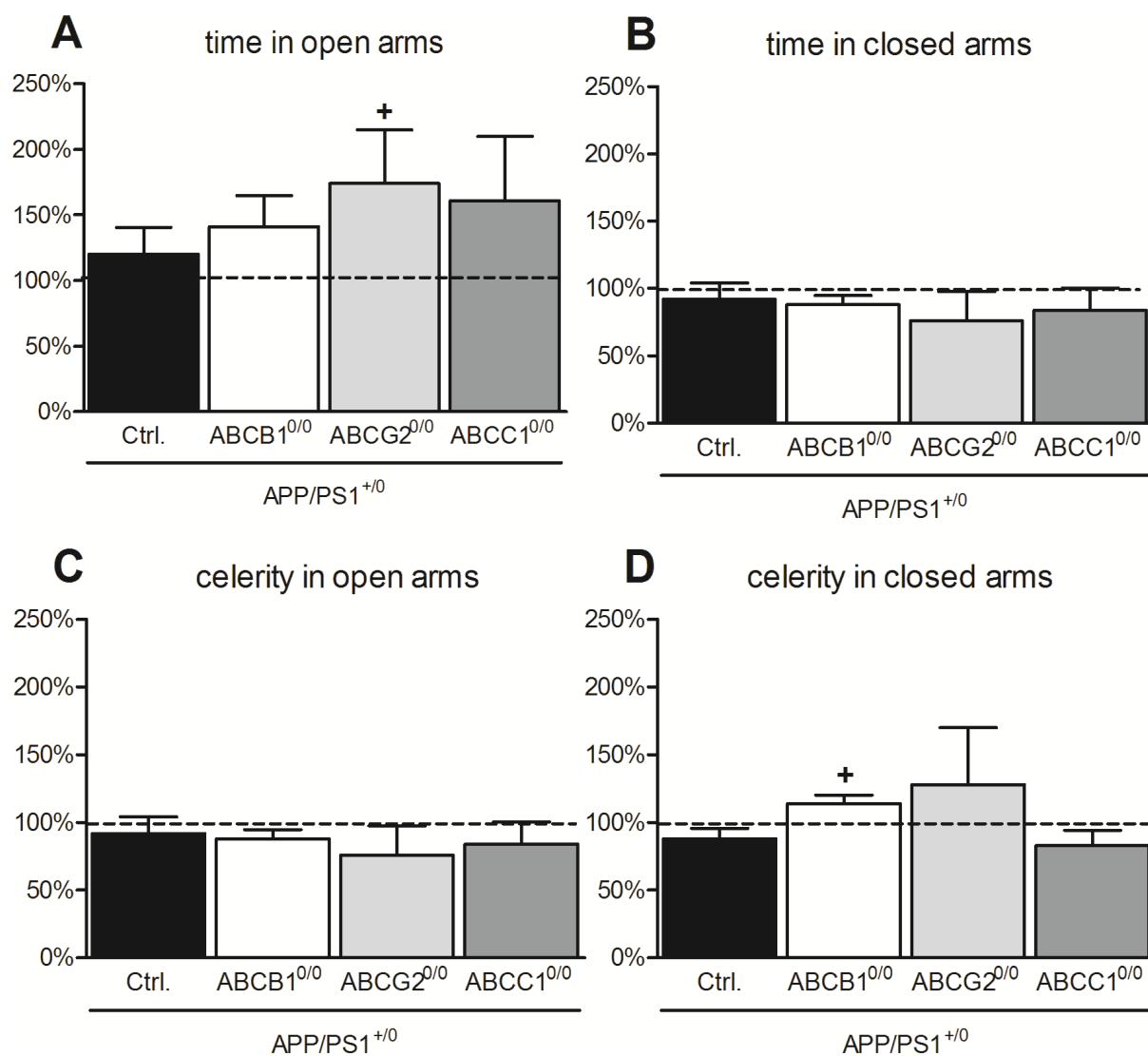
Figure 28: AD pathology alters anxiogenic behavior in ABC deficient mice. The diagram indicates the relative change of behavioral parameters of ABC deficient transgenic mice in comparison to their respective non-transgenic counterparts. Error bars: SEM; Significance vs. APP/PS1$^{+/0}$ transgenic control *p<0.05; Significance between transgenic and non-transgenic counterparts +p<0.05

EPM analysis in transgenic mouse strains						
Parameters	Strain	Mean	±SEM	tTest vs APP$^{+/0}$ Ctrl	tTest vs non-transgenic littermates	n
Time in open arms	Ctrl	120%	20.6%		p=0.466	13
	ABCB1$^{0/0}$	141%	23.9%	p=0.124	p=0.096	12
	ABCG2$^{0/0}$	174%	40.9%	p=0.995	p=0.018	4
	ABCC1$^{0/0}$	161%	49.1%	p=0.925	p=0.135	5
Time in closed arms	Ctrl	92%	12.2%		p=0.588	13
	ABCB1$^{0/0}$	88%	6.8%	p=0.052	p=0.104	12
	ABCG2$^{0/0}$	76%	21.8%	p=0.931	p=0.090	4
	ABCC1$^{0/0}$	84%	16.4%	p=0.432	p=0.297	5
Celerity in open arms	Ctrl	94%	7.1%		p=0.468	13
	ABCB1$^{0/0}$	108%	7.4%	p=0.251	p=0.377	12
	ABCG2$^{0/0}$	92%	27.3%	p=0.709	p=0.560	4
	ABCC1$^{0/0}$	68%	19.2%	p=0.165	p=0.084	5
Celerity in closed arms	Ctrl	88%	7.8%		p=0.121	13
	ABCB1$^{0/0}$	114%	6.3%	p=0.952	p=0.050	12
	ABCG2$^{0/0}$	128%	42.2%	p=0.171	p=0.161	4
	ABCC1$^{0/0}$	83%	11.5%	p=0.364	p=0.159	5

Table 37: EPM analysis in transgenic mouse strains

Also the anxious behavior, which was observed in non-transgenic control and ABC deficient mice, was not found to be statistically significant. While non-transgenic ABCB1$^{0/0}$ and ABCG2$^{0/0}$ mice showed significant anxious behavior, AD pathology lessened these effects and led to insignificant differences in between transgenic controls and ABC deficient mouse strains. The effect of Aβ deposition on behavioral parameters was most significant in ABCB1$^{0/0}$ and ABCG2$^{0/0}$ mice. The time of stay within the open arms was increased by +41% in ABCG2$^{0/0}$ APP/PS1$^{+/0}$ transgenic mice compared to non-transgenic ABCG2$^{0/0}$ animals (Figure 28A, Table 37). The other parameter, which was significantly altered by Aβ deposition, was the celerity in the closed arms, which was increased in ABCB1$^{0/0}$ transgenic mice by +14% (Figure 28D, Table 37). None of the parameters were significantly altered by ABC deficiency in transgenic mice compared to APP/PS1$^{+/0}$ controls.
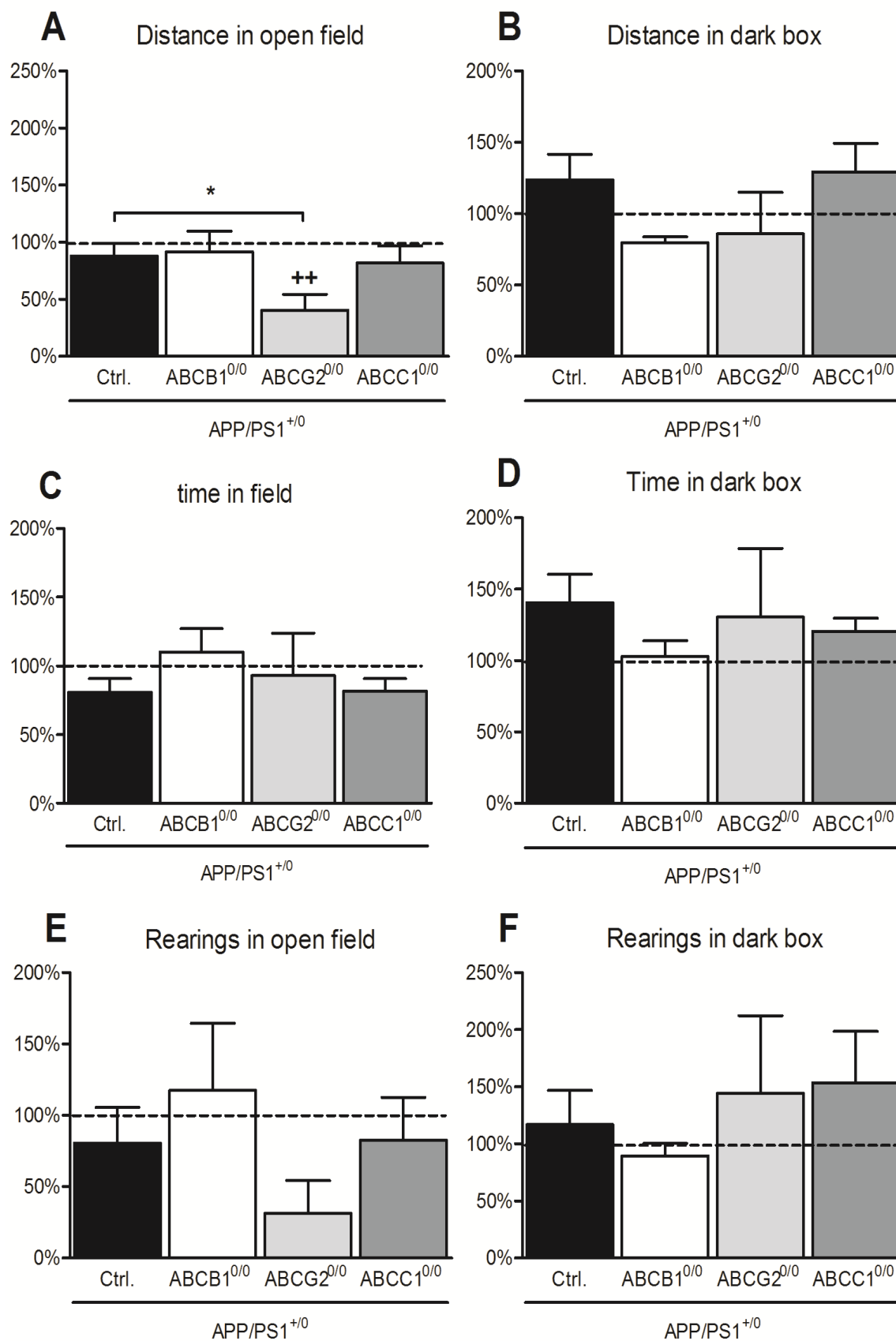
Figure 29: AD pathology enhances anxious behavior in ABCG2$^{0/0}$ mice. The diagram indicates the relative change of behavioral parameters of ABC deficient transgenic mice in comparison to their respective non-transgenic counterparts. Error bars: SEM; Significance vs. APP/PS1$^{+/0}$ transgenic control *p<0.05; Significance between transgenic and non-transgenic counterparts ++p<0.01

Also the LD-box experiments with ABC deficient AD mice showed results which were very conflicting to those made by analyzing non-transgenic mouse strains. While non-transgenic mice, deficient for ABCB1 and ABCC1, showed clear indications for impaired exploratory behavior in dependency of ABC transporter expression and stress level of their surroundings, LD-box experiments with transgenic mouse strains showed very different results. In fact the either ABCB1 or ABCG2 deficient transgenic mice showed no significant alterations in none of the analyzed parameters. Therefore, ABCG2 deficient mice harboring the human APP/PS1 transgene revealed altered exploratory behavior in the open field. The measured running distance in the open and stressful surrounding was significantly altered. This parameter, measured for $ABCG2^{0/0}$ transgenic mice, was reduced significantly by 55% compared to transgenic control mice. Compared to non-transgenic mice the reduction of the running distance was decreased even more by 60% (Figure 29A, Table 38).

LDB analysis in transgenic mouse strains						
Parameters	Strain	Mean	±SEM	tTest vs APP$^{+/0}$ Ctrl	tTest vs non-transgenic littermates	n
Distance in field	Ctrl	1287	161		p=0.411	10
	ABCB1	966	195	p=0.251	p=0.784	5
	ABCG2	576	195	p=0.028	p=0.003	4
	ABCC1	856	160	p=0.080	p=0.491	8
Distance in box	Ctrl	1003	143		p=0.307	10
	ABCB1	1065	54	p=0.770	p=0.086	5
	ABCG2	810	276	p=0.509	p=0.584	4
	ABCC1	1067	165	p=0.773	p=0.325	8
Time in field	Ctrl	54	7		p=0.116	10
	ABCB1	41	6	p=0.226	p=0.705	5
	ABCG2	51	17	p=0.832	p=0.760	4
	ABCC1	45	5	p=0.296	p=0.415	8
Time in dark box	Ctrl	45	6		p=0.113	10
	ABCB1	59	6	p=0.201	p=0.841	5
	ABCG2	47	17	p=0.876	p=0.309	4
	ABCC1	53	4	p=0.345	p=0.447	8
Rearings in open	Ctrl	15	5		p=0.512	10
	ABCB1	16	6	p=0.912	p=0.752	5
	ABCG2	5	4	p=0.224	p=0.059	4
	ABCC1	5	2	p=0.090	p=0.789	8
Rearings in box	Ctrl	16	4		p=0.625	10
	ABCB1	20	3	p=0.449	p=0.668	5
	ABCG2	13	6	p=0.743	p=0.348	4
	ABCC1	14	4	p=0.816	p=0.436	8

Table 38: LDB analysis in transgenic mouse strains

5   Discussion

The present study was planned and worked out to answer whether loss of ABC transporters would indeed lead to significant changes in neurogenesis or even to functional impairments *in vivo*. The study is motivated by repeated proposals that presumed that ABC transporters might be needed to be functionally expressed during NSPC development [53, 55, 62] due to observed transient ABC expression in NSPCs *in vitro*. Thereby it was shown for the first time that loss of ABC transporters indeed impairs neurogenic functions and leads to cognitive impairments which could possibly be even linked to the observed changes in cortical cytoarchitecture. By following different approaches and performing analyzes *in vivo* and *in vitro*, the results suggest the conclusion that the observed effects of ABC transporter loss occur mostly as a result of changes in the brain's homeostasis rather than being based upon cell-intrinsic effects. The results revealed that even ABCC1 as another ABC transporter, not mentioned before regarding NSPC functions, is critical for neurogenic functions under distinct circumstances like cortical injury.

5.1   Quantification of hippocampal neurogenesis

To evaluate changes in neurogenic functions of the adult brain with regard to lost ABC transporter functions, neuronal progenitors at different states of differentiation were labeled by means of immunofluorescence and quantified for statistical analyzes. Analyzes were performed with the goal to label early NSPCs, neuronal restricted progenitors and newly generated fully functional neurons. It was also of great importance to simultaneously label for BrdU intake as a marker of recent proliferation. Therefore marker proteins were chosen, which are reliably expressed during critical phases of NSPC differentiation and maturation. Due to the technical limitations only three fluorescence signals were simultaneously detectable, which were represented by the marker protein, BrdU and DAPI as the nuclear marker. Due to that limitation it was decided to use Sox2 as the marker for the early NSPC population, DCX for neuronal progenitors of the type-2b and type-3 phase and Calretinin for functional and newly generated neurons.

As Sox2 is expressed in radial glia cells (type-1 cell) until the late type-2a cell state, it would have been desirable if it was possible to simultaneously label for other markers of early neural stem cells like for example GFAP. But, the co-expression of GFAP and Sox2 is very difficult

to assess by immunofluorescence techniques due to GFAP protein is largely limited to the cellular processes and is nearly absent in the cell soma, which would make any conclusions about quantities of GFAP$^+$/Sox2$^+$ stem cells very questionable while marker A (GFAP) is mostly expressed in the cellular processes and marker B (Sox2) is a nuclear expressed protein. Unlike in reactive astrocytes, GFAP is also often too low expressed in common astrocytes to be even detectable by means of immunofluorescence, leading to confusing results [131]. Therefore expression of cytoplasmic GFP under control of the GFAP promoter would have been necessary [10] as it was used in a number of different studies [132, 133].

Unfortunately, for the present study, this approach is very impractical according to analyzes needed to be done in different ABC transporter knockout mouse strains, primarily not containing this transgene. Another problem is, which was even mentioned in the original paper of Nolte et al. [134] who generated the GFAP-eGFP transgenic mice, that the GFP expression does not exactly correlate to the actual localization of the GFAP protein. Especially, within the hippocampus and the supra chiasm, only a small fraction of astrocytes are actually eGFP$^+$. By labeling GFAP in retinal slices, it became most obvious that eGFP expression occurred only in distinct astrocyte populations like the Müller glial cells, while astrocytes of the same layer apparently lacked eGFP expression [134]. Even the possibility of false-positive labeled non-astrocytes by means of GFAP-driven marker expression has been discussed and cannot be excluded [131]. According to these mentioned shortcomings, co-staining for GFAP would rather not significantly improve the results.

Even the consideration of a possible advantage of co-staining for another early NSPC marker like for example Tbr2 appeared doubtful according to the following argumentation. In particular Tbr2 was often presumed as to be expressed only in early NSPCs, in 2008 Hodge and Kempermann showed that Tbr2 is even still expressed in neuronal committed type-2b neuronal progenitors, while Sox2 seems to be expressed only until the type-2a differentiation state [135]. So, Tbr2 expression would significantly overlap with DCX expression and would also label intermediate progenitors (type-2) and neuronal committed type-3 precursors. Yet, Englund et al. showed in 2005, that Tbr2 seems to be expressed during neuronal commitment in the type-2b state and is even found in 20% NeuN$^+$ cells, which from there on should be clearly considered as neurons beyond the progenitor state [136]. Indeed only 5% of the Tbr2$^+$ cells were actually positive for Nestin, a marker which is widely considered as to be expressed robustly in the earliest stem cells until type-2b differentiation [10]. Due to Nestin expression lasting even longer than that of Sox2, it appears very odd to assume having a more

robust marker for early NSPCs when labeling for Tbr2 and Sox2 if only 5% of the Tbr2^{+} cells show expression of another well-established NSPC marker. The value of Tbr2 labeling appears even more dubious in regard to another study, published in 2008 by Hodge and colleagues [135], who apparently used the same anti-Tbr2 antibody as Englund before (provided by the Lab of R.F. Hevner, without designation of the actual clone), which led to very different results showing that Tbr2 expression mostly overlaps with that of DCX.

In favor for the approach used here, the paper of Steiner and colleagues [10] should be cited, who prepared a very comprehensive analysis on morphology and marker expression of NSPCs at distinct states of differentiation. It supports the argument that, Sox2^{+} cells of the hippocampal SGZ are mostly early neuronal progenitors of the typ-1 and type-2 state. According to the microphotographs shown in their publication, only a subset of cells of at most 10-15% of the Sox2^{+} cells found in the hippocampal SGZ could perhaps be mistakenly counted S100β[+] astrocytes. Taken the progenitor cells as basis, virtually all Type-1 progenitors are Sox2^{+} while at least 80% of the type-2a progenitors are expressing Sox2. Only about 25% of the yet neuronal restricted type-2b progenitors show a significant Sox2 expression, while the expression of Sox2 becomes absent when reaching the type-3 progenitor state. The Sox2 labeled progenitor pool is thereby composed out of ca. 40% type-1 progenitors and over 50% type-2a cells while a minor fraction of under 10% are actually type-2b and type-3 cells [10]. Therefore it's absolutely valid to address the SGZ's progenitor collectivity by labeling with Sox2 alone, whereas an overwhelming majority of around 90% of those cells are or could become neuronal committed and would thereby very well reflect possible changes in progenitor quantities due to loss of distinct ABC transporter expression.

For each state of cellular differentiation several useful marker proteins whose expression is largely overlapping during these distinct phases of cellular differentiation could be cited. Nevertheless DCX and Calretinin are, as largely agreed to in the literature, very specifically expressed during early neuronal commitment in type-2b and typ-3 cells until the cells become postmitotic as in the case of DCX [123, 124], or become first expressed in postmitotic neurons during cell migration and dendritic targeting [125]. Therefore the quantification of either DCX[+] or Calretinin[+] cell populations should very well reflect changes in neuronal progenitor cell populations and those postmitotic newly generated neurons.

Inasmuch as the Sox2^{+} cell population was not significantly altered, it should be legal to address the early NSPC pool as not being impaired by lack of ABC transporter function. At least the BrdU[+] cell fraction of the Sox2 positive cells was impaired by lack of ABC

transporter expression, which might indicate alterations in the NSPC turnover. This assumption might even fit to the finding of increased numbers of BrdU incorporated cells in the Calretinin$^+$ cell fraction which might also indicate a somehow enhanced NSPC turnover in animals lacking ABC transporter expression. So, ABC transporter expression might be needed in NSPCs for maintenance of their stem cell character. Otherwise, lack of ABC function leads to fastened NSPC differentiation. Although NSPC differentiation may be fastened, neurogenesis is in contrast impaired in general due to loss of ABC transporters ABCB1 and ABCC1 as indicated by significantly decreased numbers of cells positive for DCX or Calretinin.

5.1.1 Effects of cortical injury on adult neurogenesis

By performing CCI experiments, involvement of another ABC transporter, formerly not mentioned with regard to neurogenic processes, could be disclosed as to be involved in neurogenic processes under distinct circumstances like cortical injuries. The cortical injury and the thereby demanded increased neuronal regeneration potential revealed that even ABCC1 plays a role in homeostatic processes that control neuroregenerative processes. Mice, deficient for ABCC1$^{0/0}$, showed severe impairments in neuronal differentiation, which did not occur under normal circumstances. These circumstances support the idea of ABC transporters being very important for maintaining the brain's homeostasis, especially that of the stem cell niche. Because ABC transporters convey a lot of biological and metabolic substrates [22-24], loss of ABC transporter function could severely change the brain's homeostasis leading to the observed results.

Due to the location of the stem cell niche between the vascular and the ventricular system, impairments in ABC mediated transport of metabolites might directly affect the NSPC's fate. This seems realistic due to NSPCs even interact with both systems [137] which makes the possibility even more realistic that NSPC fate is depending on ABC transporter functions. It is thinkable that in absence of ABC transporter function, distinct metabolites can reach functional or even toxic concentrations within the stem cell niche due to insufficient transport activity. Distinct cell types like for example endothelial cells are able to release soluble factors which directly affect NSPC functions [138]. Assuming such factors as to be possible ligands for ABC transporters it is very likely that ABC transporter function could indirectly intervene on neurogenic functions by maintaining the homeostasis of the microenvironment of the stem cell niche.

5.1.2   AD pathology and neurogenesis

Evaluating the effect of AD pathology, especially that of Aβ deposition, seems to be depending heavily on the used transgene model. Various mouse models used for studying the Aβ deposition aspect of Alzheimer's disease are already described in the literature. In dependency of the use of specific human APP isotypes and promoters for expressing the transgene, the effects on neurogenic functions differ heavily. Some studies suggest increased neurogenesis in general [95] or at distinct time points [97]. However, most studies reported impairing effects on neurogenic functions [101, 139]. For the combined Thy1-APPKM670/671NL - Thy1-PS1L166P AD model [105] which was used here, no studies on neurogenic functions have been performed before. Interestingly, these mice show a very early and heavy β-amyloid plaque load [36, 105] which separates them from most of the other available AD mouse models.

Due to the fact that the function of APP and its metabolites are still under heavy discussion, the differences in APP isotypes and expressional properties within the different AD models might contribute to the differential effects on neurogenic functions. While the Aβ peptides, generated as a result of amyloidogenic APP degradation, are deemed to be neurotoxic in a low oligomeric state, there is even evidence for a neuroprotective role for the β-amyloid. Indeed, Aβ was found to be cleaved from APP during early embryogenesis and seems to be important for normal brain development [140, 141]. Aβ monomers have shown to promote survival of developing neurons *in vitro* under withdrawal of neurotrophic factors [142]. Also beneficial effects of low dose administration of $A\beta_{1-40}$ and $A\beta_{1-42}$ to proliferating NSPCs were observed *in vitro* while both isoforms differentially altered the cell fate of differentiating NSPCs [143]. The properties of β-amyloids as neurotrophic and neuroprotective factors imply far-ranging influence in physiological brain functions like neurogenesis [144].

Interestingly, these pro-neurogenic effects of AD pathology were strongly depending on ABC transporter equipment of the different mouse strains. As like ABC transporter equipment heavily and differentially altered the intracortical quantities of soluble and insoluble Aβ [36], even the rate of neuroregeneration is depending on ABC transporter expression in AD pathology as results of NSPC quantification in transgenic mice revealed when compared to their non-transgenic counterparts. The fact that neurogenesis does not seem to be altered simply in a way of Aβ concentration-depending manner – neurogenesis was most significantly increased in transgenic $ABCG2^{0/0}$ mice compared to their non-transgenic counterparts, while transgenic control mice showed significantly lower Aβ-deposition which

was therefore heavily increased in ABCC$^{0/0}$ transgenic mice –moreover might depend on the exact oligomeric state of β-amyloid. Specific quantification of soluble and insoluble Aβ indeed showed decreased concentrations of soluble Aβ$_{42}$ in ABCG2$^{0/0}$ transgenic mice compared to ABCC1$^{0/0}$ and control transgenic mice while the concentration of insoluble Aβ lied somewhere between that of the ABCC1$^{0/0}$ and control AD mice. The delicate differences in concentration of soluble and insoluble Aβ imply different binding affinities of Aβ in distinct states of oligomerization to the analyzed ABC transporters. Lack of distinct transporters might therefore not only alter the overall concentration of intracortical Aβ but also alter the homeostasis of oligomeric states of the β-amyloids leading to the observed effects on adult neurogenesis.

5.2 *In vitro* analyzes of NSPC functions with regard to ABC transporter equipment

According to the presumptions of Islam and colleagues [53, 55, 62], functional ABC transporter expression should be necessary for proper NSPC functions and their loss should in contrast lead to cell-intrinsic malfunctions and impaired NSPC differentiation capacity. While the results of the *in vivo* assessment of neurogenic functionality in ABC transporter deficient mouse strains indicated that loss of ABCB1 and ABCG2 hampers NSPC maturation, the question remained open whether these effects were of cell-intrinsic nature or a result of impaired brain homeostasis. To gain more insight into this question, NSPCs were harvested from mouse brains and were cultivated *in vitro* for performing experiments on proliferation and differentiation capacity. Interestingly, proliferation experiments did not show any impairment due to loss of ABC transporter expression. In contrast, NSPCs lacking ABCG2 expression displayed even increased proliferation potential, a manner which did not fit properly to the observations made *in vivo*. Beside the small changes in proliferation capacity observed with regard to loss of ABC transporters, differentiation experiments did not show any correlation between ABC transporter expression and differentiation capacity.

However this outcome might be owed to the artificial cell culture environment which ABCG2$^{0/0}$ NSPCs might be able to cope best with. In fact these observations otherwise correctly support the idea of ABC transporters maintaining a critical microenvironment within the stem cell niche that is needed for proper stem cell functions.

5.2.1   Effects of Aβ₄₂ administration on NSPC cultures

In the view of the many differing results from studies analyzing the effects of Aβ administration on NSPC cultures *in vitro*, analogous experiments were performed for this study. To assess the nature of Aβ's influence on NSPC functions, NSPC cultures were incubated with 1μM Aβ$_{42}$ during proliferation and differentiation. The results revealed a significant pro-neuronal change in NSPC's differentiation fate at least for NSPC cultures of the control mouse strain due to significantly more generated neurons after Aβ treatment. Otherwise NSPCs showed no alterations under proliferative conditions with regard to Aβ treatment.

While several indications allow the assumption of Aβ having a neuroprotective effect because of transiently increased Aβ concentrations found in the interstitial fluid of patients with acute brain injury [145] and beneficial effects of Aβ administration to neuronal cell cultures [142, 146, 147], it is still under discussion whether cytotoxic or pro-neuronal effects predominate in NSPC functions. Here, a huge problem is Aβ's property of spontaneously aggregating into a variety of oligomers and fibrils of different sizes. Though, there are protocols in use for forcing Aβ oligomerization and providing solutions containing distinct oligomer species [115]. Studies on these distinct oligomeric species revealed different traits mostly concerning their respective level of cytotoxicity [115] but also their potential influence on stem cell functions [116]. Even though most of the experimenters abode to the original Aβ preparation protocol [115], the study's results often did not integrate easily. While oligomeric Aβ$_{42}$ was deemed to impair neuronal differentiation in neural stem cells at low micromolar concentrations [143], the opposite effect was found elsewhere [116, 148]. With regard to the different effects of distinct oligomeric Aβ species [116], it is very conceivable that minor and involuntary changes in the Aβ preparation protocol lead to unpredictable changes in the configuration of the comprising Aβ oligomer species and thereby leading to those conflicting results.

The present study's results did not reveal significant cytotoxic effects on neither proliferating nor differentiating NSPCs at concentrations around 1μM oligomeric Aβ$_{42}$. Instead Aβ$_{42}$ enhanced neuronal differentiation when applied to NSPCs of the control strain without having any significant effect on proliferation in neither of the analyzed control and ABC knock out strains. Due to the negating effect of ABC deficiency on the pro-neuronal differentiation trait of Aβ$_{42}$, it is conceivable that ABC transporters are of functional importance for cellular homeostasis with regard to trans-membrane Aβ efflux.

Unfortunately the results of the *in vitro* experiments are not directly comparable with those of the *in vivo* NSPC quantifications. However at least all APP/PS1$^{+/0}$ transgenes showed more or less increased rates of neurogenesis compared to their respective non-transgenic counterparts. But still the question remains whether enhanced neurogenesis is more or less a result of AD pathology-dependent neuronal loss or triggered by increased concentration of interstitial Aβ species.

5.3   mRNA expression analyzes

5.3.1   Expression of ABC transporter mRNA in NSPCs

Expression of distinct ABC transporters in stem cells has been excessively discussed and was observed even in neural stem and progenitor cells before [55]. Transient protein expression was directly observed for ABCB1 and ABCG2 [53, 62]. Due to the vast number of different ABC transporters, which often largely overlap in their metabolite binding profile, it is very conceivable to find these proteins highly co-regulated, like it is known for other gene families, for ensuring redundant transporter protein expression. Concerning that, expression analyzes regarding the expression of the three transport proteins of interest were performed. These analyzes showed also, that the murine ABCB1 transporter, which in contrast to the human analogue comprises out of two subtypes namely ABCB1a and ABCB1b, is differentially expressed in NSPCs. However, only the subtype ABCB1b was found to be expressed in NSPCs while ABCB1a lacked expression. Previous studies also sought for possible co-regulations in the expression of ABC transporters but remained inconclusive, though they only analyzed whole brain homogenates without concerning cell type specific expression and/or regulation [149].

According to the present results, for the first time a co-regulation between the expression of ABCB1 and ABCG2 has been found. Even ABCC1 might be altered due to state of ABCG2 expression. With regard to previous studies, that never found significant co-regulation between these genes, this regulatory effect might only occur in distinct cell types like stem and progenitor cells. Otherwise, the regulatory momentum impedes the assessment of importance of single ABC transporter expression to stem cell functions due to the co-regulations of other transporters, possibly masking the resulting impact of the lost transporter on NSPC function. Still, in view of the contradicting findings of the *in vivo* and *in vitro* analyzes concerning NSPC functions, the possibly protective effect co-regulated ABC transporter expression in NSPCs might still be overrun by the more far-ranging effects of

ABC deficiency on the brain's homeostasis, especially that of the stem cell niche, though impairing neurogenic functions.

5.3.2   *Expression of genes relevant to neurogenesis*

MibI expression

Mindbomb 1 (MibI), as an E3 ligase, is one major key member of the Notch signaling network which controls a number of cell determination events like neurogenic processes within NSPCs. Together with Neuralized (Neur), Mib1 cooperatively regulates the endocytosis of Notch ligands like Jagged1 and Delta and ubiquinates Delta [150]. Mib1 activity might also be required in the S3 cleavage of the Notch receptor to form the Notch intracellular domain 1 (NICD1), which itself has transcriptional activity on several genes, like for example the members of the hairy and enhancer split domain (HES) genes, that have great influence on the differentiation fate of NSPCs [151]. Thus, Mib1 indirectly influences the cell fate of NSPCs. Its expression level could indirectly be linked to changes in NSPC differentiation. Studies showed that Notch signaling is critical for maintaining the stem cell character of radial glia cells. By conditional inactivation of Mib1, Notch ligand endocytosis was blocked leading to loss of Notch signaling and thereby to complete depletion of radial glia cells in transgenic mice [152].

The analyzes performed on MibI mRNA expression levels revealed significantly higher expression rates of MibI *in vitro* and *in vivo*. That seemed at least to be consistent to observations of impaired neuronal differentiation capacity in ABCB1 deficient mice. As significantly impaired neuronal differentiation was only observed *in vivo* and therefore implicated that these impairments might be owed mostly to changes in brain homeostasis alone, these data might reflect also slight cell-intrinsic imbalances in signaling cascades impairing neuronal differentiation.

Mash1

Mash1 or Ascl1 for archaete scute complex homologe 1, is a pro-neuronal transcription factor which is found being expressed in a number of different progenitor populations during embryonic development of the telencephalon [153, 154]. Functional overexpression led to increased numbers of differentiated neurons in transduced progenitor cells *in vitro*. On the other hand, loss of Mash1 expression accordingly led to loss of basal ganglia neurons and cortical interneurons in the telencephalon.

Otherwise, Mash1 seems to play an ambivalent role as a regulator of NSPC differentiation. While it is often simply referred to as a neuronal specific regulator of NSPC differentiation, it was also found to be expressed in oligodendrocytic precursors [155]. Analyzes with Mash1$^{0/0}$ mutants revealed a special role for Mash1 expression in developmental processes of the telencephalon where early oligodendrocytic precursor populations are lost when lacking Mash1 expression [156]. Hence Mash1 is not simply affecting neuronal but also oligodendrocytic lineage expression.

Mash1expression levels were not affected by the status of ABC transporter expression as a cell-intrinsic effect like in vitro analyzes revealed. That was not surprising with regard to the *in vitro* NSPC differentiation results, which did not indicate any impairments of neuronal differentiation capacity due to loss of ABC transporter expression.

Otherwise, analyzes of hippocampal tissue from ABCC$^{0/0}$ mice revealed a significantly decreased mRNA expression of Mash1 compared to control animals which was not linked with impairments in neuronal differentiation as demonstrated by immunofluorescence analyzes of NSPC quantities. These data might instead indicate possible alterations in oligodendrocytic cell populations which were not further analyzed in this study.

Notch1

The Notch signaling system represents a cell-to cell signaling cascade which provides adjacent cells the ability to influence the cell fate of their direct neighbors. This cell-across feedback system has the function to maintain cellular diversity and to suppress uncontrolled cell proliferation or differentiation, ensuring the maintenance of a cell-type homeostasis. While Notch signaling is active in a given cell, this cell itself is not able to express Notch activating ligands by itself and thereby disabling the cell's possibility to activate Notch in their direct neighbors, leading to sharply distinct expression patterns in neighboring cells and a mosaic like cell distribution [157]. Different studies also suggest that Notch activation is leading to differential effects depending on the exact nature of neuronal progenitor population. Activation of Notch1 in neuronal and oligodendrocytic progenitors actually inhibits further differentiation into the according cell linage while activation in glial progenitors is promoting their differentiation into astrocytes as revealed by several loss and gain of function studies [158].

The mRNA analyzes of NSPCs *in vitro* and *in vivo* showed contradicting results. Matching the mostly unaltered proliferation capacity *in vitro*, also the Notch1 mRNA expression levels

remained inconspicuous. Therefore the expression of Notch1 seemed to be influenced by lacking ABC transporter expression *in vivo*. Analyzes of hippocampal mRNA samples showed significantly increased levels of Notch1 expression in ABCB1 deficient mice, while in contrast, Notch expression was slightly but significantly decreased in $ABCC1^{0/0}$ mice compared to controls. The increased Notch1 expression fits well to the results of NSPC quantification which indicated impaired neuronal differentiation. This effect might be owed to increasing Notch signaling in $ABCB1^{0/0}$ mice. On the other hand $ABCC1^{0/0}$ mice showed slightly decreased Notch expression while neuronal differentiation remained mostly unaffected. This slight increase in NSPC quantities might be the result of Notch signaling altered into the observed direction.

Jagged1

Beside Delta, Jagged1 is one key ligand for Notch receptor activation. Binding of Jagged1 to Notch leads to activation of the Notch pathway, which is a major signaling pathway in neurogenic functions. Thus Jagged expression is found widely expressed across the neurogenic zones of the adult central nervous system [159]. Binding of the membrane bound Notch ligand to the Notch receptor leads to intracellular cleavage of Notch and thereby to activation of the Notch pathway and the suppression of pro-neuronal gene expression.

At least the changes in Notch signaling, which were observed *in vivo*, seemed not to be the result of altered Jagged1 signaling, due to the fact that the expression of this Notch ligand remained unchanged. Therefore the expression of Notch1 appeared to be increased *in vitro* in all ABC deficient cell lines while this increase only reached statistical significance in $ABCB1^{0/0}$ cell lines compared to control lines. The alteration in Jagged1 expression *in vitro* does not easily integrate into the results of the proliferation and differentiation experiments which were also performed *in vitro*. The results of those experiments showed that differentiation was not affected by lacking ABC expression and proliferation capacity was only significantly altered in $ABCG2^{0/0}$ NSPCs. Altered Jagged1 expression might reflect the differential coping abilities of the cell lines depending on their distinct ABC transporter equipment.

Nestin

Nestin is a specific intermediate filament protein which is expressed in neuronal stem and progenitor cells. It is first expressed in type-1 cells or radial glia cells which also express the astrocytic marker GFAP and the radial glia marker BLBP while showing a characteristic

morphology. The expression of Nestin is still found in neuronal committed type-2b cells and thereby makes Nestin a classical marker for neuronal stem and progenitor cells [135, 160].

Due to the fact that Nestin is expressed during a very early phase of NSPC development, it was not surprising to find Nestin expression unaltered in regard to ABC transporter deficiency in NSPC cultures. All cells in culture have a comparable state of differentiation and are rapidly proliferating, implying a relatively stable gene expression profile.

In contrast to the findings of the in vitro experiments, expression analyzes of Nestin mRNA revealed increased mRNA levels in $ABCB1^{0/0}$ and $ABCC1^{0/0}$ mice, while the values at least reached statistical significance only in $ABCB1^{0/0}$ mice in comparison to controls. Altered Nestin gene expression levels into that direction does not easily integrate to the findings of the NSPC quantification results, where neuronal differentiation was observed as being impaired in mice lacking ABCB1 expression. But these data might indicate impaired signaling transduction within the NSPC compartment leading to malfunctions during neuronal commitment of NSPCs resulting in impaired numbers of DCX positive neuronal progenitors. The increased Nestin expression might be seen as an artifact, maybe resulting from frustrating overexpression of Nestin within NSPCs during malfunctioning differentiation processes. It could be also possible to find early NSPCs, responsible for the enhanced Nestin expression, differentiated instead into glial or oligodendroglial lineage which was not analyzed during the NSPC quantification experiments *in vivo*. Contrariwise, one would have assumed to find increased numbers of early NSPCs which was not observed by quantifying the number of Sox2 positive cells.

DCX

The microtubule associated protein DCX is mostly expressed during neuronal commitment of late typ-2 cells and type-3 cell stadium where neuronal progenitors become postmitotic late neuronal progenitors while the expression of DCX sharply decreases with the beginning expression of adult neuronal markers [161].

In order to complete the mRNA analyzes, even the proliferating NSPC cultures were tested for DCX expression. In general, the expression level of this gene would have been expected as to be very low, due to the fact that DCX is mostly expressed in later stages of NSPC differentiation. Though, studies regarding the *in vitro* proliferation capacity of NSPCs have often shown that NSPCs tend to start differentiation even under proliferative conditions and show several markers of advanced differentiated progenitor cells like Nestin and DCX [162]

Otherwise it's quite interesting that ABC transporter equipment seems to alter the expression level of DCX mRNA. While all ABC deficient cell lines showed a trend towards increased expression of the pro-neural marker DCX, statistical significance was only reached in ABCB1$^{0/0}$ deficient cell lines, which might be a hint suggesting that even though ABC transporter equipment decides about NSPC's proliferation capacity within certain limits.

It is also quite intriguing that even *in vivo*, significantly increased DCX mRNA expression was observed while the number of DCX positive cells was contrarily significantly decreased.

Unfortunately mRNA expression and protein concentration do not necessarily correlate very well. It is known that even the same mRNA expression rate of eukaryotic genes could result in a very wide range of protein concentration (up to 20-fold) [163]. There are many factors hampering the correlation of mRNA and protein levels like complicated and varied post-transcriptional mechanisms and differing protein half-lives *in vivo* [164] which could explain the contradicting results of hippocampal mRNA levels and NSPC quantification results.

5.4   Histological analyzes

The observed changes in hippocampal neurogenesis brought up the question whether these impairments might also impact upon the brain's cytoarchitecture. The ontogenesis of the brain, like even all other organs, is a very delicate process which relies on the extreme precision of all undergoing proliferative and migratory proceedings, finally culminating in the most complexity of the mammalian brain. Developmental disorders can affect the laminar positioning of cortical pyramidal neurons. Such displacements can dramatically affect cognitive functions [165]. Like it was shown for neurogenic functions of the adult brain, alterations of the brain's homeostasis might have impairing effects on neuronal differentiation also during ontogenesis and thereby on developmental processes of the whole brain, which might result in altered cytoarchitecture.

Histological analyzes have been performed to answer this question. For quantification of neuronal density and measurements of the cortical lamination, paraffin embedded brain slices were stained for the neuronal marker NeuN. To exclude possible miss-interpretations of cellular density due to unequal staining intensities, all brain slices were stained using an automated staining system and the same batch of chemicals and antibodies. All brain hemispheres were digitized using a computerized microscope and area quantifications were performed using the same software macro for all slices.

These analyzes did not reveal any significant changes in neuronal density of the neocortex as a result of lacking ABC transporter expression. However, significant changes in the cortical layer's cytoarchitecture were observed. Lack of ABC transporter ABCB1 led to a significant decrease of thickness of layer 1 while all other layers were not affected. Also ABCC1$^{0/0}$ mice showed significant alterations in cortical cytoarchitecture due to significantly increased thickness of cortical layer VI, while even here all other layers seemed not to be affected.

While impairments in cortical layer's cytoarchitecture lead to a vast number of different cognitive malfunctions [165-167], these alterations could possibly explain the behavioral phenotypes like shown in 4.5., which were most significant even in ABCB1 and ABCC1 deficient animals. While anxious behavior and drive are not primarily related to cortical functions, the changes in cytoarchitecture observed in the cortical areas might be only the tip of the iceberg, implying far ranging changes also in other brain areas.

At least for the ABCC1$^{0/0}$ mice, measurements of the cell density of the hippocampal gyrus dentatus evidenced such alterations even in other brain regions.

5.5 Behavioral experiments

Analyzes of ABC deficient animals revealed functional interactions between ABC transporter expression and neurogenic functions of the adult brain and even indicated possible alterations during brain ontogenesis due to altered cortical cytoarchitecture. These results demanded further analyzes of possible significant behavioral phenotypes in ABC knockout mice. Several behavioral tests were performed to investigate the mice's overall activity, their exploratory behavior and in general their level of anxiety.

5.5.1 Y-maze

The Y-maze is used for assessing the spontaneous alternation behavior. Studies revealed that during exploration of a y-shaped mace, rodents prefer to enter an arm which was previously not investigated, due to alternations rates significantly above chance. This behavior is considered as to be showing their willingness for exploring their environment [168] and is meant to reflect the performance of the mice's spatial working memory [169]. The alternation behavior also depends on the subject's level of anxiousness and the alternation level decreases with increasing anxiety [170].

ABC transporter deficiency seemed not to affect the performance of the mice's spatial working memory in accordance to the results of the y-maze analyzes. There were no changes

in the alternation behavior observable. In contrast, the y-maze analyzes revealed impairments in the mice's anxiety levels accompanied by a decreased exploratory drive. Both parameters, total running distance and number of arm entries were significantly decreased in animals deficient for either ABCB1 or ABCC1 compared to the control mice. Interestingly, these strains were both also most conspicuous due to altered neurogenic functions and cortical cytoarchitecture.

5.5.2 Plus-maze

The results of the y-maze analyzes suggested impaired anxiety levels and altered exploratory drive in animals deficient for distinct ABC transporters. As a result of these indications, further analyzes needed to be done to assess anxiety behavior. The elevated plus-maze is an advanced procedure based on the early work of Montgomery, who used different y-shaped mazes with different open and enclosed alleys, observing increased exploratory behavior in rats within the enclosed arms [118]. Years of debate followed the studies of Montgomery concerning the relationship between novelty fear and exploration. Finally in 1984, Handley and Mithani introduced their "elevated x-maze" which was formed plus-shaped, was elevated above ground level and comprised two open and enclosed arms [171]. Studies on anxiolytic drugs using the elevated plus maze revealed its potency in studying anxious behavior in rodents [172]. From there on the plus-maze was the medium of choice when coming to assess anxious behavior in rodents.

The distance traveled in the different arms is evaluated as the locomotive activity of the subjects, while parameter of rearing frequency is supposed to reflect the animal's exploratory drive [173]. While even the number of counted transitions between the open and enclosed compartments comprises an explorative momentum, this parameter should be considered as to be much more influenced by the anxiety level. At last, the length of stay in the enclosed compartment should be considered as a direct indicator of the subject's anxiety level.

The results of the plus-maze support the implications from the y-maze, that ABC-deficiency is impairing the explorative drive of the animals by altering the anxiety level of these animals. Again, strains deficient for expression of either ABCB1 or ABCC1 appeared most conspicuous during the plus-maze experiments. ABCB1$^{0/0}$ mice showed the most significant preference for the enclosed compartments and appeared even more active and explorative in the enclosed compartments compared to the controls, while their behavior did not appear conspicuous in the open areas. ABCC1 deficient animals showed themselves only to be less explorative in the open field and less often switched between open and enclosed areas. Hence,

the impact of ABCB1 deficiency on behavioral parameters appeared more severe than that after loss of ABCC1. ABCB1 deficiency seemed to affect both, anxiety level and explorative drive in general. Here the motivation for explorative behavior might be even increased but overrun by increased anxiety level. In ABCC1$^{0/0}$ mice, only the frequency of rearing is decreased in the open areas and the frequency of switching into these areas, indicating that here only anxiety levels might by slightly increased

5.5.3 LDB maze

To complete the assessment for spontaneous behavior in terms of locomotive activity, exploration and anxiety, the mice were finally tested in the light-dark-box maze. The LDB setup is based on the ethological view of shifting the relative propensities of exploring a new surrounding and avoiding to be exposed within the open space. It was first developed by Crawley and Goodwin [174] and was used from thereon in numbers of behavioral studies. The test, as like as exploration tests in general, reflects a type of anxiety linked with uncontrollable stress or a kind of depressive anxiety due to the fact that the animal is exposed to an aversive environment from which it cannot escape [175].

Complex behavioral alterations in ABC deficient mouse strains were revealed by LD-box experiments. Here, both ABCB1$^{0/0}$ and ABCC1$^{0/0}$ mice showed a significant avoidance of the lighted compartment compared to the controls. Interestingly, ABCB1$^{0/0}$ mice revealed an increased exploratory behavior under non-stress conditions in the dark area while behavior is not altered under stressful light exposure. Otherwise, ABCC1$^{0/0}$ showed no altered behavior under non-stress conditioned while seemed to be more anxious under light exposure. These data indicate complex alteration within the neuronal networking due to lost ABC transporter function.

While altered neurogenic functions might also contribute to cognitive performance in spatial learning and orientation tasks [176], the mouse strains used in this study were unfortunately not suitable for use in tests based on visual cues. Due to a mutation of the retinal phosphodiesterase, FVB/N mice suffer from retinal degeneration leading to visual deficits within the first 30 days of live [177, 178]. The performance in other behavioral tasks should not be impaired by this mutation due to the left ability for light perception and the rodent's nature of strongly relying on tactile stimuli for orientation [179]. Like shown in previous studies the mice are able to orient within the mazes narrow corridors and can easily recognize open areas, as like in the LDB, or the abyss of the plus-maze [180].

Still it remains unclear whether the impaired transport capacity leads to an actual impairment of the wiring of distinct neuronal networks, as indicated by altered cortical cytoarchitecture, or rather the behavioral alterations are an effect based on changes of the biological milieu within the brain. In fact steroids for example are ABC transporter substrates [181] and are also able to alter anxious behavior within a special set of hippocampal neurons [182]. Further investigation should be performed on possible ontogenetic effects of ABC transporter deficiency and the exact nature of changed milieu within the brain.

5.5.4 *Behavioral phenotypes of APP/PS1$^{+/0}$ transgenic mouse strains*

Due to the fact that alterations in ABC transporter expression had significant effects on the behavioral phenotypes, the question remained whether AD pathology additionally affects mice's behavior and in which dimension it does. Since transgenic AD mouse models were generated to model aspects of AD pathology like Aβ deposition, studies on behavioral phenotypes were performed and mostly found significant behavioral deficits analogous to Alzheimer's disease in humans. Independent from the used human APP transgenes and their promoters used for driving their expression, most mouse strains showed behavioral deficits like neophobia [117], increased anxiety and aggressiveness [183] and either increased [183, 184] or decreased [185] activity/motility levels. They also revealed a significantly declined cognitive performance due to decreased alternation rates in the y-maze [117, 128, 184, 185] and decreased escape latencies in the Morris-water-maze [185]. Quantitative differences of behavioral deficits between the various transgenic AD mouse models might result from the different quantities of Aβ deposition and localization depending on the used transgenes and promoters driving their expression.

The results from behavior assessment of the ABC deficient APP/PS1$^{+/0}$ transgenic mice did not easily integrate. While y-maze analyzes revealed only significantly increased activity rates for ABCC1$^{0/0}$ transgenic mice compared to their respective non transgenic counterparts and APP/PS1$^{+/0}$ controls, results of the plus-maze and LDB analyzes only showed significantly altered anxious behavior for ABCG2$^{0/0}$ transgenic mice. Those animals showed themselves to be most affected by open surroundings in the open arms of the plus-maze and the lighted compartment of the LDB, resulting in increased anxiety related behavior. Comparing the relative changes in behavioral parameters between transgenic and non-transgenic animals, the changes were not found to be congruent throughout the different ABC-deficient strains and the controls.

A possible explanation for these incongruent relative changes in behavioral parameters throughout the analyzed transgenic mouse strains might be the ABC transporter specific transport capacity for distinct Aβ species. One of the latest publications of our workgroup showed the distinct effects of ABC transporter deficiency on the cortical Aβ deposition rate [36]. The study confirmed distinct transport capacities for each of the analyzed transporters. These specific clearance capacities resulted in specific deposition rates of insoluble Aβ and even more significantly differing concentrations of its soluble forms. The data also showed cyclic correlations between concentrations of soluble and insoluble Aβ species over time. This suggests a complex connection between Aβ production, clearance and deposition, significantly depending on ABC transporter specific transport capacities. Although overall Aβ burden might became predictable using mathematical modeling, still the exact localization of each Aβ deposition remains random. The defects of neuronal circuitry and the resulting effects stay unpredictable and might contribute to the scattering results of the behavioral assessment.

5.6   Conclusions

The present study contributes basic knowledge about the various physiological functions of ATP binding cassette transporters. The results documented herein could partly support the hypothesis of ABC transporters, ABCB1 and ABCG2 in particular, being involved in neuroregenerative processes. But according to the presented results, this functional involvement is taken place less likely on the cellular level of the NSPCs themselves. It seems that ABC transporter deficit much more likely intrigues the delicate homeostasis of the stem cell niche, thereby altering neurogenic functions in the way it has been observed here. Just as like as ABC transporters are responsible for extrusion of cytotoxic metabolites across the blood brain barrier to prevent pathogenesis of proteopathies like Alzheimer's disease, they are even necessary for maintaining the brain's stem cell pool and thereby secure the brain's regeneration capacity even into late adulthood. Indication has been found that loss of single ABC transporter is actually able to affect brain homeostasis resulting even in altered cytoarchitecture and behavioral phenotypes.

With regard to the vast number of ABC transporter modulating drugs used in treatment of chronic and acute diseases, more understanding of the specific transport capacities for metabolites, cytokines and such alike has to be achieved in order to fully understand the links between disease pathologies and regenerative processes. Such knowledge would allow the

invention of new treatment options for various kinds of neurodegenerative diseases by simply modulating the transport activity for distinct compounds for instance to advocate the extrusion of toxic compounds or otherwise selectively modulate transport of physiologically active metabolites to enhance regenerative processes.

6   Appendix

6.1   References

1.   Sidman, R.L., I.L. Miale, and N. Feder, *Cell proliferation and migration in the primitive ependymal zone: an autoradiographic study of histogenesis in the nervous system.* Exp Neurol, 1959. **1**: p. 322-33.
2.   Altman, J. and G.D. Das, *Autoradiographic and histological evidence of postnatal hippocampal neurogenesis in rats.* J Comp Neurol, 1965. **124**(3): p. 319-35.
3.   Kaplan, M.S. and J.W. Hinds, *Neurogenesis in the adult rat: electron microscopic analysis of light radioautographs.* Science, 1977. **197**(4308): p. 1092-4.
4.   Paton, J.A. and F.N. Nottebohm, *Neurons generated in the adult brain are recruited into functional circuits.* Science, 1984. **225**(4666): p. 1046-8.
5.   Reynolds, B.A. and S. Weiss, *Generation of neurons and astrocytes from isolated cells of the adult mammalian central nervous system.* Science, 1992. **255**(5052): p. 1707-10.
6.   Richards, L.J., T.J. Kilpatrick, and P.F. Bartlett, *De novo generation of neuronal cells from the adult mouse brain.* Proc Natl Acad Sci U S A, 1992. **89**(18): p. 8591-5.
7.   Eriksson, P.S., et al., *Neurogenesis in the adult human hippocampus.* Nat Med, 1998. **4**(11): p. 1313-7.
8.   Gage, F.H., *Mammalian neural stem cells.* Science, 2000. **287**(5457): p. 1433-8.
9.   Kriegstein, A. and A. Alvarez-Buylla, *The glial nature of embryonic and adult neural stem cells.* Annu Rev Neurosci, 2009. **32**: p. 149-84.
10.   Steiner, B., et al., *Type-2 cells as link between glial and neuronal lineage in adult hippocampal neurogenesis.* Glia, 2006. **54**(8): p. 805-14.
11.   Ming, G.L. and H. Song, *Adult neurogenesis in the mammalian brain: significant answers and significant questions.* Neuron, 2011. **70**(4): p. 687-702.
12.   Huangfu, D. and K.V. Anderson, *Cilia and Hedgehog responsiveness in the mouse.* Proc Natl Acad Sci U S A, 2005. **102**(32): p. 11325-30.
13.   Mirzadeh, Z., et al., *Neural stem cells confer unique pinwheel architecture to the ventricular surface in neurogenic regions of the adult brain.* Cell Stem Cell, 2008. **3**(3): p. 265-78.
14.   Doetsch, F., et al., *Subventricular zone astrocytes are neural stem cells in the adult mammalian brain.* Cell, 1999. **97**(6): p. 703-16.
15.   Lois, C. and A. Alvarez-Buylla, *Long-distance neuronal migration in the adult mammalian brain.* Science, 1994. **264**(5162): p. 1145-8.
16.   Carleton, A., et al., *Becoming a new neuron in the adult olfactory bulb.* Nat Neurosci, 2003. **6**(5): p. 507-18.
17.   Brill, M.S., et al., *Adult generation of glutamatergic olfactory bulb interneurons.* Nat Neurosci, 2009. **12**(12): p. 1524-33.
18.   Zhao, C., W. Deng, and F.H. Gage, *Mechanisms and functional implications of adult neurogenesis.* Cell, 2008. **132**(4): p. 645-60.
19.   Kosaka, T. and K. Hama, *Three-dimensional structure of astrocytes in the rat dentate gyrus.* J Comp Neurol, 1986. **249**(2): p. 242-60.
20.   Filippov, V., et al., *Subpopulation of nestin-expressing progenitor cells in the adult murine hippocampus shows electrophysiological and morphological characteristics of astrocytes.* Mol Cell Neurosci, 2003. **23**(3): p. 373-82.
21.   Seri, B., et al., *Cell types, lineage, and architecture of the germinal zone in the adult dentate gyrus.* J Comp Neurol, 2004. **478**(4): p. 359-78.
22.   Ferreira, M.J. and I. Sa-Nogueira, *A multitask ATPase serving different ABC-type sugar importers in Bacillus subtilis.* J Bacteriol, 2010. **192**(20): p. 5312-8.
23.   Gisin, J., et al., *A Rhodobacter capsulatus member of a universal permease family imports molybdate and other oxyanions.* J Bacteriol, 2010. **192**(22): p. 5943-52.
24.   Linton, K.J., *Structure and function of ABC transporters.* Physiology (Bethesda), 2007. **22**: p. 122-30.
25.   Tournier, N., et al., *Opioid transport by ATP-binding cassette transporters at the blood-brain barrier: implications for neuropsychopharmacology.* Curr Pharm Des, 2011. **17**(26): p. 2829-42.
26.   Hirano, T., *At the heart of the chromosome: SMC proteins in action.* Nat Rev Mol Cell Biol, 2006. **7**(5): p. 311-22.
27.   Hopfner, K.P., et al., *Structural biology of Rad50 ATPase: ATP-driven conformational control in DNA double-strand break repair and the ABC-ATPase superfamily.* Cell, 2000. **101**(7): p. 789-800.
28.   Kozak, L., et al., *Elf1p, a member of the ABC class of ATPases, functions as a mRNA export factor in Schizosacchromyces pombe.* J Biol Chem, 2002. **277**(37): p. 33580-9.
29.   Dean, M., Y. Hamon, and G. Chimini, *The human ATP-binding cassette (ABC) transporter superfamily.* J Lipid Res, 2001. **42**(7): p. 1007-17.
30.   Dean, M. and T. Annilo, *Evolution of the ATP-binding cassette (ABC) transporter superfamily in vertebrates.* Annu Rev Genomics Hum Genet, 2005. **6**: p. 123-42.
31.   Sarkadi, B., et al., *ABCG2 -- a transporter for all seasons.* FEBS Lett, 2004. **567**(1): p. 116-20.
32.   Juliano, R.L. and V. Ling, *A surface glycoprotein modulating drug permeability in Chinese hamster ovary cell mutants.* Biochim Biophys Acta, 1976. **455**(1): p. 152-62.

33. Kartner, N., et al., *Daunorubicin-resistant Chinese hamster ovary cells expressing multidrug resistance and a cell-surface P-glycoprotein.* Cancer Res, 1983. **43**(9): p. 4413-9.

34. Pahnke, J., M. Krohn, and K. Scheffler, *[The role of blood-brain barrier in the pathogenesis of Alzheimer dementia--implications for immunological therapies for plaque dissolution].* Fortschr Neurol Psychiatr, 2009. **77 Suppl 1**: p. S21-4.

35. Pahnke, J., et al., *Alzheimer's disease and blood-brain barrier function-Why have anti-beta-amyloid therapies failed to prevent dementia progression?* Neurosci Biobehav Rev, 2009. **33**(7): p. 1099-108.

36. Krohn, M., et al., *Cerebral amyloid-beta proteostasis is regulated by the membrane transport protein ABCC1 in mice.* J Clin Invest, 2011. **121**(10): p. 3924-31.

37. Hoof, T., et al., *Cystic fibrosis-type mutational analysis in the ATP-binding cassette transporter signature of human P-glycoprotein MDR1.* J Biol Chem, 1994. **269**(32): p. 20575-83.

38. Choudhuri, S. and C.D. Klaassen, *Structure, function, expression, genomic organization, and single nucleotide polymorphisms of human ABCB1 (MDR1), ABCC (MRP), and ABCG2 (BCRP) efflux transporters.* Int J Toxicol, 2006. **25**(4): p. 231-59.

39. Borst, P. and A.H. Schinkel, *Genetic dissection of the function of mammalian P-glycoproteins.* Trends Genet, 1997. **13**(6): p. 217-22.

40. Gottesman, M.M. and I. Pastan, *Biochemistry of multidrug resistance mediated by the multidrug transporter.* Annu Rev Biochem, 1993. **62**: p. 385-427.

41. Higgins, C.F. and M.M. Gottesman, *Is the multidrug transporter a flippase?* Trends Biochem Sci, 1992. **17**(1): p. 18-21.

42. Jones, P.M. and A.M. George, *The ABC transporter structure and mechanism: perspectives on recent research.* Cell Mol Life Sci, 2004. **61**(6): p. 682-99.

43. Karwatsky, J., et al., *Binding of a photoaffinity analogue of glutathione to MRP1 (ABCC1) within two cytoplasmic regions (L0 and L1) as well as transmembrane domains 10-11 and 16-17.* Biochemistry, 2003. **42**(11): p. 3286-94.

44. Loscher, W. and H. Potschka, *Drug resistance in brain diseases and the role of drug efflux transporters.* Nat Rev Neurosci, 2005. **6**(8): p. 591-602.

45. Leschziner, G.D., et al., *ABCB1 genotype and PGP expression, function and therapeutic drug response: a critical review and recommendations for future research.* Pharmacogenomics J, 2007. **7**(3): p. 154-79.

46. Cordon-Cardo, C., et al., *Multidrug-resistance gene (P-glycoprotein) is expressed by endothelial cells at blood-brain barrier sites.* Proc Natl Acad Sci U S A, 1989. **86**(2): p. 695-8.

47. Schinkel, A.H., *P-Glycoprotein, a gatekeeper in the blood-brain barrier.* Adv Drug Deliv Rev, 1999. **36**(2-3): p. 179-194.

48. Lam, F.C., et al., *beta-Amyloid efflux mediated by p-glycoprotein.* J Neurochem, 2001. **76**(4): p. 1121-8.

49. Vogelgesang, S., et al., *The role of P-glycoprotein in cerebral amyloid angiopathy; implications for the early pathogenesis of Alzheimer's disease.* Curr Alzheimer Res, 2004. **1**(2): p. 121-5.

50. Cirrito, J.R., et al., *P-glycoprotein deficiency at the blood-brain barrier increases amyloid-beta deposition in an Alzheimer disease mouse model.* J Clin Invest, 2005. **115**(11): p. 3285-90.

51. Alison, M.R., *Tissue-based stem cells: ABC transporter proteins take centre stage.* J Pathol, 2003. **200**(5): p. 547-50.

52. Borovski, T., et al., *Cancer stem cell niche: the place to be.* Cancer Res, 2011. **71**(3): p. 634-9.

53. Islam, M.O., et al., *Characterization of ABC transporter ABCB1 expressed in human neural stem/progenitor cells.* FEBS Lett, 2005. **579**(17): p. 3473-80.

54. Yamamoto, A., et al., *ABCB1 is predominantly expressed in human fetal neural stem/progenitor cells at an early development stage.* J Neurosci Res, 2009. **87**(12): p. 2615-23.

55. Lin, T., O. Islam, and K. Heese, *ABC transporters, neural stem cells and neurogenesis - a different perspective.* Cell Res, 2006. **16**(11): p. 857-71.

56. Bates, S.E., et al., *The role of half-transporters in multidrug resistance.* J Bioenerg Biomembr, 2001. **33**(6): p. 503-11.

57. Litman, T., et al., *The multidrug-resistant phenotype associated with overexpression of the new ABC half-transporter, MXR (ABCG2).* J Cell Sci, 2000. **113 (Pt 11)**: p. 2011-21.

58. Rocchi, E., et al., *The product of the ABC half-transporter gene ABCG2 (BCRP/MXR/ABCP) is expressed in the plasma membrane.* Biochem Biophys Res Commun, 2000. **271**(1): p. 42-6.

59. Leslie, E.M., R.G. Deeley, and S.P. Cole, *Multidrug resistance proteins: role of P-glycoprotein, MRP1, MRP2, and BCRP (ABCG2) in tissue defense.* Toxicol Appl Pharmacol, 2005. **204**(3): p. 216-37.

60. Krishnamurthy, P., et al., *The stem cell marker Bcrp/ABCG2 enhances hypoxic cell survival through interactions with heme.* J Biol Chem, 2004. **279**(23): p. 24218-25.

61. Diestra, J.E., et al., *Frequent expression of the multi-drug resistance-associated protein BCRP/MXR/ABCP/ABCG2 in human tumours detected by the BXP-21 monoclonal antibody in paraffin-embedded material.* J Pathol, 2002. **198**(2): p. 213-9.

62. Islam, M.O., et al., *Functional expression of ABCG2 transporter in human neural stem/progenitor cells.* Neurosci Res, 2005. **52**(1): p. 75-82.

63. Leslie, E.M., R.G. Deeley, and S.P. Cole, *Toxicological relevance of the multidrug resistance protein 1, MRP1 (ABCC1) and related transporters.* Toxicology, 2001. **167**(1): p. 3-23.

64. Cole, S.P., et al., *Overexpression of a transporter gene in a multidrug-resistant human lung cancer cell line.* Science, 1992. **258**(5088): p. 1650-4.

65. Gradhand, U. and R.B. Kim, *Pharmacogenomics of MRP transporters (ABCC1-5) and BCRP (ABCG2).* Drug Metab Rev, 2008. **40**(2): p. 317-54.

66.   Rao, V.V., et al., *Choroid plexus epithelial expression of MDR1 P glycoprotein and multidrug resistance-associated protein contribute to the blood-cerebrospinal-fluid drug-permeability barrier.* Proc Natl Acad Sci U S A, 1999. **96**(7): p. 3900-5.

67.   Chaudhary, P.M. and I.B. Roninson, *Expression and activity of P-glycoprotein, a multidrug efflux pump, in human hematopoietic stem cells.* Cell, 1991. **66**(1): p. 85-94.

68.   Wolf, N.S., et al., *In vivo and in vitro characterization of long-term repopulating primitive hematopoietic cells isolated by sequential Hoechst 33342-rhodamine 123 FACS selection.* Exp Hematol, 1993. **21**(5): p. 614-22.

69.   Goodell, M.A., et al., *Isolation and functional properties of murine hematopoietic stem cells that are replicating in vivo.* J Exp Med, 1996. **183**(4): p. 1797-806.

70.   Lechner, A., et al., *Nestin-positive progenitor cells derived from adult human pancreatic islets of Langerhans contain side population (SP) cells defined by expression of the ABCG2 (BCRP1) ATP-binding cassette transporter.* Biochem Biophys Res Commun, 2002. **293**(2): p. 670-4.

71.   Norwood, K., et al., *An in vivo propagated human acute myeloid leukemia expressing ABCA3.* Leuk Res, 2004. **28**(3): p. 295-9.

72.   Chiba, T., et al., *Side population purified from hepatocellular carcinoma cells harbors cancer stem cell-like properties.* Hepatology, 2006. **44**(1): p. 240-51.

73.   Ueda, T., et al., *Cloning and functional analysis of the rhesus macaque ABCG2 gene. Forced expression confers an SP phenotype among hematopoietic stem cell progeny in vivo.* J Biol Chem, 2005. **280**(2): p. 991-8.

74.   Bunting, K.D., et al., *Enforced P-glycoprotein pump function in murine bone marrow cells results in expansion of side population stem cells in vitro and repopulating cells in vivo.* Blood, 2000. **96**(3): p. 902-9.

75.   Broccardo, C., et al., *ABCA2 is a marker of neural progenitors and neuronal subsets in the adult rodent brain.* J Neurochem, 2006. **97**(2): p. 345-55.

76.   Sulkava, R., et al., *Accuracy of clinical diagnosis in primary degenerative dementia: correlation with neuropathological findings.* J Neurol Neurosurg Psychiatry, 1983. **46**(1): p. 9-13.

77.   De Strooper, B. and W. Annaert, *Proteolytic processing and cell biological functions of the amyloid precursor protein.* J Cell Sci, 2000. **113 (Pt 11)**: p. 1857-70.

78.   Anderson, J.P., et al., *An alternative secretase cleavage produces soluble Alzheimer amyloid precursor protein containing a potentially amyloidogenic sequence.* J Neurochem, 1992. **59**(6): p. 2328-31.

79.   Mattson, M.P., et al., *Evidence for excitoprotective and intraneuronal calcium-regulating roles for secreted forms of the beta-amyloid precursor protein.* Neuron, 1993. **10**(2): p. 243-54.

80.   Small, D.H., et al., *A heparin-binding domain in the amyloid protein precursor of Alzheimer's disease is involved in the regulation of neurite outgrowth.* J Neurosci, 1994. **14**(4): p. 2117-27.

81.   Barrantes, F.J., V. Borroni, and S. Valles, *Neuronal nicotinic acetylcholine receptor-cholesterol crosstalk in Alzheimer's disease.* FEBS Lett, 2010. **584**(9): p. 1856-63.

82.   Haass, C., *Take five--BACE and the gamma-secretase quartet conduct Alzheimer's amyloid beta-peptide generation.* Embo J, 2004. **23**(3): p. 483-8.

83.   Suh, Y.H. and F. Checler, *Amyloid precursor protein, presenilins, and alpha-synuclein: molecular pathogenesis and pharmacological applications in Alzheimer's disease.* Pharmacol Rev, 2002. **54**(3): p. 469-525.

84.   Nicoll, J.A., et al., *Abeta species removal after abeta42 immunization.* J Neuropathol Exp Neurol, 2006. **65**(11): p. 1040-8.

85.   Lesne, S., L. Kotilinek, and K.H. Ashe, *Plaque-bearing mice with reduced levels of oligomeric amyloid-beta assemblies have intact memory function.* Neuroscience, 2008. **151**(3): p. 745-9.

86.   Chen, Y.R. and C.G. Glabe, *Distinct early folding and aggregation properties of Alzheimer amyloid-beta peptides Abeta40 and Abeta42: stable trimer or tetramer formation by Abeta42.* J Biol Chem, 2006. **281**(34): p. 24414-22.

87.   Bernstein, S.L., et al., *Amyloid-beta protein oligomerization and the importance of tetramers and dodecamers in the aetiology of Alzheimer's disease.* Nat Chem, 2009. **1**(4): p. 326-31.

88.   Maurer, K. and S. Hoyer, *Alois Alzheimer revisited: differences in origin of the disease carrying his name.* J Neural Transm, 2006. **113**(11): p. 1645-58.

89.   Jin, K., et al., *Increased hippocampal neurogenesis in Alzheimer's disease.* Proc Natl Acad Sci U S A, 2004. **101**(1): p. 343-7.

90.   Yang, Y., E.J. Mufson, and K. Herrup, *Neuronal cell death is preceded by cell cycle events at all stages of Alzheimer's disease.* J Neurosci, 2003. **23**(7): p. 2557-63.

91.   Phillips, W., A.W. Michell, and R.A. Barker, *Neurogenesis in diseases of the central nervous system.* Stem Cells Dev, 2006. **15**(3): p. 359-79.

92.   Boekhoorn, K., M. Joels, and P.J. Lucassen, *Increased proliferation reflects glial and vascular-associated changes, but not neurogenesis in the presenile Alzheimer hippocampus.* Neurobiol Dis, 2006. **24**(1): p. 1-14.

93.   Lovell, M.A., et al., *Isolation of neural precursor cells from Alzheimer's disease and aged control postmortem brain.* Neurobiol Aging, 2006. **27**(7): p. 909-17.

94.   Ziabreva, I., et al., *Altered neurogenesis in Alzheimer's disease.* J Psychosom Res, 2006. **61**(3): p. 311-6.

95.   Jin, K., et al., *Enhanced neurogenesis in Alzheimer's disease transgenic (PDGF-APPSw,Ind) mice.* Proc Natl Acad Sci U S A, 2004. **101**(36): p. 13363-7.

96.   Donovan, M.H., et al., *Decreased adult hippocampal neurogenesis in the PDAPP mouse model of Alzheimer's disease.* J Comp Neurol, 2006. **495**(1): p. 70-83.

97.   Ermini, F.V., et al., *Neurogenesis and alterations of neural stem cells in mouse models of cerebral amyloidosis.* Am J Pathol, 2008. **172**(6): p. 1520-8.

98.   Wen, P.H., et al., *The presenilin-1 familial Alzheimer disease mutant P117L impairs neurogenesis in the hippocampus of adult mice.* Exp Neurol, 2004. **188**(2): p. 224-37.

99.   Verret, L., et al., *Alzheimer's-type amyloidosis in transgenic mice impairs survival of newborn neurons derived from adult hippocampal neurogenesis.* J Neurosci, 2007. **27**(25): p. 6771-80.

100. Zhang, C., et al., *Long-lasting impairment in hippocampal neurogenesis associated with amyloid deposition in a knock-in mouse model of familial Alzheimer's disease.* Exp Neurol, 2007. **204**(1): p. 77-87.

101. Haughey, N.J., et al., *Disruption of neurogenesis by amyloid beta-peptide, and perturbed neural progenitor cell homeostasis, in models of Alzheimer's disease.* J Neurochem, 2002. **83**(6): p. 1509-24.

102. Schinkel, A.H., et al., *Normal viability and altered pharmacokinetics in mice lacking mdr1-type (drug-transporting) P-glycoproteins.* Proc Natl Acad Sci U S A, 1997. **94**(8): p. 4028-33.

103. Jonker, J.W., et al., *The breast cancer resistance protein protects against a major chlorophyll-derived dietary phototoxin and protoporphyria.* Proc Natl Acad Sci U S A, 2002. **99**(24): p. 15649-54.

104. Wijnholds, J., et al., *Increased sensitivity to anticancer drugs and decreased inflammatory response in mice lacking the multidrug resistance-associated protein.* Nat Med, 1997. **3**(11): p. 1275-9.

105. Radde, R., et al., *Abeta42-driven cerebral amyloidosis in transgenic mice reveals early and robust pathology.* EMBO Rep, 2006. **7**(9): p. 940-6.

106. Gratzner, H.G., *Monoclonal antibody to 5-bromo- and 5-iododeoxyuridine: A new reagent for detection of DNA replication.* Science, 1982. **218**(4571): p. 474-5.

107. Kernie, S.G., T.M. Erwin, and L.F. Parada, *Brain remodeling due to neuronal and astrocytic proliferation after controlled cortical injury in mice.* J Neurosci Res, 2001. **66**(3): p. 317-26.

108. Yu, T.S., et al., *Traumatic brain injury-induced hippocampal neurogenesis requires activation of early nestin-expressing progenitors.* J Neurosci, 2008. **28**(48): p. 12901-12.

109. Ferrari, D., et al., *Isolation of neural stem cells from neural tissues using the neurosphere technique.* Curr Protoc Stem Cell Biol, 2010. **Chapter 2**: p. Unit2D 6.

110. Mullis, K., et al., *Specific enzymatic amplification of DNA in vitro: the polymerase chain reaction.* Cold Spring Harb Symp Quant Biol, 1986. **51 Pt 1**: p. 263-73.

111. Chomczynski, P. and N. Sacchi, *Single-step method of RNA isolation by acid guanidinium thiocyanate-phenol-chloroform extraction.* Anal Biochem, 1987. **162**(1): p. 156-9.

112. Higuchi, R., et al., *Simultaneous amplification and detection of specific DNA sequences.* Biotechnology (N Y), 1992. **10**(4): p. 413-7.

113. VanGuilder, H.D., K.E. Vrana, and W.M. Freeman, *Twenty-five years of quantitative PCR for gene expression analysis.* Biotechniques, 2008. **44**(5): p. 619-26.

114. Livak, K.J. and T.D. Schmittgen, *Analysis of relative gene expression data using real-time quantitative PCR and the 2(-Delta Delta C(T)) Method.* Methods, 2001. **25**(4): p. 402-8.

115. Dahlgren, K.N., et al., *Oligomeric and fibrillar species of amyloid-beta peptides differentially affect neuronal viability.* J Biol Chem, 2002. **277**(35): p. 32046-53.

116. Shruster, A., et al., *Wnt signaling pathway overcomes the disruption of neuronal differentiation of neural progenitor cells induced by oligomeric amyloid beta-peptide.* J Neurochem, 2011. **116**(4): p. 522-9.

117. Hsiao, K.K., et al., *Age-related CNS disorder and early death in transgenic FVB/N mice overexpressing Alzheimer amyloid precursor proteins.* Neuron, 1995. **15**(5): p. 1203-18.

118. Montgomery, K.C., *The relation between fear induced by novel stimulation and exploratory behavior.* J Comp Physiol Psychol, 1955. **48**(4): p. 254-60.

119. Arendash, G.W., et al., *Progressive, age-related behavioral impairments in transgenic mice carrying both mutant amyloid precursor protein and presenilin-1 transgenes.* Brain Res, 2001. **891**(1-2): p. 42-53.

120. Maldonado, E. and J.F. Navarro, *Effects of 3,4-methylenedioxy-methamphetamine (MDMA) on anxiety in mice tested in the light-dark box.* Prog Neuropsychopharmacol Biol Psychiatry, 2000. **24**(3): p. 463-72.

121. Graham, V., et al., *SOX2 functions to maintain neural progenitor identity.* Neuron, 2003. **39**(5): p. 749-65.

122. Kandasamy, M., et al., *Stem cell quiescence in the hippocampal neurogenic niche is associated with elevated transforming growth factor-beta signaling in an animal model of Huntington disease.* J Neuropathol Exp Neurol, 2010. **69**(7): p. 717-28.

123. von Bohlen Und Halbach, O., *Immunohistological markers for staging neurogenesis in adult hippocampus.* Cell Tissue Res, 2007. **329**(3): p. 409-20.

124. Ming, G.L. and H. Song, *Adult neurogenesis in the mammalian central nervous system.* Annu Rev Neurosci, 2005. **28**: p. 223-50.

125. Kempermann, G., et al., *Milestones of neuronal development in the adult hippocampus.* Trends Neurosci, 2004. **27**(8): p. 447-52.

126. Bye, N., et al., *Neurogenesis and glial proliferation are stimulated following diffuse traumatic brain injury in adult rats.* J Neurosci Res, 2011. **89**(7): p. 986-1000.

127. Conrad, C.D., et al., *The effects of type I and type II corticosteroid receptor agonists on exploratory behavior and spatial memory in the Y-maze.* Brain Res, 1997. **759**(1): p. 76-83.

128. Holcomb, L., et al., *Accelerated Alzheimer-type phenotype in transgenic mice carrying both mutant amyloid precursor protein and presenilin 1 transgenes.* Nat Med, 1998. **4**(1): p. 97-100.

129. Cruz, A.P., F. Frei, and F.G. Graeff, *Ethopharmacological analysis of rat behavior on the elevated plus-maze.* Pharmacol Biochem Behav, 1994. **49**(1): p. 171-6.

130. Rodgers, R.J. and A. Dalvi, *Anxiety, defence and the elevated plus-maze.* Neurosci Biobehav Rev, 1997. **21**(6): p. 801-10.

131. Wang, D.D. and A. Bordey, *The astrocyte odyssey.* Prog Neurobiol, 2008. **86**(4): p. 342-67.

132. Wigley, R., et al., *Morphological and physiological interactions of NG2-glia with astrocytes and neurons.* J Anat, 2007. **210**(6): p. 661-70.

133. Leoni, G., M. Rattray, and A.M. Butt, *NG2 cells differentiate into astrocytes in cerebellar slices.* Mol Cell Neurosci, 2009. **42**(3): p. 208-18.

134. Nolte, C., et al., *GFAP promoter-controlled EGFP-expressing transgenic mice: a tool to visualize astrocytes and astrogliosis in living brain tissue.* Glia, 2001. **33**(1): p. 72-86.

135.   Hodge, R.D., et al., *Intermediate progenitors in adult hippocampal neurogenesis: Tbr2 expression and coordinate regulation of neuronal output.* J Neurosci, 2008. **28**(14): p. 3707-17.
136.   Englund, C., et al., *Pax6, Tbr2, and Tbr1 are expressed sequentially by radial glia, intermediate progenitor cells, and postmitotic neurons in developing neocortex.* J Neurosci, 2005. **25**(1): p. 247-51.
137.   Shen, Q., et al., *Adult SVZ stem cells lie in a vascular niche: a quantitative analysis of niche cell-cell interactions.* Cell Stem Cell, 2008. **3**(3): p. 289-300.
138.   Shen, Q., et al., *Endothelial cells stimulate self-renewal and expand neurogenesis of neural stem cells.* Science, 2004. **304**(5675): p. 1338-40.
139.   Feng, R., et al., *Deficient neurogenesis in forebrain-specific presenilin-1 knockout mice is associated with reduced clearance of hippocampal memory traces.* Neuron, 2001. **32**(5): p. 911-26.
140.   Herms, J., et al., *Cortical dysplasia resembling human type 2 lissencephaly in mice lacking all three APP family members.* Embo J, 2004. **23**(20): p. 4106-15.
141.   Guenette, S., et al., *Essential roles for the FE65 amyloid precursor protein-interacting proteins in brain development.* Embo J, 2006. **25**(2): p. 420-31.
142.   Giuffrida, M.L., et al., *Beta-amyloid monomers are neuroprotective.* J Neurosci, 2009. **29**(34): p. 10582-7.
143.   Chen, Y. and C. Dong, *Abeta40 promotes neuronal cell fate in neural progenitor cells.* Cell Death Differ, 2009. **16**(3): p. 386-94.
144.   Chasseigneaux, S. and B. Allinquant, *Functions of Abeta, sAPPalpha and sAPPbeta : similarities and differences.* J Neurochem, 2012. **120 Suppl 1**: p. 99-108.
145.   Brody, D.L., et al., *Amyloid-beta dynamics correlate with neurological status in the injured human brain.* Science, 2008. **321**(5893): p. 1221-4.
146.   Franke, T.F., D.R. Kaplan, and L.C. Cantley, *PI3K: downstream AKTion blocks apoptosis.* Cell, 1997. **88**(4): p. 435-7.
147.   Soucek, T., et al., *The regulation of glucose metabolism by HIF-1 mediates a neuroprotective response to amyloid beta peptide.* Neuron, 2003. **39**(1): p. 43-56.
148.   Heo, C., et al., *Effects of the monomeric, oligomeric, and fibrillar Abeta42 peptides on the proliferation and differentiation of adult neural stem cells from subventricular zone.* J Neurochem, 2007. **102**(2): p. 493-500.
149.   Lee, Y.J., et al., *Investigation of efflux transport of dehydroepiandrosterone sulfate and mitoxantrone at the mouse blood-brain barrier: a minor role of breast cancer resistance protein.* J Pharmacol Exp Ther, 2005. **312**(1): p. 44-52.
150.   Koo, B.K., et al., *An obligatory role of mind bomb-1 in notch signaling of mammalian development.* PLoS One, 2007. **2**(11): p. e1221.
151.   Barsi, J.C., et al., *Mind bomb1 is a ubiquitin ligase essential for mouse embryonic development and Notch signaling.* Mech Dev, 2005. **122**(10): p. 1106-17.
152.   Yoon, K.J., et al., *Mind bomb 1-expressing intermediate progenitors generate notch signaling to maintain radial glial cells.* Neuron, 2008. **58**(4): p. 519-31.
153.   Casarosa, S., C. Fode, and F. Guillemot, *Mash1 regulates neurogenesis in the ventral telencephalon.* Development, 1999. **126**(3): p. 525-34.
154.   Horton, S., et al., *Correct coordination of neuronal differentiation events in ventral forebrain requires the bHLH factor MASH1.* Mol Cell Neurosci, 1999. **14**(4-5): p. 355-69.
155.   Parras, C.M., et al., *Mash1 specifies neurons and oligodendrocytes in the postnatal brain.* Embo J, 2004. **23**(22): p. 4495-505.
156.   Parras, C.M., et al., *The proneural gene Mash1 specifies an early population of telencephalic oligodendrocytes.* J Neurosci, 2007. **27**(16): p. 4233-42.
157.   Brooker, R., K. Hozumi, and J. Lewis, *Notch ligands with contrasting functions: Jagged1 and Delta1 in the mouse inner ear.* Development, 2006. **133**(7): p. 1277-86.
158.   Louvi, A. and S. Artavanis-Tsakonas, *Notch signalling in vertebrate neural development.* Nat Rev Neurosci, 2006. **7**(2): p. 93-102.
159.   Stump, G., et al., *Notch1 and its ligands Delta-like and Jagged are expressed and active in distinct cell populations in the postnatal mouse brain.* Mech Dev, 2002. **114**(1-2): p. 153-9.
160.   Ehninger, D. and G. Kempermann, *Neurogenesis in the adult hippocampus.* Cell Tissue Res, 2008. **331**(1): p. 243-50.
161.   Brown, J.P., et al., *Transient expression of doublecortin during adult neurogenesis.* J Comp Neurol, 2003. **467**(1): p. 1-10.
162.   Steffenhagen, C., et al., *Identity, fate and potential of cells grown as neurospheres: species matters.* Stem Cell Rev, 2011. **7**(4): p. 815-35.
163.   Gygi, S.P., et al., *Correlation between protein and mRNA abundance in yeast.* Mol Cell Biol, 1999. **19**(3): p. 1720-30.
164.   Greenbaum, D., et al., *Comparing protein abundance and mRNA expression levels on a genomic scale.* Genome Biol, 2003. **4**(9): p. 117.
165.   Spalice, A., et al., *Neuronal migration disorders: clinical, neuroradiologic and genetics aspects.* Acta Paediatr, 2009. **98**(3): p. 421-33.
166.   Lipoff, D.M., et al., *Neocortical molecular layer heterotopia in substrains of C57BL/6 and C57BL/10 mice.* Brain Res, 2011. **1391**: p. 36-43.
167.   Schwartzkroin, P.A. and C.A. Walsh, *Cortical malformations and epilepsy.* Ment Retard Dev Disabil Res Rev, 2000. **6**(4): p. 268-80.
168.   Lalonde, R., *The neurobiological basis of spontaneous alternation.* Neurosci Biobehav Rev, 2002. **26**(1): p. 91-104.

169.   Hooper, N., C. Fraser, and T.W. Stone, *Effects of purine analogues on spontaneous alternation in mice.* Psychopharmacology (Berl), 1996. **123**(3): p. 250-7.

170.   Bats, S., et al., *The effects of a mild stressor on spontaneous alternation in mice.* Behav Brain Res, 2001. **118**(1): p. 11-5.

171.   Handley, S.L. and S. Mithani, *Effects of alpha-adrenoceptor agonists and antagonists in a maze-exploration model of 'fear'-motivated behaviour.* Naunyn Schmiedebergs Arch Pharmacol, 1984. **327**(1): p. 1-5.

172.   Pellow, S., et al., *Validation of open:closed arm entries in an elevated plus-maze as a measure of anxiety in the rat.* J Neurosci Methods, 1985. **14**(3): p. 149-67.

173.   Moser, P.C., *An evaluation of the elevated plus-maze test using the novel anxiolytic buspirone.* Psychopharmacology (Berl), 1989. **99**(1): p. 48-53.

174.   Crawley, J. and F.K. Goodwin, *Preliminary report of a simple animal behavior model for the anxiolytic effects of benzodiazepines.* Pharmacol Biochem Behav, 1980. **13**(2): p. 167-70.

175.   Bourin, M. and M. Hascoet, *The mouse light/dark box test.* Eur J Pharmacol, 2003. **463**(1-3): p. 55-65.

176.   Snyder, J.S., et al., *A role for adult neurogenesis in spatial long-term memory.* Neuroscience, 2005. **130**(4): p. 843-52.

177.   Errijgers, V., et al., *FVB.129P2-Pde6b(+) Tyr(c-ch)/Ant, a sighted variant of the FVB/N mouse strain suitable for behavioral analysis.* Genes Brain Behav, 2007. **6**(6): p. 552-7.

178.   Crawley, J.N., et al., *Behavioral phenotypes of inbred mouse strains: implications and recommendations for molecular studies.* Psychopharmacology (Berl), 1997. **132**(2): p. 107-24.

179.   Krupa, D.J., et al., *Behavioral properties of the trigeminal somatosensory system in rats performing whisker-dependent tactile discriminations.* J Neurosci, 2001. **21**(15): p. 5752-63.

180.   Mineur, Y.S. and W.E. Crusio, *Behavioral and neuroanatomical characterization of FVB/N inbred mice.* Brain Res Bull, 2002. **57**(1): p. 41-7.

181.   Becker, K.F., H. Allmeier, and V. Hollt, *New mechanisms of hormone secretion: MDR-like gene products as extrusion pumps for hormones?* Horm Metab Res, 1992. **24**(5): p. 210-3.

182.   Korte, S.M., *Corticosteroids in relation to fear, anxiety and psychopathology.* Neurosci Biobehav Rev, 2001. **25**(2): p. 117-42.

183.   Moechars, D., et al., *Expression in brain of amyloid precursor protein mutated in the alpha-secretase site causes disturbed behavior, neuronal degeneration and premature death in transgenic mice.* Embo J, 1996. **15**(6): p. 1265-74.

184.   Holcomb, L.A., et al., *Behavioral changes in transgenic mice expressing both amyloid precursor protein and presenilin-1 mutations: lack of association with amyloid deposits.* Behav Genet, 1999. **29**(3): p. 177-85.

185.   Galvan, V., et al., *Reversal of Alzheimer's-like pathology and behavior in human APP transgenic mice by mutation of Asp664.* Proc Natl Acad Sci U S A, 2006. **103**(18): p. 7130-5.

6.2   Acknowledgements/Danksagung

6.3   Curriculum vitae

Personal Information

Name: Toni Schumacher

Date & Place of Birth   14.03.1982 in Rostock, Germany

Education

10/2008 – 05/2012	PhD thesis in the Neurodegeneration Research Lab of Prof. J. Pahnke , University of Rostock
10/2001 – 02/2008	Studies of Biology and Diploma at the University of Rostock
09/1995 – 06/ 2000	High School "Erasmus-Gymnasium" in Rostock, Abitur
09/1992 – 06/1995	High School "Albert Schweitzer" in Rostock
09/1988 – 06/1992	Comprehensive School "Egon Schulz", Rostock

Practical Experience

Since 10/2008	*Doctoral student* in the Neurodegeneration Research Lab – Performed research regarding the role of ABC transporters in neuroregeneration in vivo and in vitro
03/2008 – 10/2008	*Research assistant* at Neuroproof GmbH Rostock, Germany – Functional screening with primary neuronal networks for drug development
2007 – 2008	*Undergraduate student assistant* at the Clinic for Internal Medicine in Rostock, Germany – Molecular diagnosis of lung pathogens like Pneumocystis jerovecii
2004 – 2007	*Undergraduate student assistant* at the "Institut für Zellbiologie und Systemtechnik" in Rostock, Germany – Field potential analyzes of neuronal networks by multiple electrode arrays

Scholarship

10/2008 – 10/2011   *Scholarship holder of the "Landesgraduiertenförderung M.-V."*

Publications

Peer-reviewed articles

1 **Schumacher T**, Krohn M, Hofrichter J, Lange C, Stenzel J, et al. (2012) *ABC Transporters B1, C1 and G2 Differentially Regulate Neuroregeneration in Mice.* PLoS ONE 7(4): e35613. doi:10.1371/journal.pone.0035613

2 Krohn M, Lange C, Hofrichter J, Scheffler K, Stenzel J, Steffen J, **Schumacher T**, et al. (2011) *Cerebral amyloid-β proteostasis is regulated by the membrane transport protein ABCC1 in mice.* J Clin Invest. 2011 October 3; 121(10): 3924–3931. doi: 10.1172/JCI57867

3 Scheffler K, Stenzel J, Krohn M, Lange C, Hofrichter J, **Schumacher T**, et al. (2011) *Determination of spatial and temporal distribution of microglia by 230nm-high-resolution, high-throughput automated analysis reveals different amyloid plaque populations in an APP/PS1 mouse model of Alzheimer's disease.* Curr Alzheimer Res. 2011 November; 8(7):781-788

Poster

1 **Schumacher T**, Pahnke J. (2009) *Transient ABC transporter expression during neurogenesis – Cause or effect of stem cell differentiation?* Acta Neuropathol. (2009) 118 (3), 460-461

6.4   Declaration/ Eidesstattliche Erklärung

Ich gebe folgende Erklärung ab:

1. Die Gelegenheit zum vorliegenden Promotionsvorhaben ist mir nicht kommerziell vermittelt worden. Insbesondere habe ich keine Organisation eingeschaltet, die gegen Entgelt Betreuerinnen/Betreuer für die Anfertigung von Dissertationen sucht oder die mir obliegenden Pflichten hinsichtlich der Prüfungsleistungen für mich ganz oder teilweise erledigt.

2. Ich versichere hiermit an Eides statt, dass ich die vorliegende Arbeit selbstständig angefertigt und ohne fremde Hilfe verfasst habe. Dazu habe ich keine außer den von mir angegebenen Hilfsmitteln und Quellen verwendet und die den benutzten Werken inhaltlich und wörtlich entnommenen Stellen habe ich als solche kenntlich gemacht.

Toni Schumacher   Rostock, den 11. Mai 2012